Malignant Liver Tumors

4

Yi Dong, Wen-Ping Wang, Pei-Li Fan, Feng Mao,
Han-Sheng Xia, Jia-Ying Cao, and Bei-Jian Huang

Abbreviations

CDFI	Color Doppler flow imaging
CEUS	Contrast enhanced ultrasound
CT	Computed tomography
DWI	Diffusion-weighted imaging
HCC	Hepatocellular carcinoma
HGDN	High-grade dysplastic nodule
ICC	Intrahepatic cholangiocarcinoma
ICGHN	International Consensus Group for Hepatocellular Neoplasia
IWP	International Working Party
LGDN	Low-grade dysplastic nodule
MRI	Magnetic resonance image
OATP	Organic anionic transporting polypeptide
PET	Positron emission tomography
RN	Regenerative nodule
UCA	Ultrasound contrast agent
US	Ultrasonography
WHO	World Health Organization

4.1 Hepatocellular Carcinoma

Yi Dong and Wen-Ping Wang

4.1.1 Introduction

- Hepatocellular carcinoma (HCC) is the most common primary liver malignant tumors and a major cause of morbidity and death worldwide. Currently, it is the second leading cause of cancer-related death [1]. It is the sixth most common cancer and the fourth cause of cancer death, with a 5-year survival rate of 18%. It is estimated that in 2030 more than 1 million patients will die of liver cancer [2].
- HCC develops in various chronic liver disease backgrounds: chronic hepatitis caused by hepatitis B or C virus (HBV or HCV), nonalcoholic or alcoholic steatohepatitis, etc.
- HCC develops in a multistep fashion. Various precancerous lesions, including regenerative nodules (RN), and dysplastic nodules (DN), progress to early HCCs, well differentiated, moderately differentiated, or poorly differentiated HCCs (Fig. 4.1).

4.1.2 Indications of Liver CEUS

- For all focal liver lesions detected during routine ultrasound or surveillance in the cirrhotic or noncirrhotic liver, CEUS is indicated to characterize and to establish a diagnosis of HCC (followed by CT and MRI for staging).
- To characterize focal liver lesions not suitable for biopsy, especially those remained indeterminate after CT or MR examinations.
- For patients with multiple focal liver lesions, CEUS is recommended to select a nodule or nodules with different contrast enhancement patterns for biopsy.

Y. Dong (✉) · W.-P. Wang · P.-L. Fan · F. Mao · H.-S. Xia
J.-Y. Cao · B.-J. Huang
Department of Ultrasound, Zhongshan Hospital, Fudan University, Shanghai, China
e-mail: dong.yi@zs-hospital.sh.cn; fan.peili@zs-hospital.sh.cn; mao.feng@zs-hospital.sh.cn; xia.hansheng@zs-hospital.sh.cn; cao.jiaying@zs-hospital.sh.cn; huang.beijian@zs-hospital.sh.cn

MALIGNANT	Arterial Phase		Portal venous/Late Phase	
Hepatocellular Carcinima	Hyperenhancement	Dysmorphic Vessels	**Early<1 min** Hyper/Iso Enhancement	**Late>1 min** Weak Wash-out
Liver Metastasis	Hyperenhancement	Rim Enhancement	Hyperenhancement	Punched Wash-out
BENIGN	Arterial Phase		Portal venous/Late Phase	
Hemangioma	Peripheral Nodular Hyperenhancement/Centripetel Fill		Incomplete	Hyper/Iso Enhancement
Focal Nodular Hyperplasia	Hyperenhancement/Centrifugal Fill		Central Scar	Hyper/Iso Enhancement
Adenoma	Hyperenhancement/Centripetel Fill		Hyper/Iso Enhancement	Weak Wash-out

Fig. 4.1 Schematic algorithm of enhancement of focal liver masses with CEUS. *AP* arterial phase, *PVP* portal venous phase, *LP* late phase, *APHE* arterial phase hyperenhancement

- CEUS is used to reach further diagnosis in patients with inconclusive histologic or cytologic results.
- To monitor dynamic changes in contrast enhancement patterns over time for follow up of suspected malignant hepatocellular lesions.
- Based on contrast enhancement, to differentiate tumor in vein from bland thrombus in vein.
- To monitor and target ablation therapy response of HCC during and after ablation or chemotherapy treatments.

4.1.3 CEUS Features of HCC

- More than 95% of focal liver lesions in liver cirrhosis are HCCs.
- Typical contrast enhanced ultrasound features of HCCs including: hyperenhancement in the early arterial phase, typically mild wash-out in the late phase. For HCC lesions, mild wash-out most often does not occur until very late in the late phase (>3 min) (Figs. 4.2 and 4.3).
- Well-differentiated HCCs may lack wash-out in the late phase. In cirrhotic liver, only arterial phase hyperenhance-

ment might be sufficient for the preoperative diagnosis of HCC [3] (Figs. 4.4 and 4.5).
- On the condition that the lesion did not show wash-out after 3 min, a further observation after 4–6 min is necessary.
- A second contrast agents injection can be repeated and focuses on the wash-out area 7–10 min later after first injection, for lesions located at difficult place, or small lesion sizes which arterial phase hyperenhancement is missed, or unsatisfied imaging due to patient being unable to hold breath, and for extra findings of an indeterminate wash-out nodule in the portal venous or late phase.

4.1.4 Additional Benefit for CEUS vs CT or MRI

- CT/MRI shows wash-out of focal liver lesions in the portal venous or late phase, but does not show definite arterial phase enhancement of the lesion.
- CT/MRI shows arterial phase hyperenhancement but does not show definite wash-out.
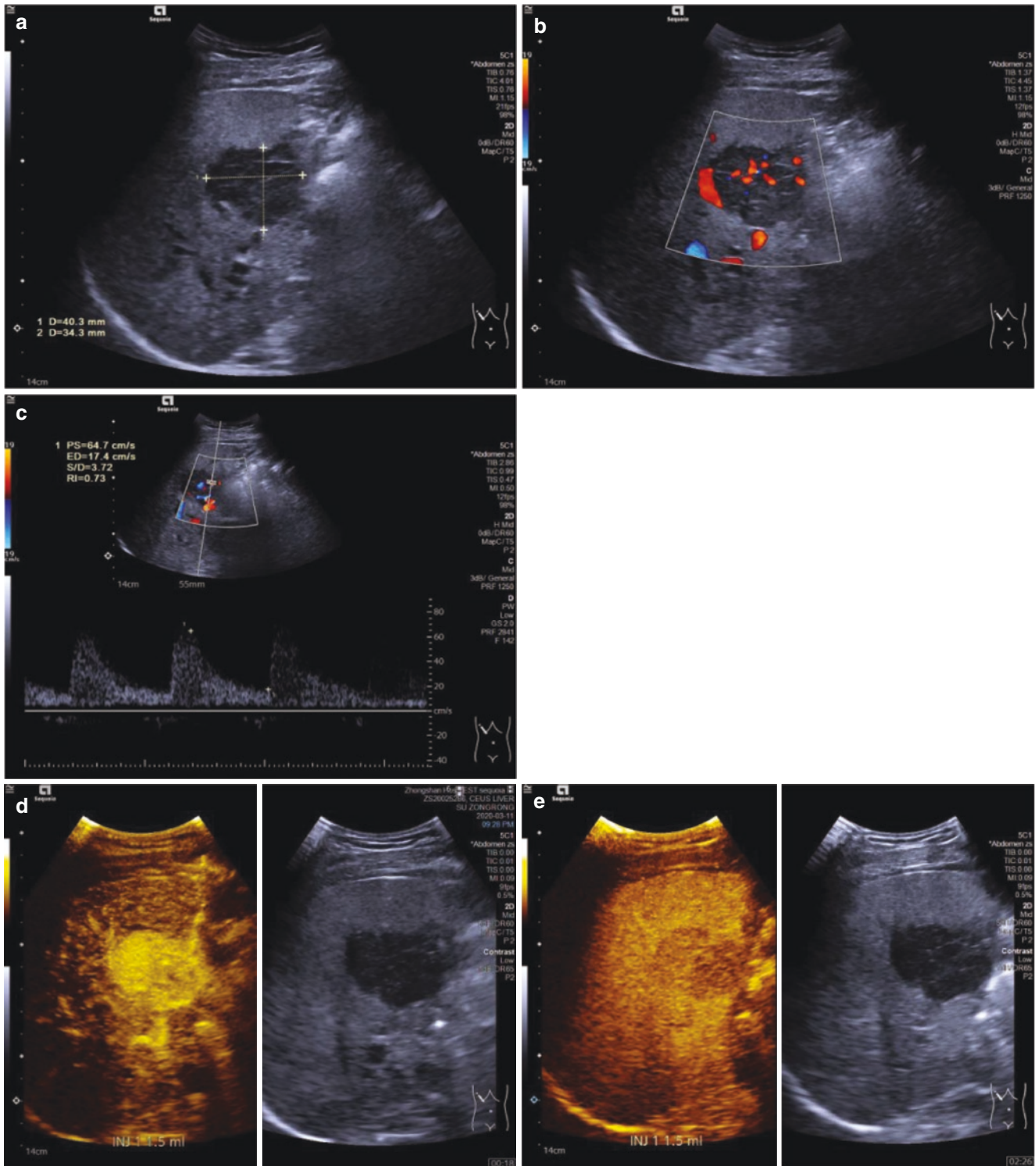
Fig. 4.2 A typical case of hepatocellular carcinoma (HCC). A gray-scale image revealed a hypoechoic focal liver lesion in right lobe of liver (**a**). Color flow signals could be detected inside the lesion (**b**). Arterial Doppler spectrum with high resistance index (RI) as 0.73 was measured (**c**). At 18 s after injection of contrast agents, the lesion showed complete hyperenhancement during arterial phase (**d**). At 2 min 26 s, the lesion showed late and mild wash-out (**e**)
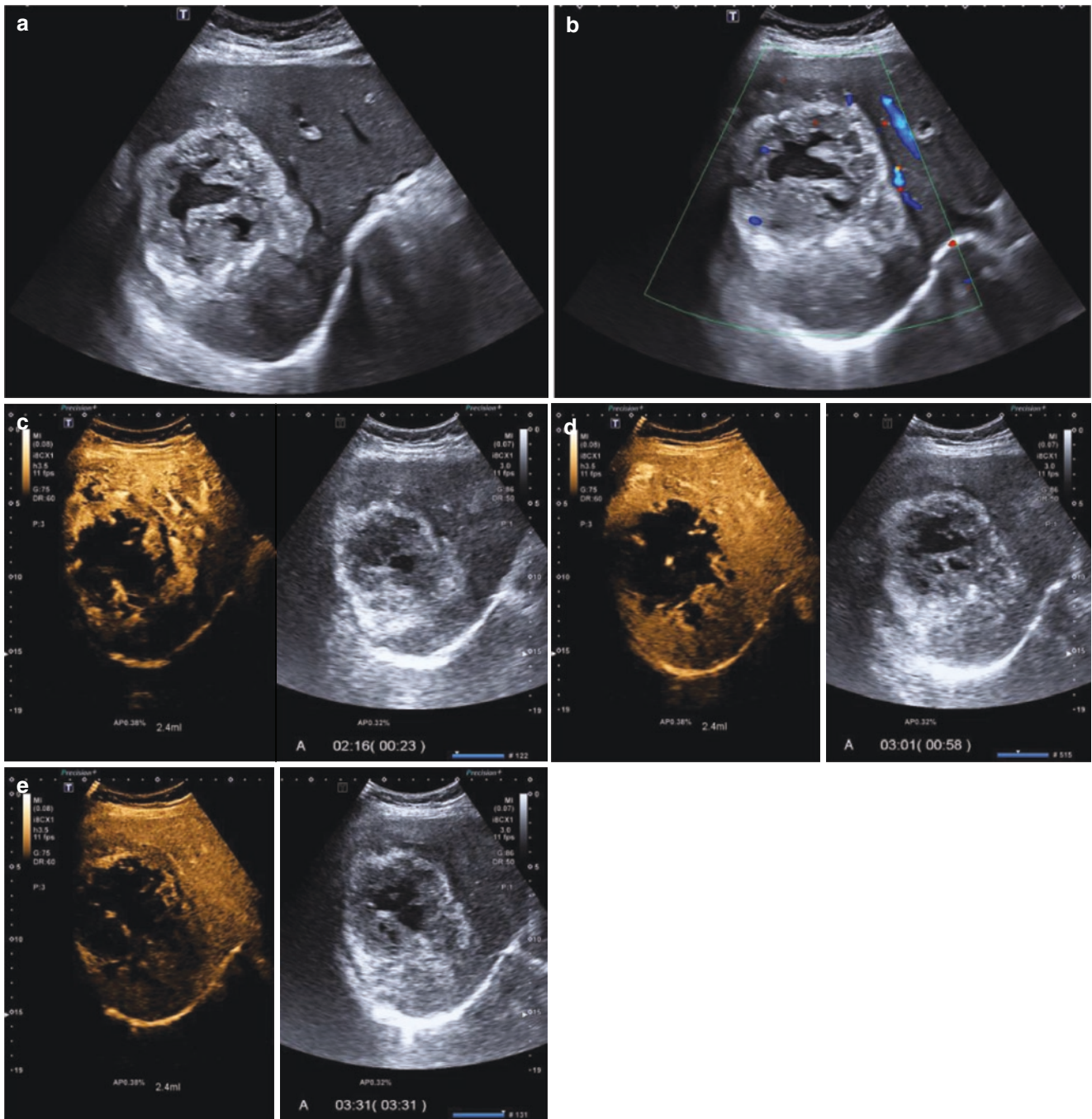
Fig. 4.3 A case of surgery and histopathologically proved hepatocellular carcinoma (HCC) in non-liver cirrhosis. A gray-scale image reveals a heterogenous hyperchoic focal liver lesion in right lobe of liver (**a**). Minor color flow signal could be detected inside the lesion (**b**). The lesion showed hyperenhancement in the surrounding area during early arterial phase with non-enhanced necrosis area inside (**c**). The lesion showed slight wash-out during portal venous phase (**d**) and turned into hypoenhancement during late phase of contrast enhanced ultrasound (**e**)
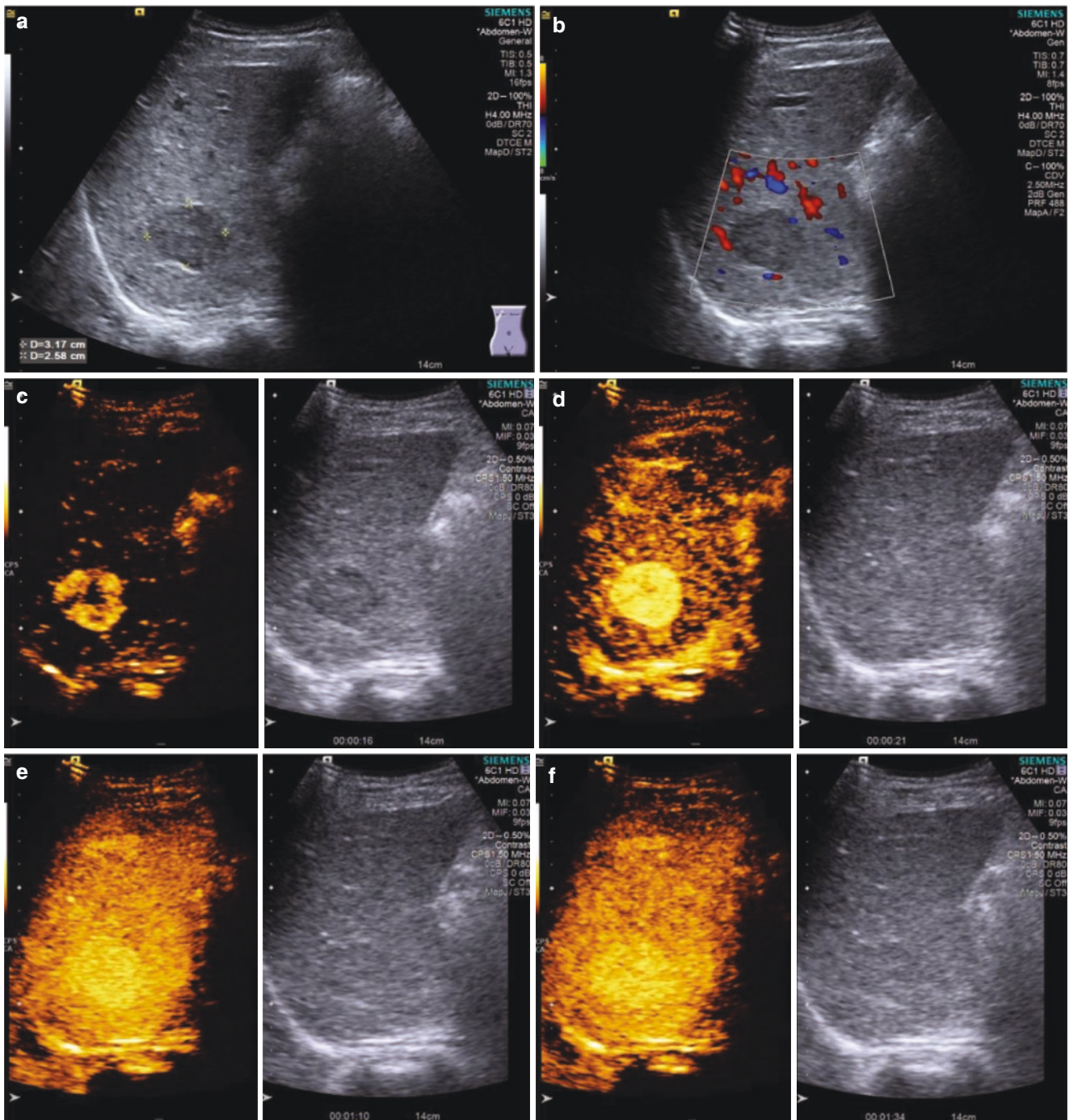
Fig. 4.4 A case of well-differentiated hepatocellular carcinoma (HCC) lack contrast wash-out in the late phase. A gray-scale image reveals a hypoechoic focal liver lesion in right lobe of liver (**a**). No color flow signal could be detected inside the lesion (**b**). The lesion showed nodular hyperenhancement during early arterial phase (**c**) and quickly turned into complete hyperenhancement (**d**). The lesion showed no wash-out and was slightly hyperenhanced during portal venous and late phase of contrast enhanced ultrasound (**e**)
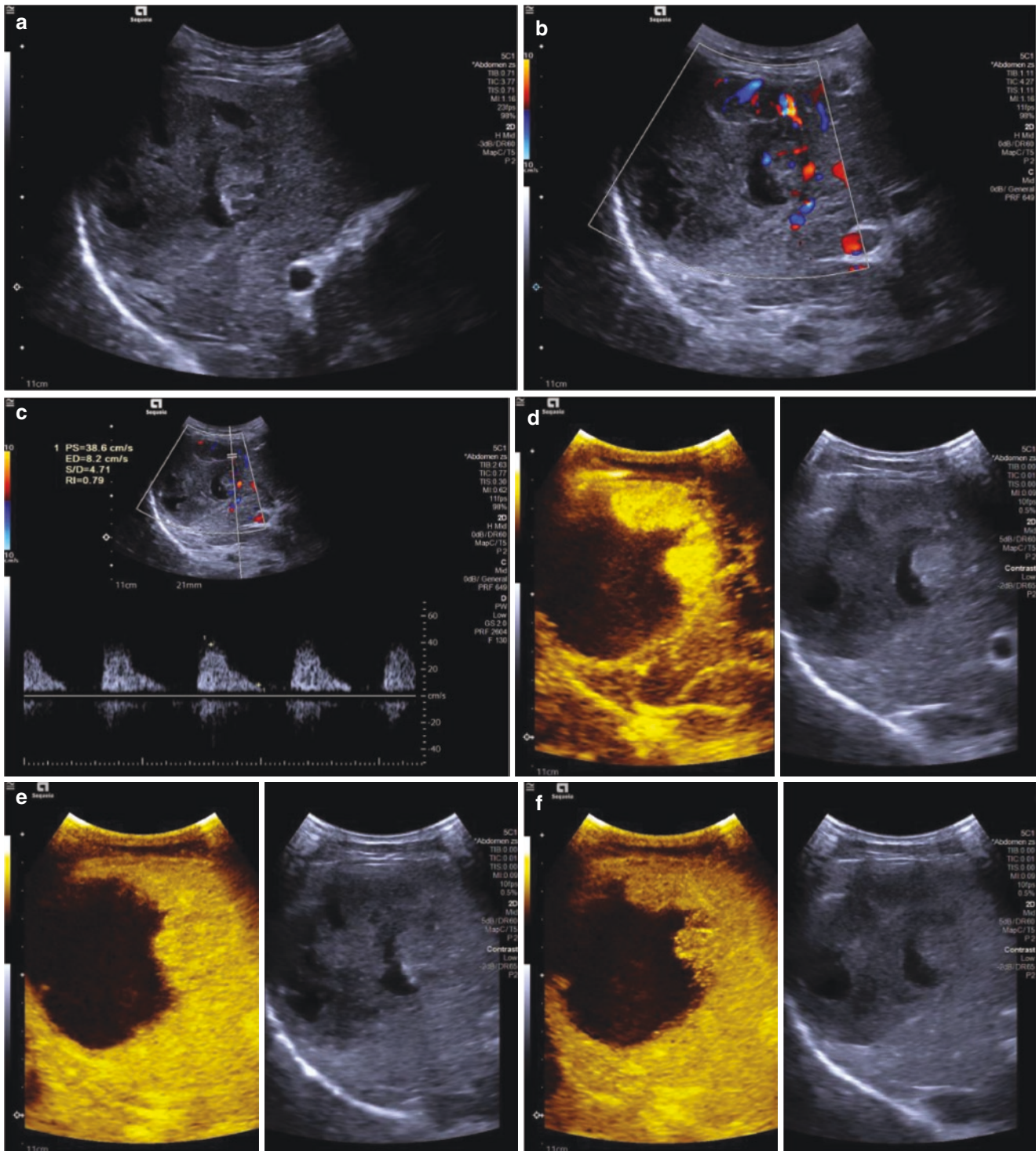
Fig. 4.5 A case of large hepatocellular carcinoma (HCC) with inner necrosis. B mode ultrasound image revealed a large cystic solid focal liver lesion in right lobe of liver (**a**). Color flow signal could be detected inside the lesion (**b**). Arterial Doppler spectrum with high resistance index (RI) as 0.79 was measured (**c**). The lesion showed partial hyper-enhancement during arterial phase (**d**). The lesion showed no wash-out during portal venous (**e**) and late phase of contrast enhanced ultrasound (**f**)

- Depending on its unique advantages of real-time scan and continuous acquisition, CEUS can provide continuous evaluation of wash-in and wash-out process for 5 min.

4.1.5 Limitations of Liver CEUS

Some common limitations with B mode ultrasound also exist in CEUS, such as subdiaphragmatic or deep located lesions, limited penetration in large size patients, infrequent interference of bowel or gastric gas, and lesion located in severe hepatic steatosis.

- Nodules located deeper than 10 cm from the skin surface. On those conditions, sound beam attenuation will cause excess subcutaneous or hepatic fat not well depicted with CEUS.
- In some patients, the upper right subdiaphragmatic regions of the liver cannot be visualized clearly through a proper acoustic window.
- Focal liver lesions with a diameter smaller than 10 mm, especially located in heterogeneous cirrhotic liver.
- Patients who could not cooperate satisfactorily during CEUS scan (Table 4.1).

4.1.6 Surveillance

Ultrasound is a widely accepted cost-effective first-line surveillance modality for the diagnosis of HCC. It is recommended by major international liver societies, including the European Association for the Study of the Liver (EASL) and the American Association for the Study of Liver Diseases (AASLD). During surveillance of HCC, ultra-

Table 4.1 Comparison of CEUS features to CT and MRI features

CEUS	CT and MRI
Real-time dynamic imaging	Static images
Use of a pure intravascular contrast agent	Use of extracellular contrast agent
No vascular pseudolesions	Subject to vascular pseudolesions
Multiple injections of contrast agent are possible	Only one injection of contrast agent
No motion artifacts	MRI is very sensitive to motion artifacts
Operator dependent and high technical expertise required	Non-operator dependent
May have blind area due to difficult to scan	Image of entire liver is routine

sound with a-fetoprotein (AFP) has been regarded as a standard surveillance tool. With the application of contrast enhanced ultrasound, the suboptimal detection rates and false referral rates of ultrasound have been overcome (Figs. 4.6 and 4.7).

Contrast enhanced ultrasound has not been recommended for surveillance of HCC because it does not enable examination of the entire liver. Although the detection rate for early-stage HCC was not significantly improved by adding CEUS, the false positive rate was significantly reduced [4]. The contrast agent Sonzaoid® is phagocytized by liver-specific macrophages including Kupffer cells. Since Kupffer cells may be less or even absent in HCC, hypoenhancement in the postvascular phase is a highly sensitive imaging feature of HCC [5–8]. CEUS may be used as a second-line imaging tool for a lesion suspicious for HCC, which was detected with B mode ultrasound surveillance.

Contrast enhanced ultrasound scan in the delayed phase permits detection of HCC lesions. However, CEUS is not recommended for surveillance. The entire liver cannot be scanned by contrast enhanced ultrasound [9]. Instead, CEUS permits the characterization of one or several identified nodules.

4.1.7 CEUS LI-RADS

- To make accurate characterization of focal liver lesions in the cirrhotic liver is among one of the most challenging imaging problems.
- The use of a microbubble-based contrast enhanced ultrasound and the implementation of the Liver Imaging Reporting and Data System (LI-RADS) for CEUS will greatly promote the future use of CEUS in patients who are at high risk for HCC.
- The LI-RADS uses a diagnostic algorithm to assign categories and reflect the relative probability of HCC. It was created with the aim to standardize liver imaging in patients at high risk for HCC.
- CEUS LI-RADS could improve the integration of CEUS into the clinical multimodality approach for the diagnosis and treatment of the liver at risk for HCC, providing additional important information to that obtained with CT and MRI (Table 4.2).

CEUS LI-RADS includes five diagnostic categories: LR-1 (definitely benign), LR-2 (probably benign), LR-3 (intermediate malignancy probability) (Fig. 4.8), LR-4 (probably HCC) (Fig. 4.9), and LR-5 (definitely HCC) (Figs. 4.10, 4.11, and 4.12).
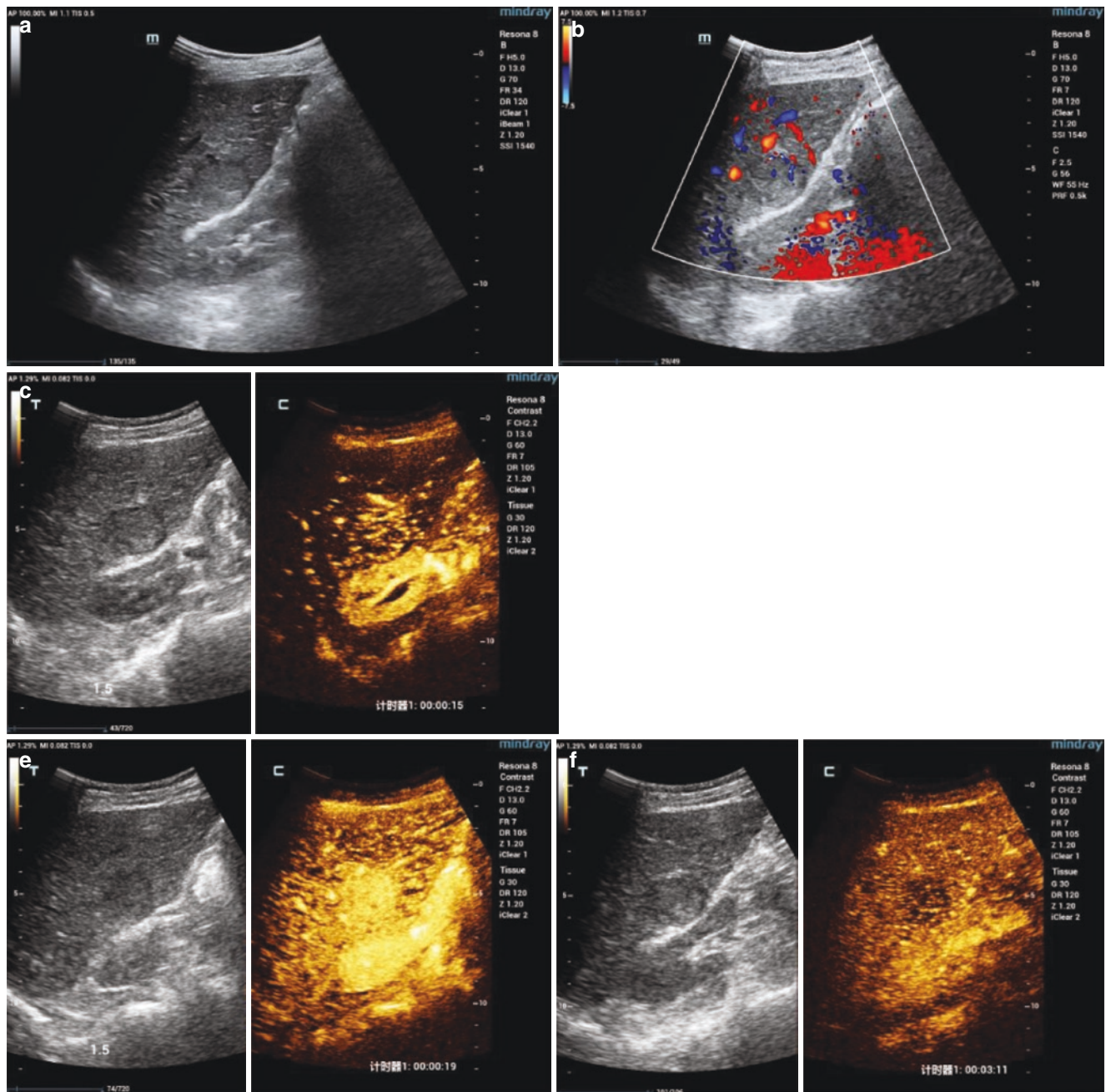
Fig. 4.6 A case of hepatocellular carcinoma (HCC) with typical contrast enhancement pattern. B mode ultrasound image revealed a hypoechoic solid focal liver lesion in right lobe of liver (**a**). A dotted color flow signal could be detected inside the lesion (**b**). The lesion showed heterogenous hyperenhancement during arterial phase (**c**) and soon reached peak and complete hyperenhancement (**d**). In the late phase, the lesion was hypoenhanced (**e**)

LR-NC (not categorized due to image degradation), LR-TIV (tumor in vein) (Figs. 4.13, 4.14, and 4.15) and LR-M (probably or definitely malignant but not HCC specific) diagnostic categories are also included in CEUS LI-RADS. CEUS has high sensitivity and accuracy in the detection and correct differentiation of a tumor thrombus from a bland thrombus [10]. CEUS LR-TIV should lead to alternative imaging assessment or repeat imaging, biopsy, or treatment.

Clinically HCCs can invade surrounding liver vessels with a prevalence of up to 20%. Portal vein thrombosis is a common imaging finding in liver cirrhosis. Differentiation between tumor thrombus and bland portal vein thrombosis is crucial for further therapeutic management. During CEUS
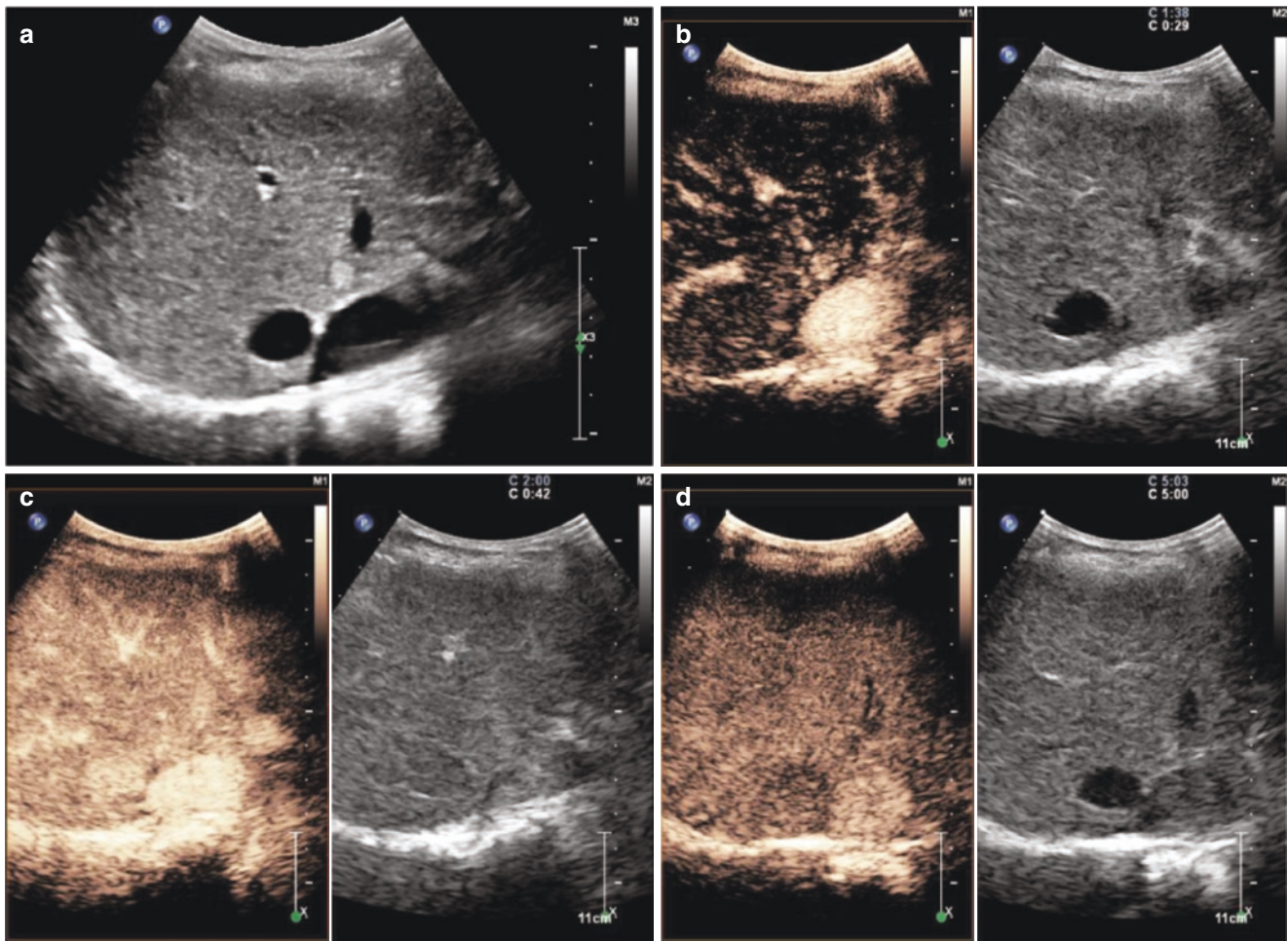
Fig. 4.7 A case of surgery and histopathologically proved hepatocellular carcinoma (HCC). B mode ultrasound image revealed a hyperechoic small (8 mm) solid focal liver lesion in right lobe of liver (**a**). After injection of contrast agents, the lesion showed heterogenous hyperenhancement during arterial phase (**b**). No wash-out could be detected during portal venous phase (**c**). The lesion was isoenhanced during the late phase (**d**)

no contrast uptake is seen in bland portal vein thrombosis inside the lumen of the portal vein. However, contrast enhancement of the thrombus indicates tumor thrombus. In the case of HCC invading the portal vein, the tumor thrombus typically shows arterial phase hyperenhancement during arterial phase and mild wash-out in the late phase.

In addition to major CEUS imaging features, ancillary features (AFs) are used to modify the likelihood that an observation is HCC [11]. Some similar phenomena described on CE-CT and CE-MRI can also be seen on CEUS, including pseudomasses, capsule vessels, and arterioportal shunts. The 2018 version of the LI-RADS guidelines provided new rules regarding the application of AFs. AFs should only be used if their presence is unequivocal; they should not be utilized if their presence is uncertain. Three CEUS AFs favor malignancy, among which, "definite growth" favors malignancy in general, nodule-in-nodule appearance (Figs. 4.16 and 4.17) and mosaic

appearance (Figs. 4.18 and 4.19) favor HCC in particular [11]. These Afs may be applied to upgrade the observation by one category to a maximum classification of LR-4. They cannot be used to upgrade the category to LR-5, and their absence should not be used to downgrade the LR category [11].

4.1.8 Small HCC

The diagnostic algorithm of the international societies identifies 1 cm size as the starting point for radiological diagnosis of HCC. However, the current APASL algorithm based on the dynamic pattern of contrast imaging suggests diagnosis of HCC independently on tumor size. The reported specificity and sensitivity of CEUS in the diagnosis of HCC ≤2 cm in a cirrhotic liver were 87% and 100%, respectively [12] (Figs. 4.20 and 4.21).

Table 4.2 Contrast enhanced ultrasound LI-RADS diagnostic categories

Category	Criteria
LR-1	Simple cyst, classic hemangioma, focal fatty change, or focal fatty sparing
LR-2	Nodule size <10 mm, no AP enhancement, no wash-out, no additional enhancement patterns OR LI-RADS 3 observation stable for ≥2 years
LR-3	Nodule size ≥10 mm, no AP enhancement, no wash-out, no additional enhancement patterns OR nodule size <10 mm, AP enhancement, no wash-out OR nodule size <20 mm, no AP hyperenhancement, and wash-out (≥60 s)
LR-4	Nodule size ≥10 mm, AP hyperenhancement, no wash-out OR nodule size <10 mm, AP hyperenhancement, and wash-out OR nodule size ≥20 mm, no AP hyperenhancement, and wash-out (≥60 s)
LR-5	Nodule size ≥10 mm, AP hyperenhancement, and wash-out
LR-M	Nodule of any size and wash-out (<60 s) OR marked wash-out within 2 min OR rim enhancement and wash-out
LR-NC	Not categorizable due to image degradation or omission
LR-TIV	Tumor within the portal vein, hepatic vein, or both

Arterial phase (AP) hyperenhancement is defined as diffuse enhancement with unequivocal nodule hypervascularity and no evidence of peripheral globular or rim-like enhancement. LI-RADS = Liver Imaging Reporting and Data System, LR-1 = definitely benign, LR-2 = probably benign, LR-3 = intermediate malignancy probability, LR-4 = probably hepatocellular carcinoma (HCC), LR-5 = definitely HCC, LR-NC = cannot be categorized due to image degradation, LR-TIV = tumor in vein, and LR-M = probably or definitely malignant but not HCC specific

4.1.9 Treatment Response Follow Up

4.1.9.1 Ablation Therapy

- In ablative therapy of liver tumors, the clinical application of CEUS including selection of patient, intraprocedural real-time guidance, and posttreatment immediate assessment. CEUS makes it possible to detect residual tumor vascularity immediately after ablation, to make additional treatments, and to increase ablation efficacy finally.
- The reactive inflammatory changes as peripheral hyperemia of the treated lesion may show rim hyperenhancement, which may last for 2–3 weeks after local ablation therapy. It is always necessary to distinguish the reactive hyperemia from residual or recurrent tumor. Comparison with pretreatment CEUS images is helpful in these patients (Fig. 4.22).
- CEUS is sensitive and accurate in detecting residual or recurrent tumors after ablation. The residual tumor demonstrates the typical hyperenhancement pattern as HCC, which is characterized by arterial phase hyperenhancement with late mild wash-out (Fig. 4.23).

- CEUS can be used to characterize the recurrence after treatment. Any new nodular demonstrating arterial hyperenhancement during CEUS, regardless of wash-out or not, is highly suspicious for HCC recurrence (Fig. 4.24).
- In addition, during the regular surveillance after ablative therapy, CEUS could be used to scan the entire liver for detection and evaluation of new nodules. During follow-up procedure, arterial phase hyperenhancement is the diagnostic characteristic of recurrence HCC on CEUS.

4.1.9.2 Transarterial Chemoembolization

- A significant proportion of HCC patients are diagnosed at intermediate or late stage. For those patients, transarterial chemoembolization (TACE) is the most widely used first-line therapy.
- The accurate evaluation of local tumor responses to the first TACE session has an important clinical impact on the overall clinical management of HCC patients.
- Currently, serological biomarkers and magnetic resonance imaging (MRI) are main methods for the prediction of HCC responses to TACE.
- CEUS has distinguished advantages in assessing treatment response after TACE. It could assess treatment response as early as 1 day after the TACE procedure. CEUS also allows assessment of microvascular perfusion changes of residual tumor (Fig. 4.25).
- CEUS has been proved to have equivalent or superior efficacy for assessing the treatment response of HCC to TACE. It makes short-time follow-up possible (Figs. 4.26 and 4.27).

4.1.9.3 Targeted Therapy

- In 2006, sorafenib (Nexavar®, Bayer AG, Germany), a multikinase inhibitor, was approved for the treatment of patients with advanced HCC. Two major angiogenesis pathways inhibited by Sorafenib were vascular endothelial growth factor receptor 2 (VEGFR2) and platelet-derived growth factor receptor (PDGFR).
- Sorafenib has been regarded as the first-line treatment for patients with advanced HCC.
- The Response Evaluation Criteria in Cancer of the Liver (RECICL) criteria to address therapeutic response in liver malignancies also puts an emphasis on the detection and measurement of necrosis. However, all of these parameters can only partially reflect the early tumor response to treatment.
- It is possible to make specific and precise evaluations for early prediction of tumor response in HCC patients by CEUS. Also, CEUS could be an excellent tool for selecting potential patients for targeted therapy.
- The unique advantages of CEUS in evaluating antitumor treatment including low cost, rapid, easy to repeat, no radiation or side effects. It is well accepted by patients.
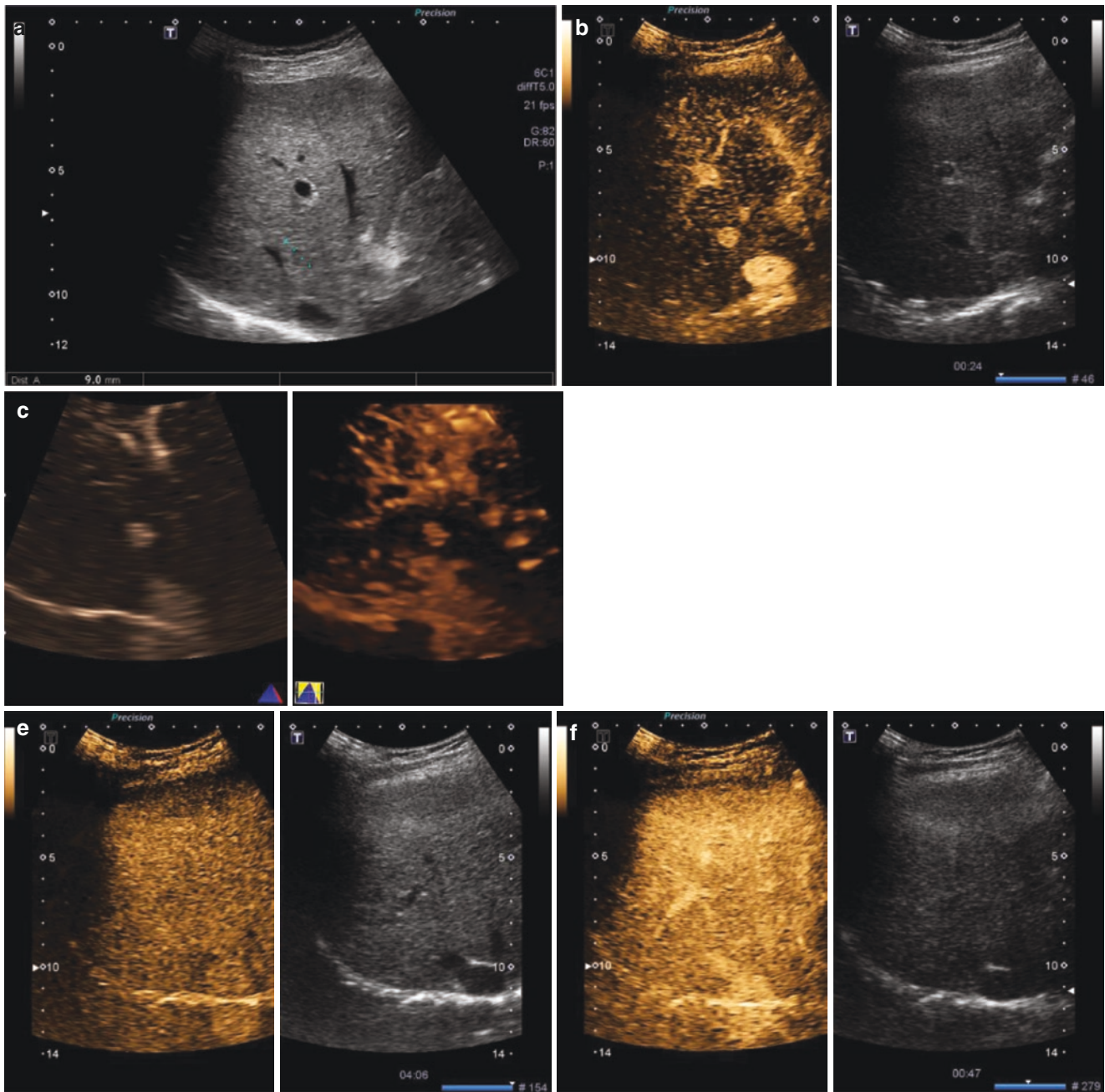
Fig. 4.8 Images of contrast enhanced ultrasound (CEUS) LR-3, indeterminate malignancy probability, in a 39-year-old man with hepatitis B-related cirrhosis. B mode ultrasound image showed a 9 mm diameter hyperechoic nodule located in right lobe of liver (**a**). The lesion showed hyperenhancement during arterial phase both in 2D CEUS (**b**) and in 3D CEUS (**c**). The lesion was isoenhanced during portal venous phase (**d**) and showed wash-out during late phase (**e**). Subsequent surgery and histopathological results revealed a hepatocellular carcinoma (HCC)

- Time intensity curves and quantitative evaluation of dynamic CEUS parameters may provide additional information in evaluations of the treatment effects of anti-angiogenesis treatment. TTP may be an early and sensitive parameter to evaluate response to sorafenib treatment [13].

- Three-dimensional CEUS (3D-CEUS) has recently been successfully used to make accurate and clear depiction of the tumor microvascular perfusion.
- A correlation has been proved to exist between 3D-CEUS parameters and pathological changes in HCC after treatment.
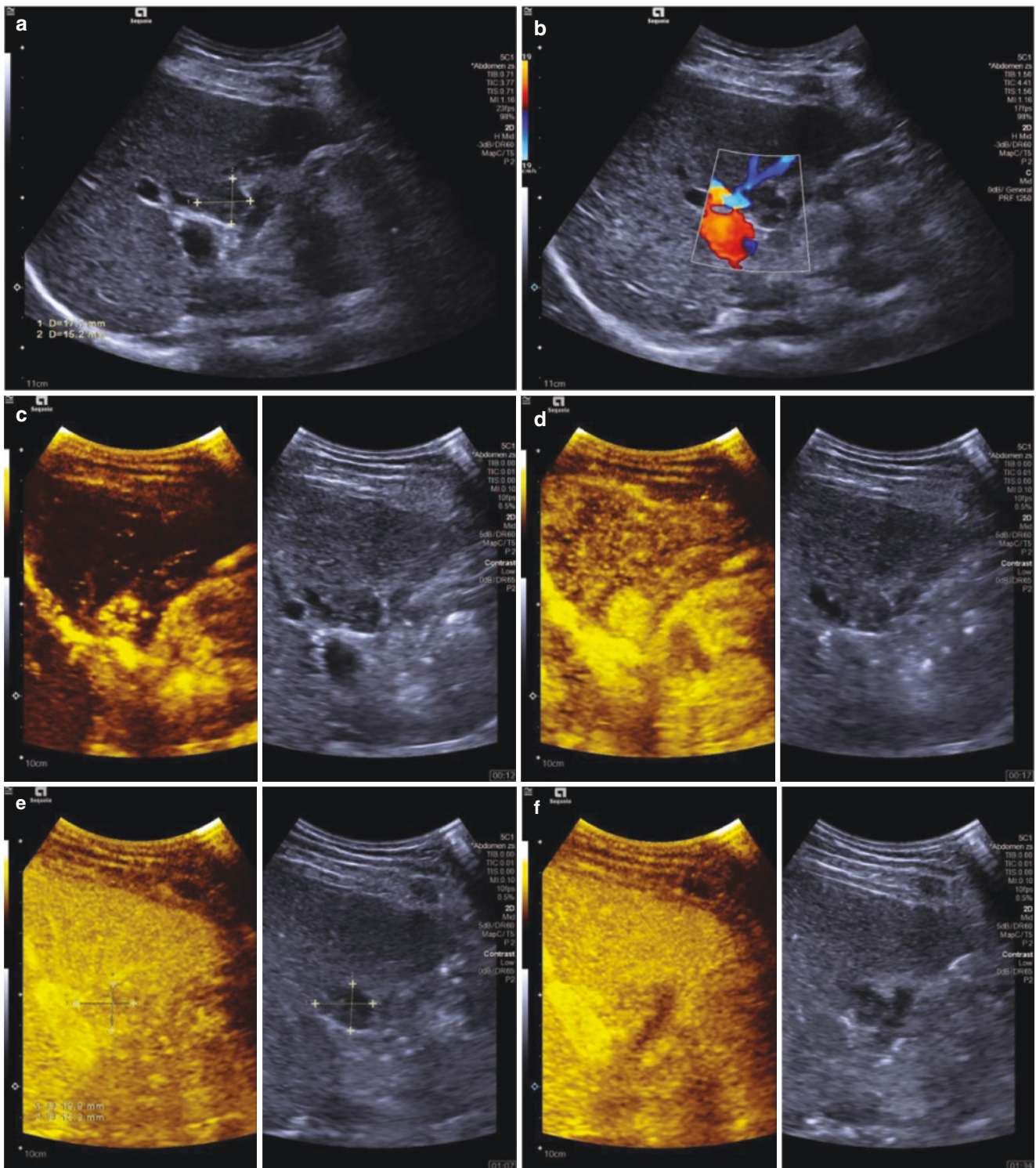
Fig. 4.9 Images of contrast enhanced ultrasound (CEUS) LR-4, probably hepatocellular carcinoma (HCC), in a 29-year-old man with hepatitis B-related cirrhosis. B mode ultrasound image showed a 17-mm diameter hyperechoic nodule located in right lobe of liver (**a**). No color flow signal could be detected inside the lesion (**b**). The lesion showed nodular hyperenhancement during arterial phase in comparison with the adjacent liver (**c**) and showed complete and quick hyperenhancement in 17 s after injection of contrast agents (**d**). Mild wash-out was observed during late portal venous (**e**) and late phase (**f**). Subsequent surgery and histopathological results showed the lesion was a well-differentiated stage II HCC
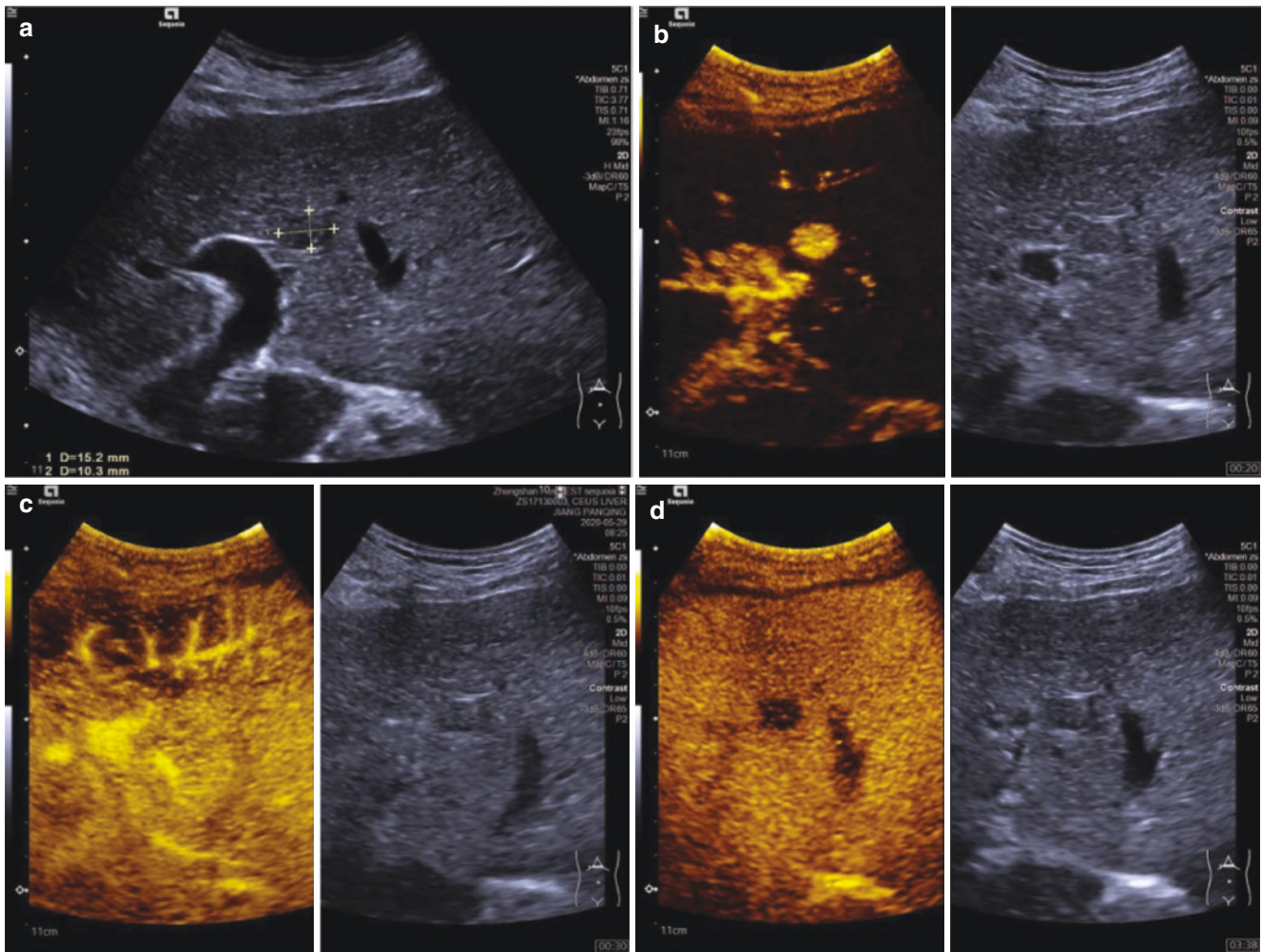
Fig. 4.10 Images of contrast enhanced ultrasound (CEUS) LR-5, definitely hepatocellular carcinoma (HCC), in a 45-year-old man with hepatitis B-related cirrhosis. Surveillance US image shows a 15 mm diameter hypoechoic nodule (**a**). The lesion showed hyperenhancement during arterial phase compared with the adjacent liver (**b**). CEUS image obtained 30 s after microbubble injection showed unequivocal slight contrast wash-out (**c**). Obvious wash-out was observed during late phase (**d**). Subsequent surgery and histopathological results showed the lesion was a stage III HCC

4.2   Intrahepatic Cholangiocarcinoma

Pei-Li Fan, Feng Mao, and Wen-Ping Wang

4.2.1   Definitions

Intrahepatic cholangiocarcinoma (ICC) is the second most common primary hepatic malignant tumor after hepatocellular carcinoma (HCC). ICC is biliary epithelial differentiation and occurs in intrahepatic biliary tree, from the segmental ducts to the smallest bile ducts. ICC could be classified into three types: mass-forming type, intraductal-growth type, and periductal infiltrating type. Mass-forming type is the most common type of ICC [14, 15].

4.2.2   Imaging

4.2.2.1 Conventional Ultrasound Findings
Mass-forming type
The mass-forming type of ICC is an expansile mass lesion with ill-defined border in the hepatic parenchyma (Fig. 4.28).
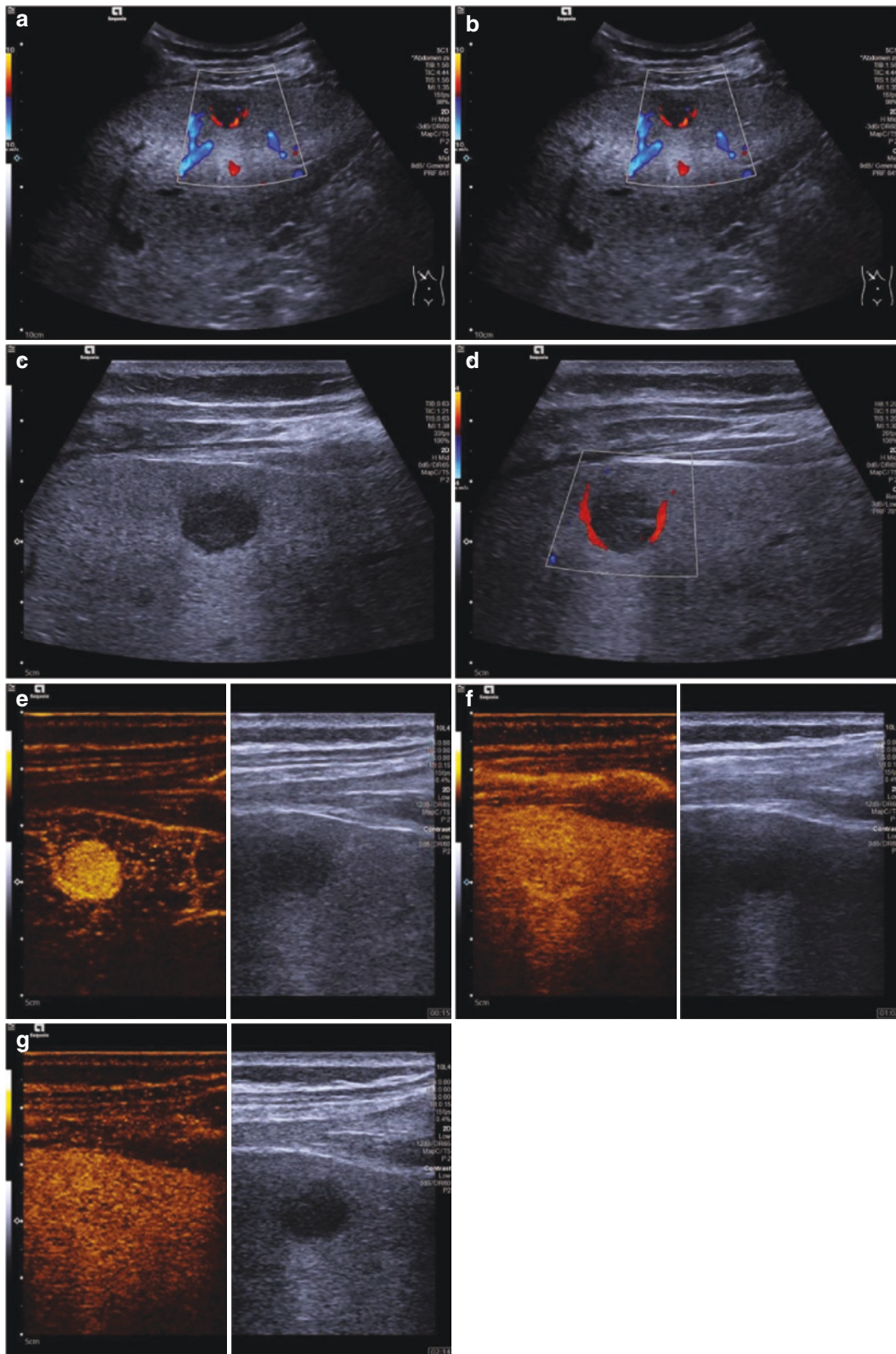
Fig. 4.11 Images of contrast enhanced ultrasound (CEUS) LR-5, definitely hepatocellular carcinoma (HCC), in a 49-year-old man with hepatitis B related cirrhosis. B mode ultrasound image showed a 13 mm diameter small hypoechoic nodule in the superficial area of right lobe of liver (**a**). Color flow signals could be detected in the surrounding area of the lesion (**b**). While using the high-frequency linear transducer, posterior hyperechoic could be observed on B mode ultrasound (**c**) with similar color flow signals (**d**). The lesion showed hyperenhancement during arterial phase compared with the adjacent liver (**e**). CEUS image obtained 60 s after microbubble injection showed isoenhancement. Unequivocal slight contrast wash-out could be observed during late phase (**f**). Subsequent surgery and histopathological results showed the lesion was a stage III HCC
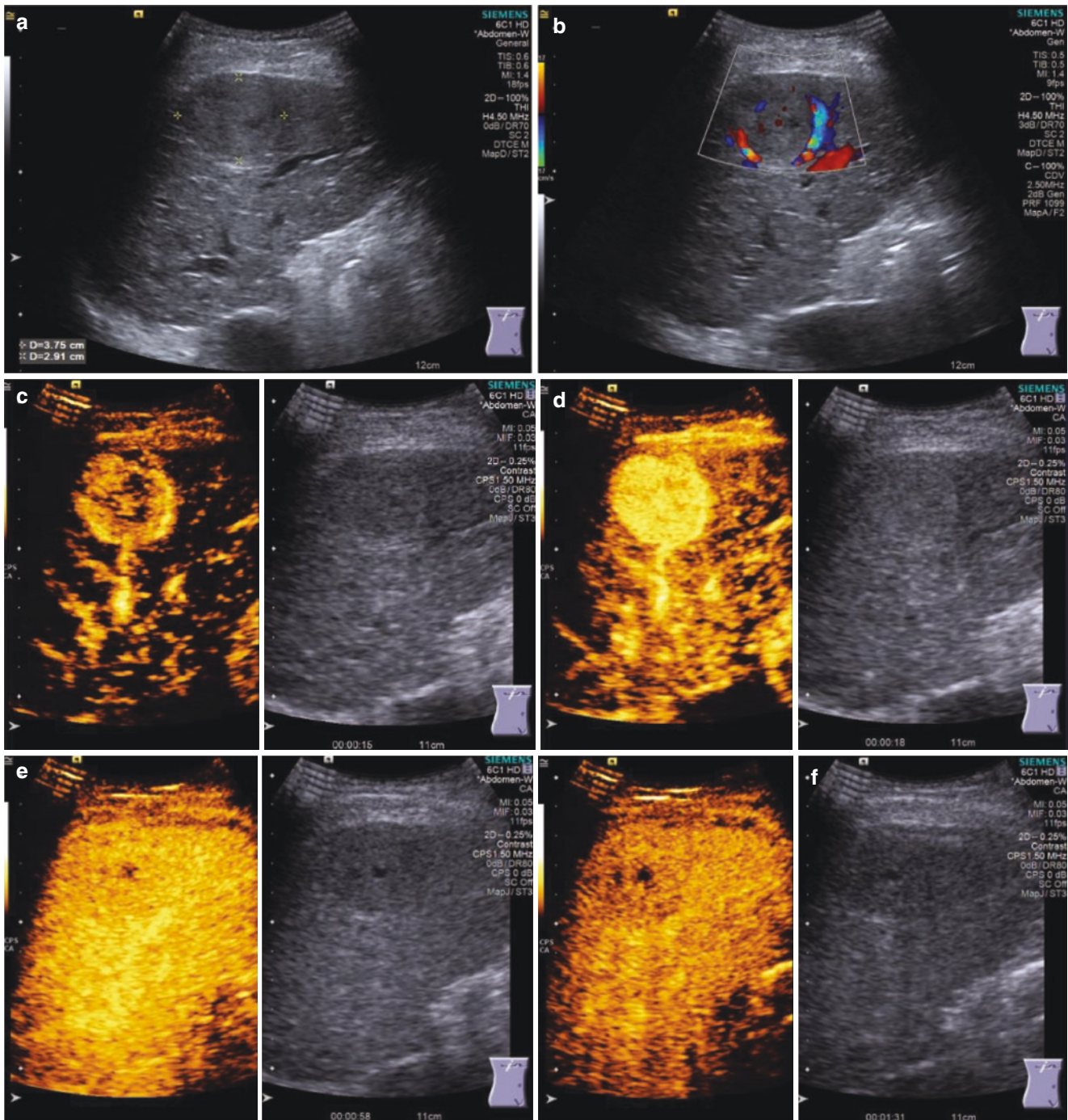
Fig. 4.12 Images of contrast enhanced ultrasound (CEUS) LR-5, definitely hepatocellular carcinoma (HCC), in a 54-year-old man with hepatitis B-related cirrhosis. B mode ultrasound image showed a 37-mm diameter hypoechoic nodule in the right lobe of liver (**a**). Color flow signals could be detected both inside the lesion and in the surrounding area of the lesion (**b**). The lesion showed heterogenously hyperenhancement during arterial phase compared with the adjacent liver (**c**) and reached peak enhancement in 18 s after injection of contrast agents (**d**). Unequivocal slight contrast wash-out could be observed during portal venous (**e**) and late phase (**f**). Subsequent surgery and histopathological results showed the lesion was a stage III HCC
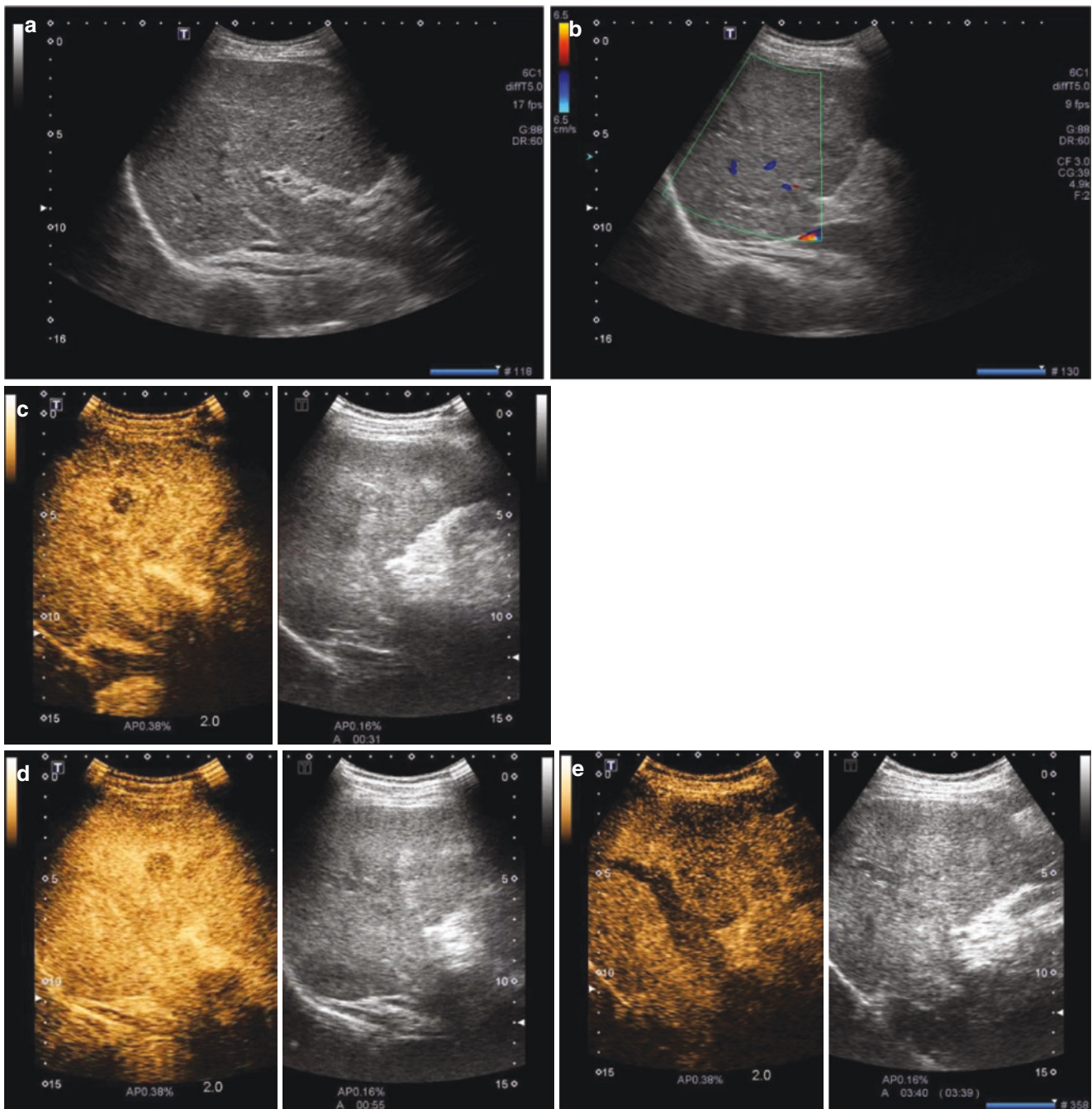
Fig. 4.13 Images of contrast enhanced ultrasound (CEUS) LR-TIV, hepatocellular carcinoma (HCC) with tumor thrombus, in a 49-year-old man with hepatitis B-related cirrhosis. B mode ultrasound image showed a large hypoechoic nodule in the right lobe of liver, hypoechoic tumor thrombus was suspected inside the right branch of portal vein (**a**). No color flow signals could be detected inside the portal vein (**b**). After injection of contrast agents, real-time direct visualization of arterial phase hyperenhancement in the tumor thrombus could be observed (**c**). Hypoenhancement of thrombus could be observed during portal venous (**d**) and late phase (**e**)
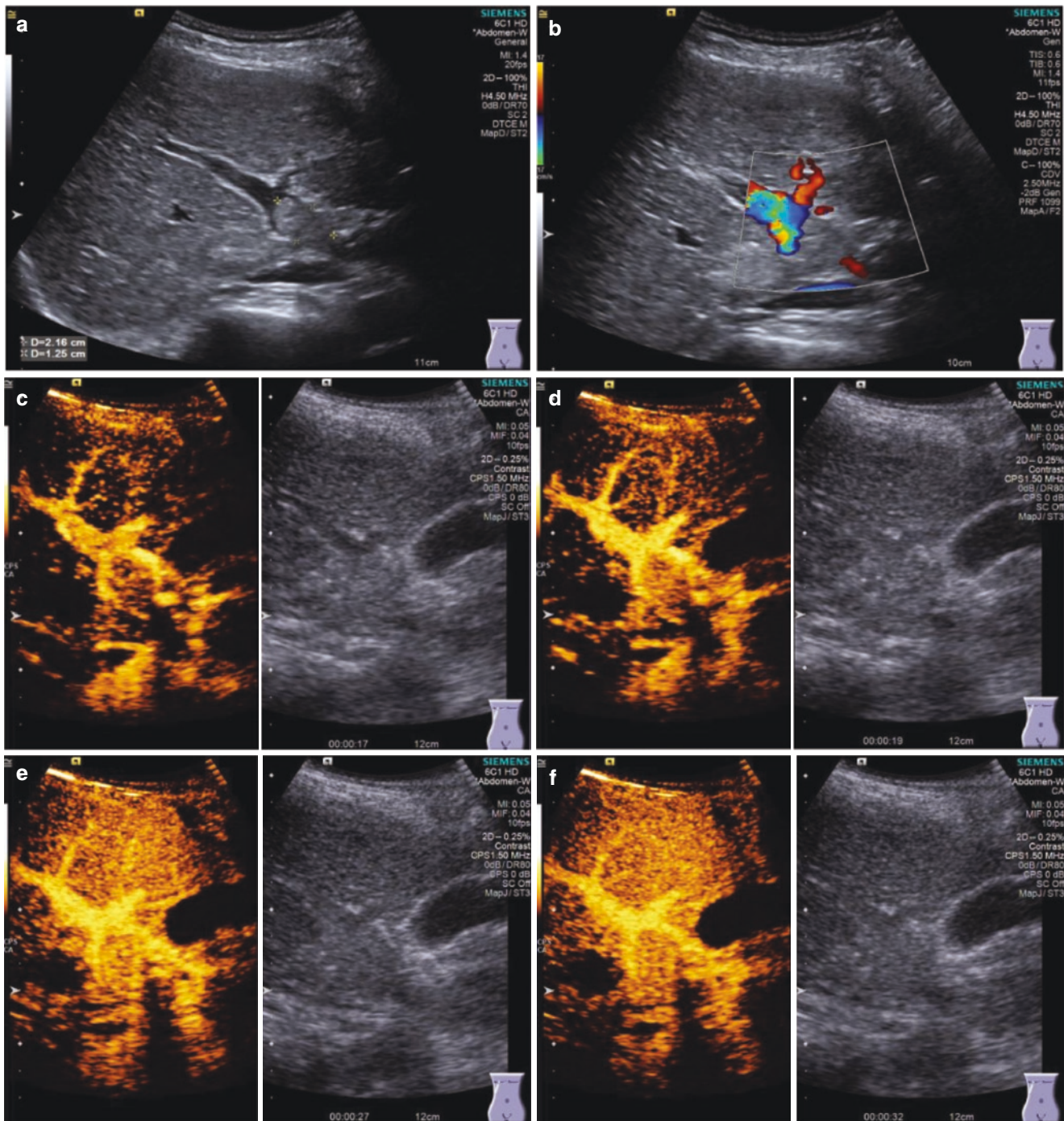
Fig. 4.14 Images of contrast enhanced ultrasound (CEUS) LR-TIV, hepatocellular carcinoma (HCC) with focal tumor thrombus, in a 79-year-old man with hepatitis B-related cirrhosis. B mode ultrasound image showed a 21-mm focal hypoechoic tumor thrombus in the right branch of portal vein (**a**). No color flow signals could be detected inside the lesion (**b**). After injection of contrast agents, real-time visualization of arterial phase hyperenhancement in the tumor thrombus could be observed in 17 s (**c**), 19 s (**d**), 27 s (**e**), and 32 s (**f**) during arterial phase
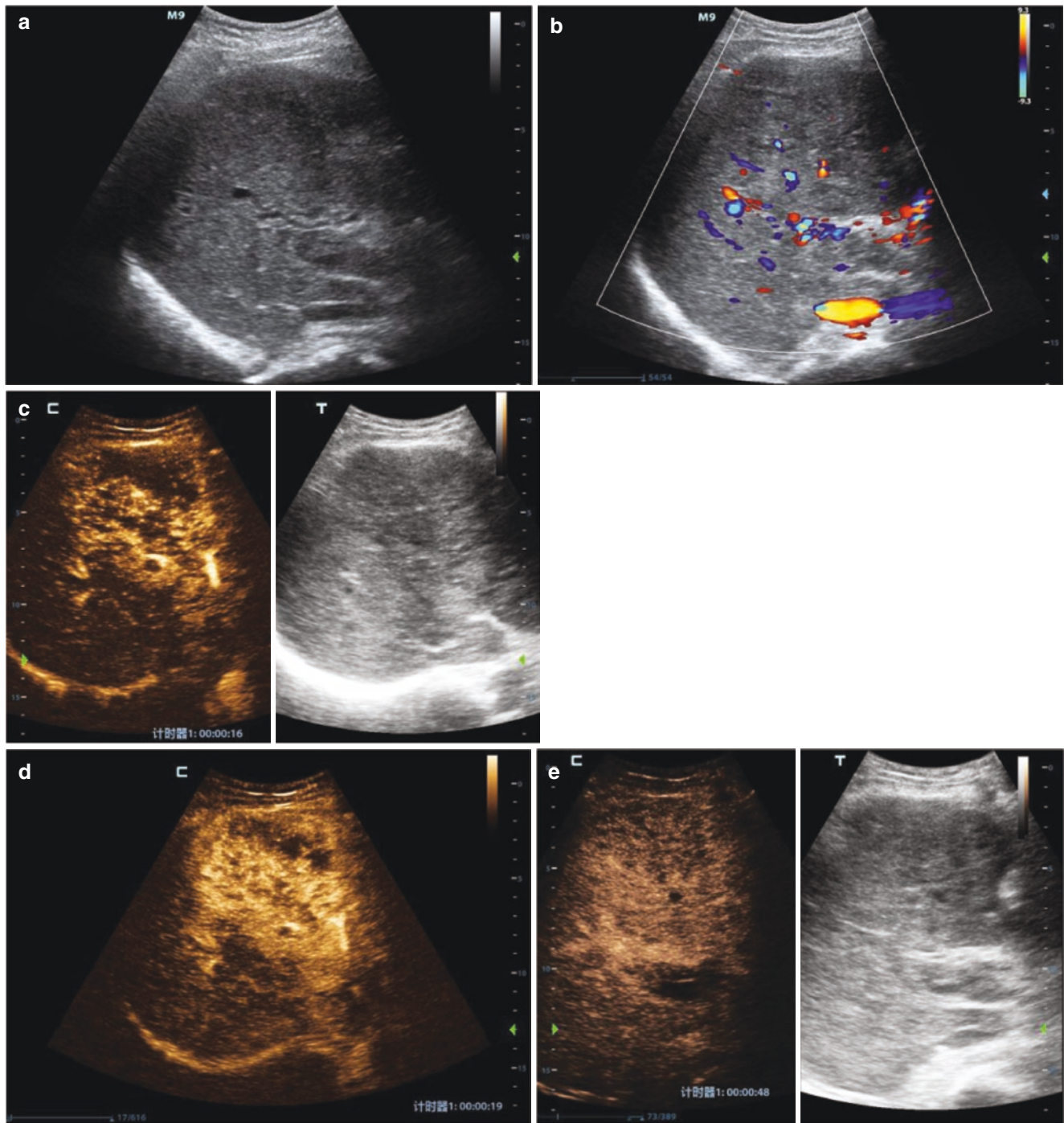
Fig. 4.15 Hepatocellular carcinoma (HCC) with thrombus, in a 65-year-old man with hepatitis B-related cirrhosis. B mode ultrasound image showed a large hypoechoic nodule in the right lobe of liver, hypoechoic tumor thrombus was suspected inside the right branch of portal vein (**a**). No color flow signals could be detected inside the portal vein (**b**). After injection of contrast agents, a persistently nonenhancing bland thrombus could be observed during arterial phase (**c**), portal venous phase (**d**), and late phase (**e**)
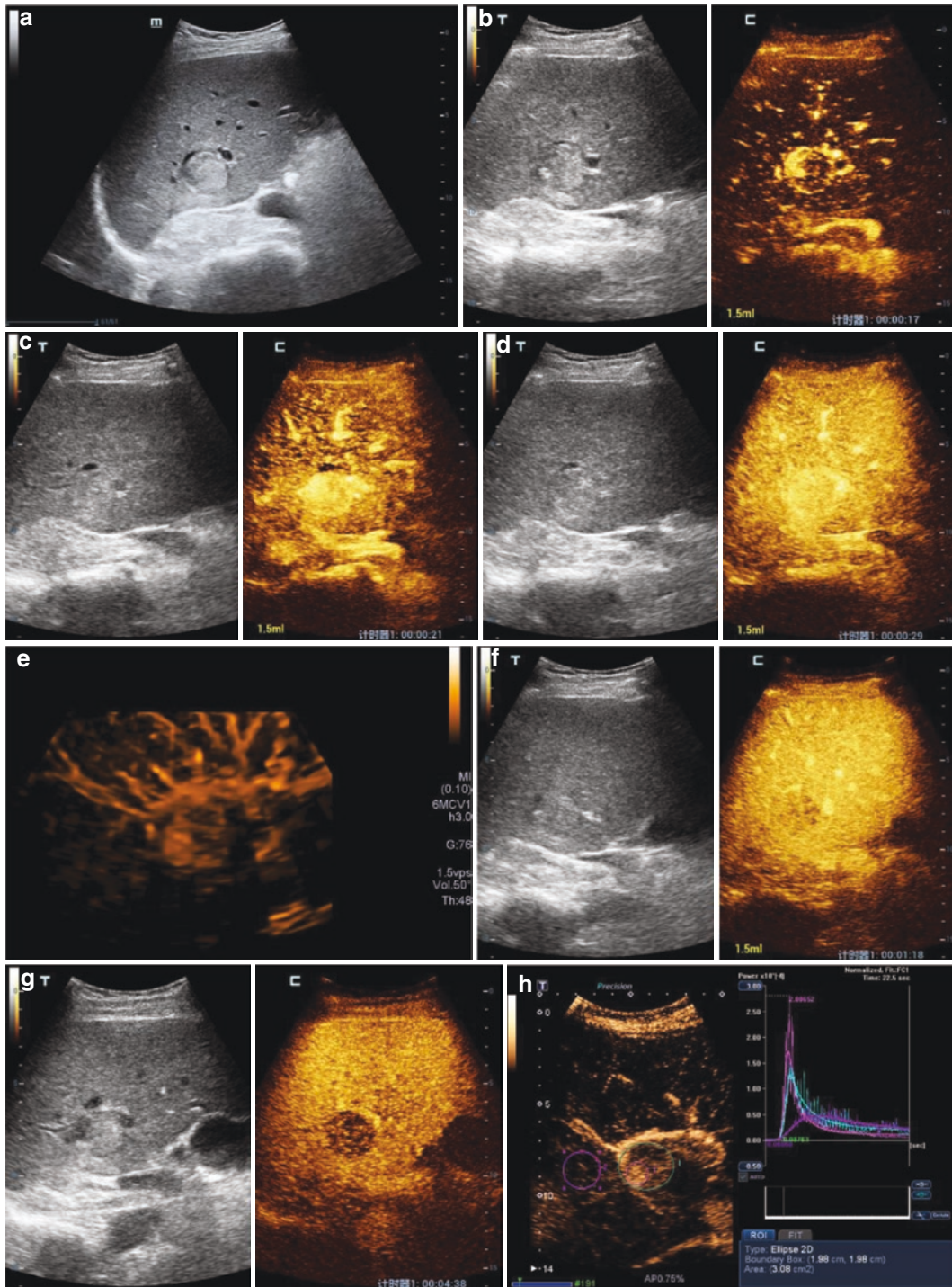
Fig. 4.16 Nodule-in-nodule appearance. The patient is a 62-year-old man with hepatitis B cirrhosis and an LR-5 lesion on B mode ultrasound (**a**). Contrast enhanced ultrasound showed a 24-mm nodule with a nodule-in-nodule appearance in the arterial phase (arrows) (**b–e**). The entire nodule displays hyperenhancement in the arterial phase, while an extremely hyperenhanced nodular could be detected inside the lesion (arrows) (**b–e**). On portal venous phase at 1 min (**f**) and on late phase after 4 min (**g**), the lesion showed mild wash-out. Dynamic CEUS and time intensity curves analysis also indicate different wash-in and wash-out mode between the nodule and the whole lesion (**h**). With regard to surgery and histopathological appearance, this is typical of a poor-differentiated hepatocellular carcinoma (HCC) nodular developed in a well-differentiated HCC lesion (**i–k**)
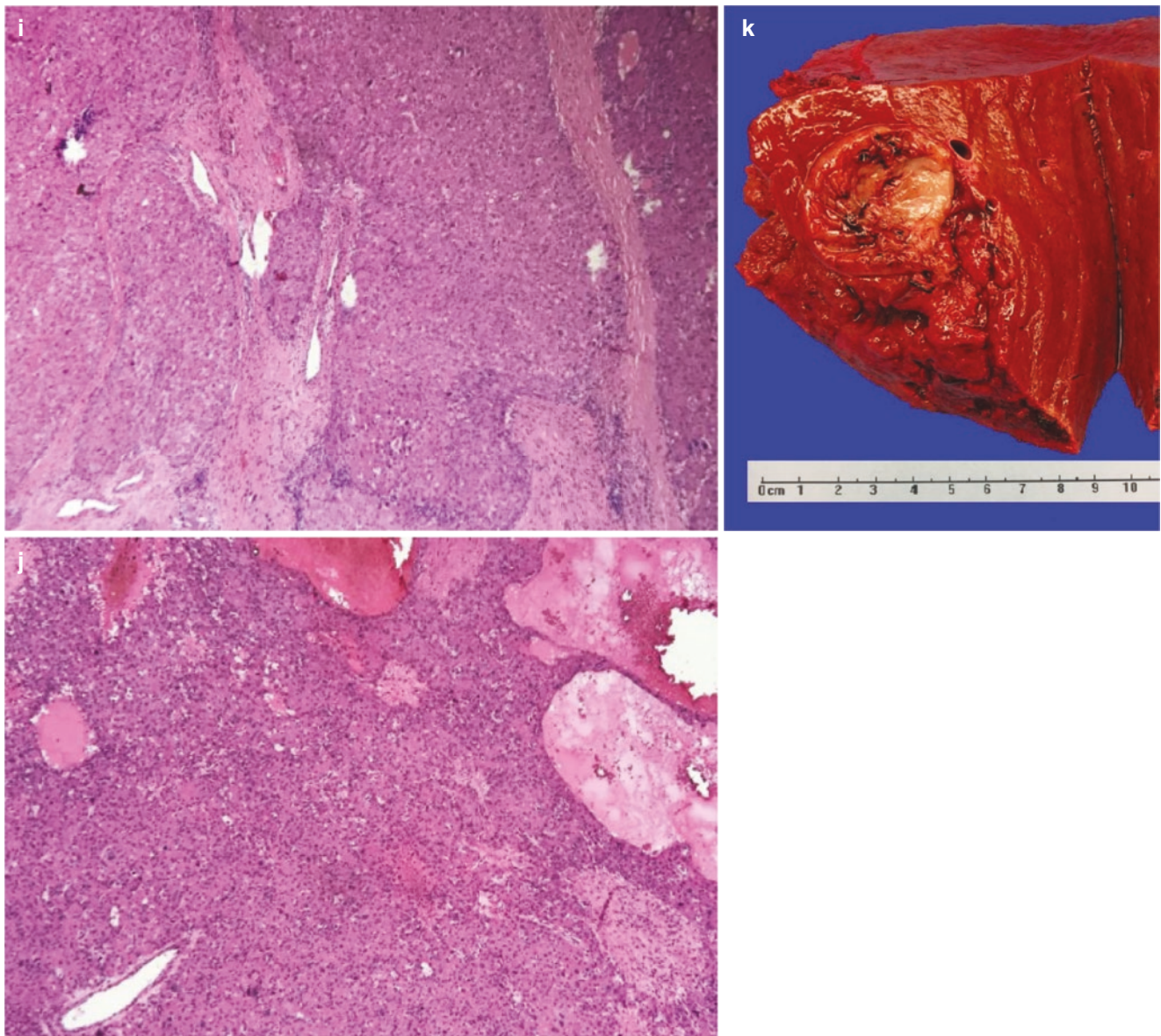
Fig. 4.16 (continued)

Intraductal-growth type

The intraductal-growth type of ICC is confined within the dilated part of an intrahepatic large bile duct. Tumor commonly shows a polypoid or papillary mural nodule within the dilated bile duct lumen (Figs. 4.29 and 4.30). Sometimes mild extension beyond bile duct walls can be seen. Ultrasound can identify marked, localized dilatation of affected ducts.

Periductal-infiltrating type

The periductal-infiltrating type of ICC develops along the intrahepatic bile ducts and appears as a solid mass extending along portal tracts. As a result of tumoral obstruction, the upstream ducts occur secondary dilatation (Fig. 4.31). The anatomical location of the involved ducts can be evaluated by caliber changes or ducts rigidity. This type is hard to be detected by ultrasound before surgery.

These three types may overlap in the same case. Advanced ICC often has a mixed pattern of growth with central necrosis and/or intrahepatic metastases. Ultrasound can easily detect secondary dilated bile ducts around the tumor [16–18].

4.2.2.2 Contrast Enhanced Ultrasound Findings
Mass-forming type

ICCs with mass-forming type have a variety of patterns in the arterial phase on contrast enhanced ultrasound (CEUS). Peripheral rim-like hyperenhancement in the arterial phase is the typical pattern (Fig. 4.32) [19]. This typical pattern could
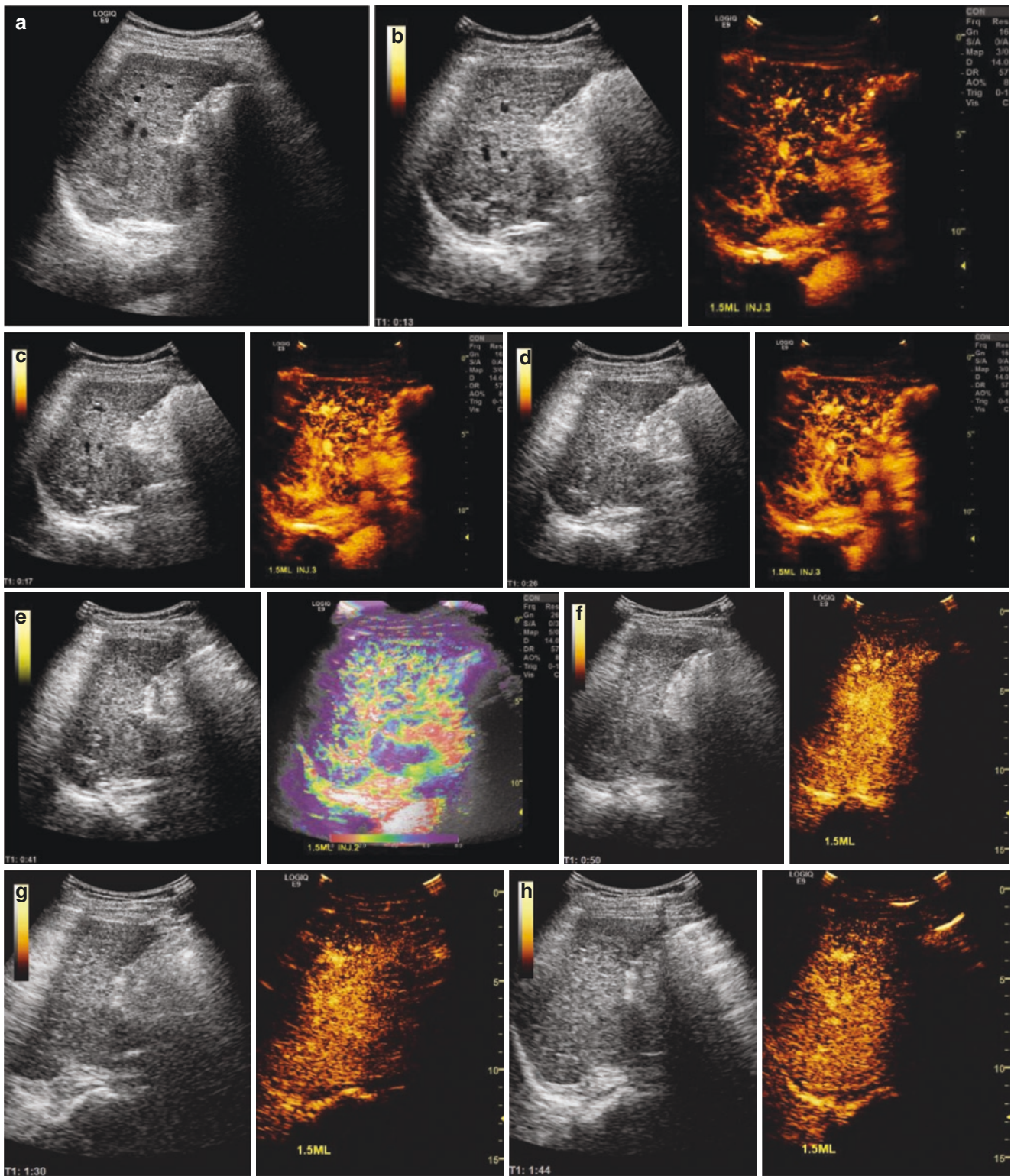
Fig. 4.17 Nodule-in-nodule appearance. The patient is a 47-year-old man with hepatitis B cirrhosis and an LR-4 lesion on B mode ultrasound (**a**). Contrast-enhanced ultrasound showed a 32-mm nodule with a nodule-in-nodule appearance in the arterial phase (arrows) (**b**–**e**). The entire nodule displays hypoenhancement in the arterial phase, while a hyperenhanced nodular could be detected inside the lesion (arrows) (**b**–**e**). The whole lesion showed isoenhancement both on portal venous phase (**f**) and on late phase (**g**, **h**). With regard to surgery and histopathological results, this is typical of a well-differentiated hepatocellular carcinoma (stage II) focus developed in a dysplastic nodule (**i**–**m**)
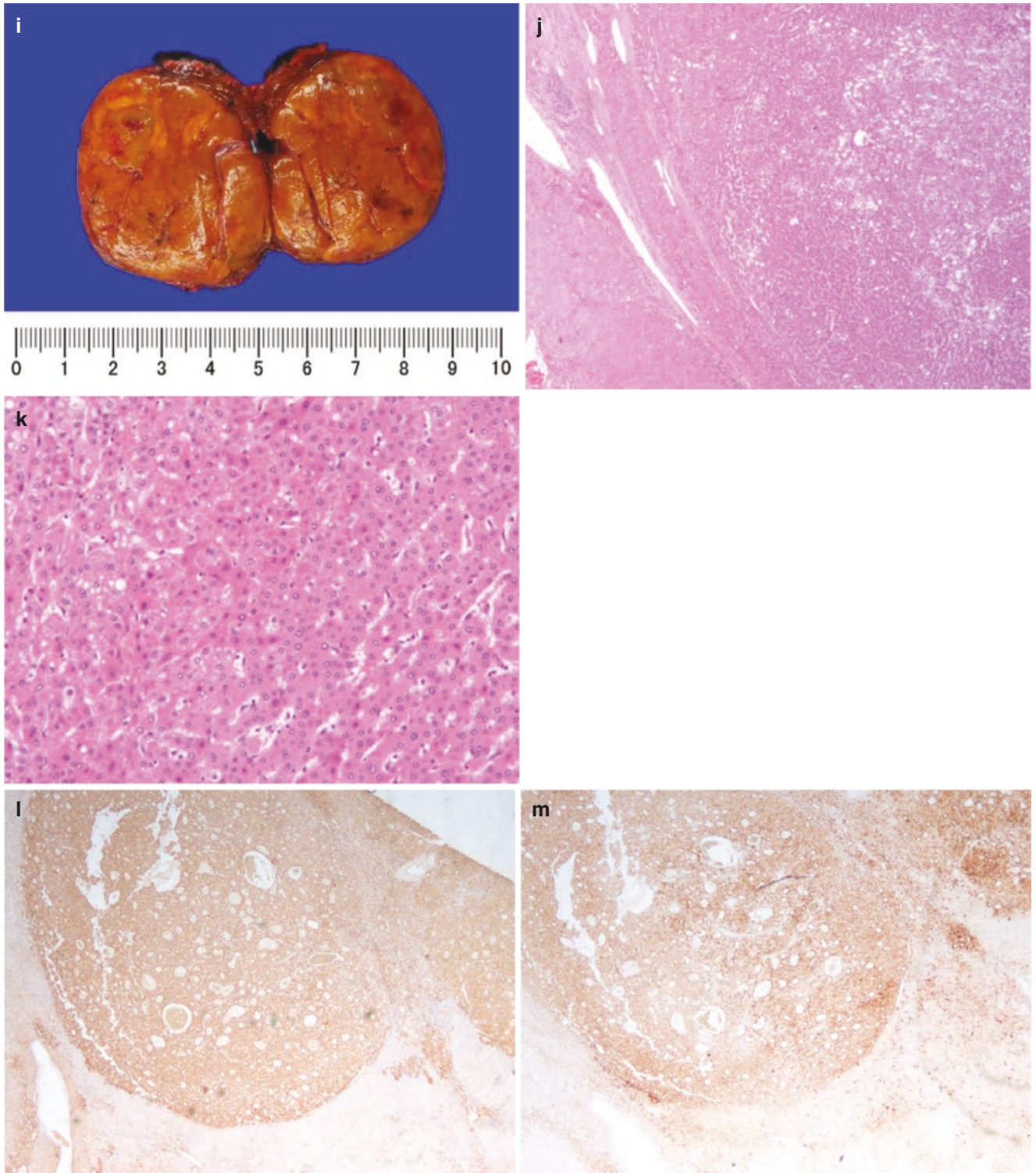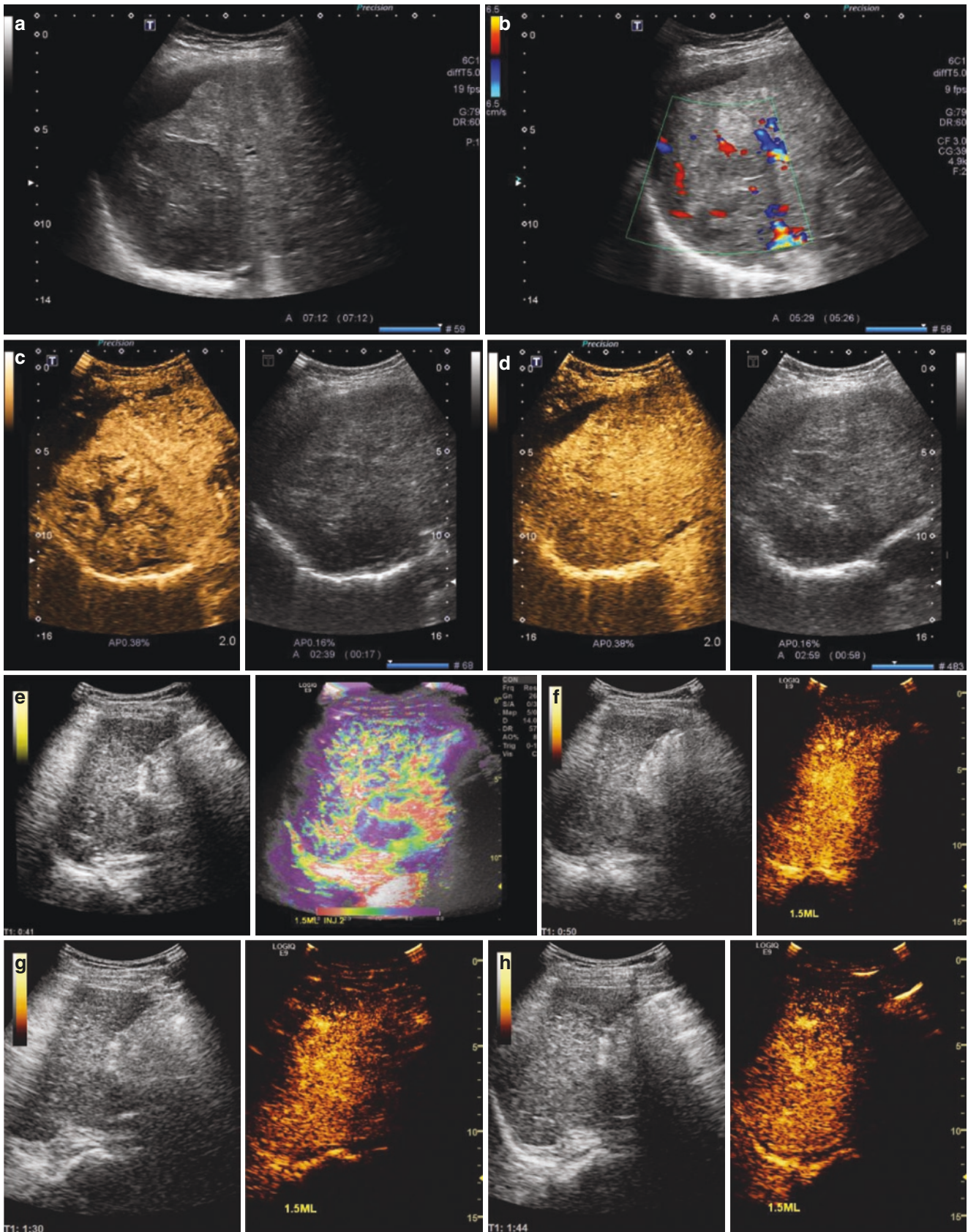
Fig. 4.17 (continued)

Fig. 4.18 Mosaic appearance. The patient is a 63-year-old man with hepatitis B virus cirrhosis and hepatocellular carcinoma (**a**). Color flow signals could be detected inside the lesion (**b**). After injection of contrast agents, heterogeneous enhancement could be detected both in arterial phase (**c**) and in portal venous phase (**d**)
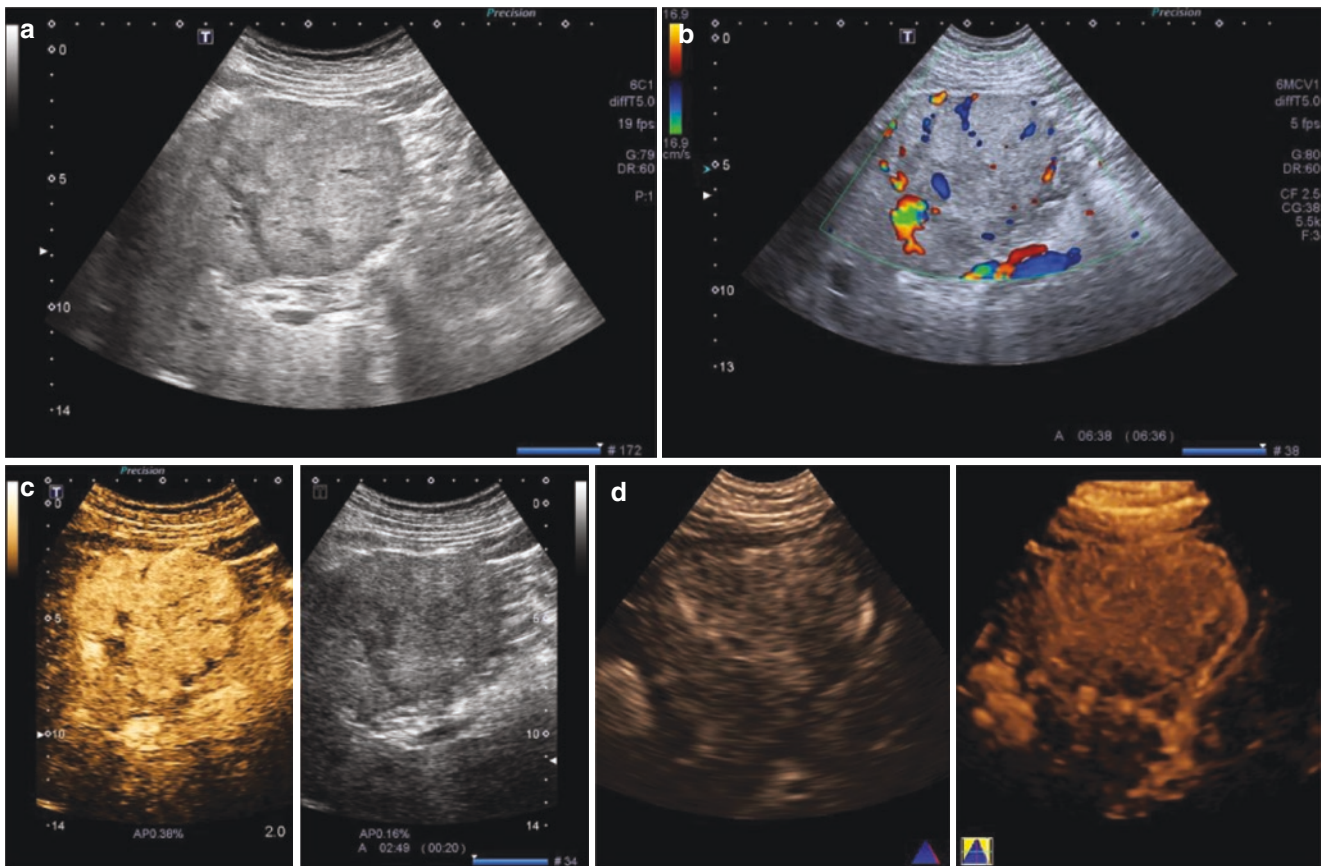
Fig. 4.19 Mosaic appearance. The patient is a 41-year-old woman with hepatitis B virus cirrhosis and hepatocellular carcinoma. A heterogenous 8.5-cm LR-5 hypoechoic lesion could be detected on B mode ultrasound (**a**). Color flow signals could be detected inside the lesion (**b**). During arterial phase, the lesion showed heterogeneous hyperenhancement both on two-dimensional contrast enhanced ultrasound (CEUS) (**c**) and three-dimensional CEUS (**d**)

be observed in 38–69% of ICCs. The peripheral hyperenhancement areas always indicate abundant tumor cells and the central areas correspond to fibrotic stroma at pathological examination. The other enhancement patterns are heterogeneously branched hyperenhancement (Fig. 4.28), hyperenhancement with vague boundary (Fig. 4.33), and heterogeneous hypoenhancement (Fig. 4.34). In patients with cirrhosis or small tumor size, the wash-in patterns of ICC on CEUS could be similar to those of HCC, which manifest homogeneous and heterogeneous hyperenhancement. Recent studies further revealed that wash-out of ICC was much earlier (<60 s) than that of HCC, and wash-out degree was more marked in ICC than that in HCC [20–24].

Intraductal-growth type
ICCs with intraductal-growth type often show that the intraductal tumor manifests slightly hyperenhancement in the arterial phase and gradually enhancement, followed by portal venous/late phase wash-out (Figs. 4.29 and 4.30).

Periductal-infiltrating type
ICCs with periductal-infiltrating types are rare. It is hard to detect tumors with this type before surgery. Fibrosis is more commonly found in this type, therefore this type often shows slightly hyperenhancement or isoenhancement in the arterial phase followed by early wash-out (Fig. 4.31).

4.2.2.3 CT Findings
ICCs usually manifest to be hypodense hepatic masses with irregular margins on unenhanced CT. On arterial phase of dynamic enhanced CT, ICCs usually show peripheral enhancement, and the center of the tumor (with few cells and abundant stroma) remains poorly enhanced. The center of the tumor gradually enhances on late phase (delayed
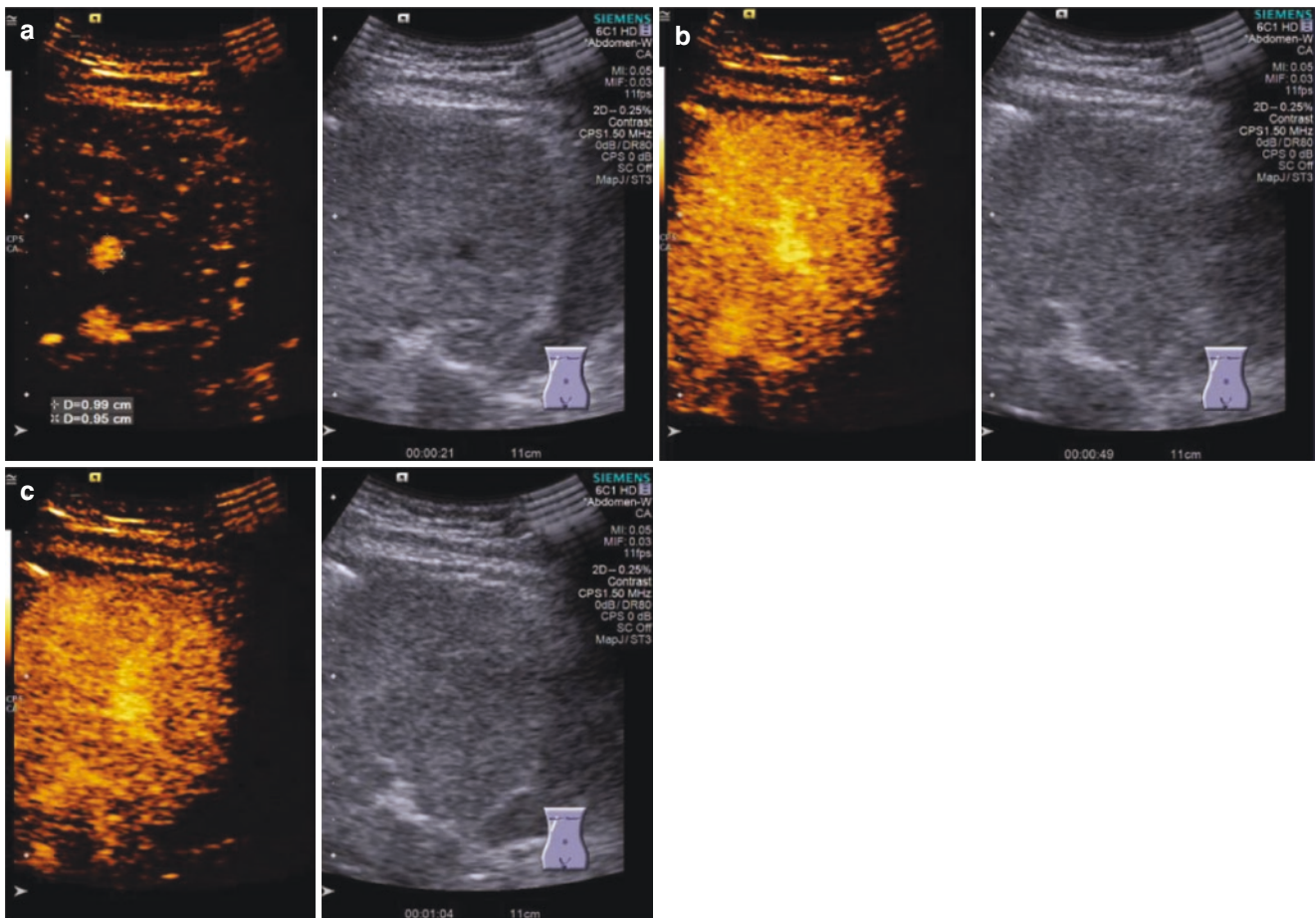
Fig. 4.20 Images of contrast enhanced ultrasound (CEUS) LR-4, probably hepatocellular carcinoma (HCC), in a 57-year-old man with hepatitis B-related cirrhosis. B mode ultrasound image showed a 9-mm diameter hyperechoic nodule located in right lobe of liver. The lesion showed hyperenhancement during arterial phase (**a**) in comparison with the adjacent liver. No wash-out was observed during portal venous (**b**) or late phase (**c**). Subsequent biopsy was positive for well-differentiated HCC

enhancement). This progressive enhancement differs ICC from HCC. HCC shows arterial phase enhancement followed by late phase wash-out. This feature may reflect that fibrosis is late enhancement but retains the contrast agent [14, 25].

4.2.2.4 MRI Findings
On MRI, ICC typically appears hypointense on T1WI and hyperintense on T2WI. T2WI may show central hypointensity due to fibrosis. Dynamic enhanced MRI shows arterial phase peripheral enhancement followed by progressive and centripetal filling in Fig. 4.32. Pooling of contrast agent in the delayed phase indicates fibrosis and may suggest ICC. MRI with cholangiopancreatography (MRCP) is helpful in visualizing the ductal system and in determining the anatomic extent of tumor [14, 25].

4.2.2.5 Other Imaging Findings
Fluorodeoxyglucose positron emission tomography (FDG-PET) can detect mass-forming type of ICC with high sensitivity, but PET is less useful for periductal infiltrating type. When CEUS, CT, or MRI has already been performed, PET-CT for diagnosis of ICC is controversial. The additional utility of PET is also questioned when extrahepatic suspicious lesion on CT or MRI is absent. The benefit of PET for staging ICC is not clear and thus PET should be used selectively [14, 25].

4.2.2.6 Best Imaging Protocol Advices
- Ultrasound, CT, MRI/MRCP, and PET are the most common imaging methods to diagnose and stage ICC.
- Ultrasound is the first imaging method for patients with abdominal pain or obstructive jaundice.
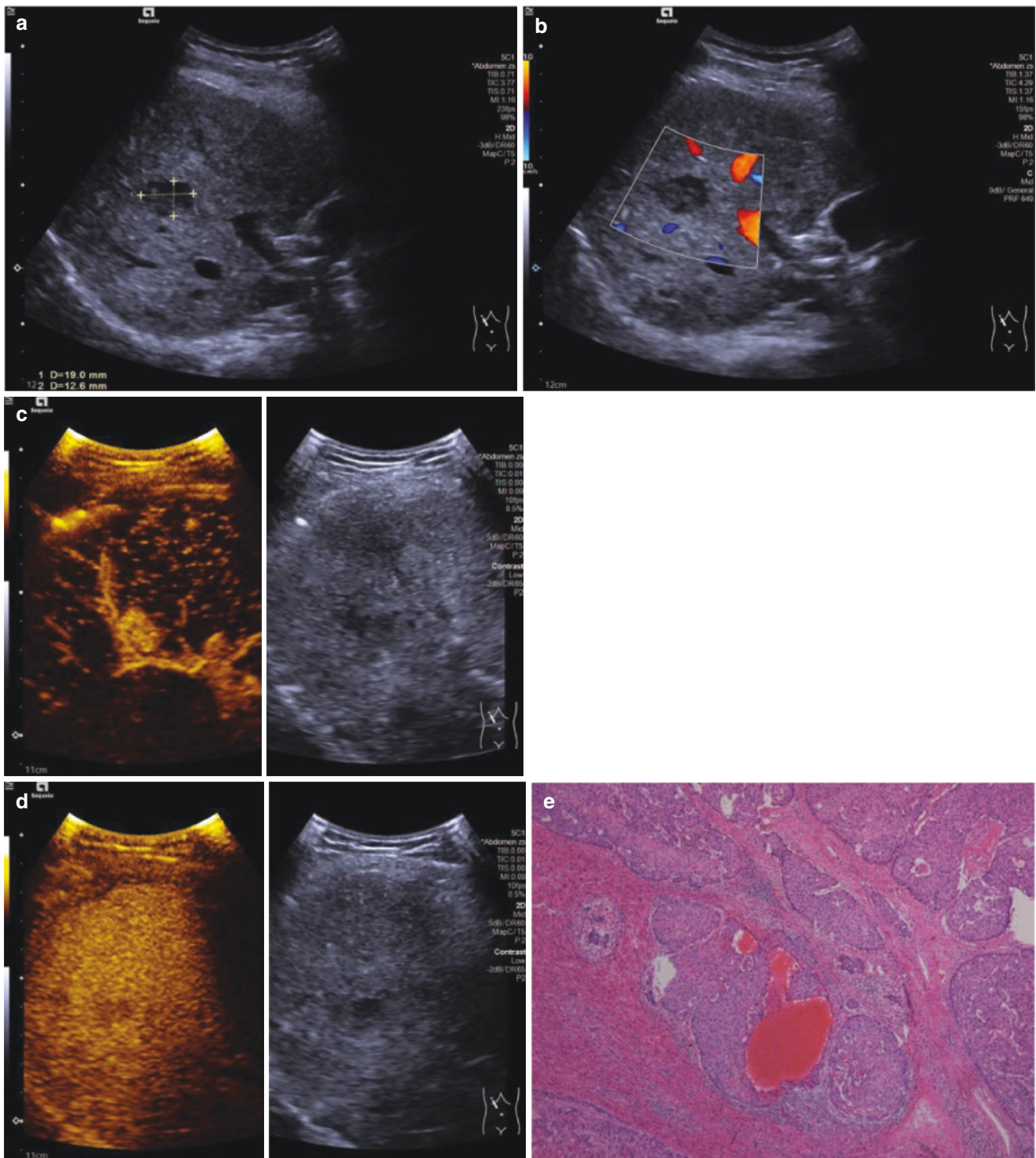
Fig. 4.21 Small hepatocellular carcinoma (HCC) in a 57-year-old man with hepatitis B-related cirrhosis. B mode ultrasound image showed a 19-mm diameter hyperechoic nodule located in right lobe of liver (**a**). No color flow signals could be detected inside the lesion (**b**). The lesion showed hyperenhancement during arterial phase (**c**) and hypoenhancement during late phase (**d**). Subsequent surgery and histopathological result was positive for grade III HCC with microvascular invasion (**e**)
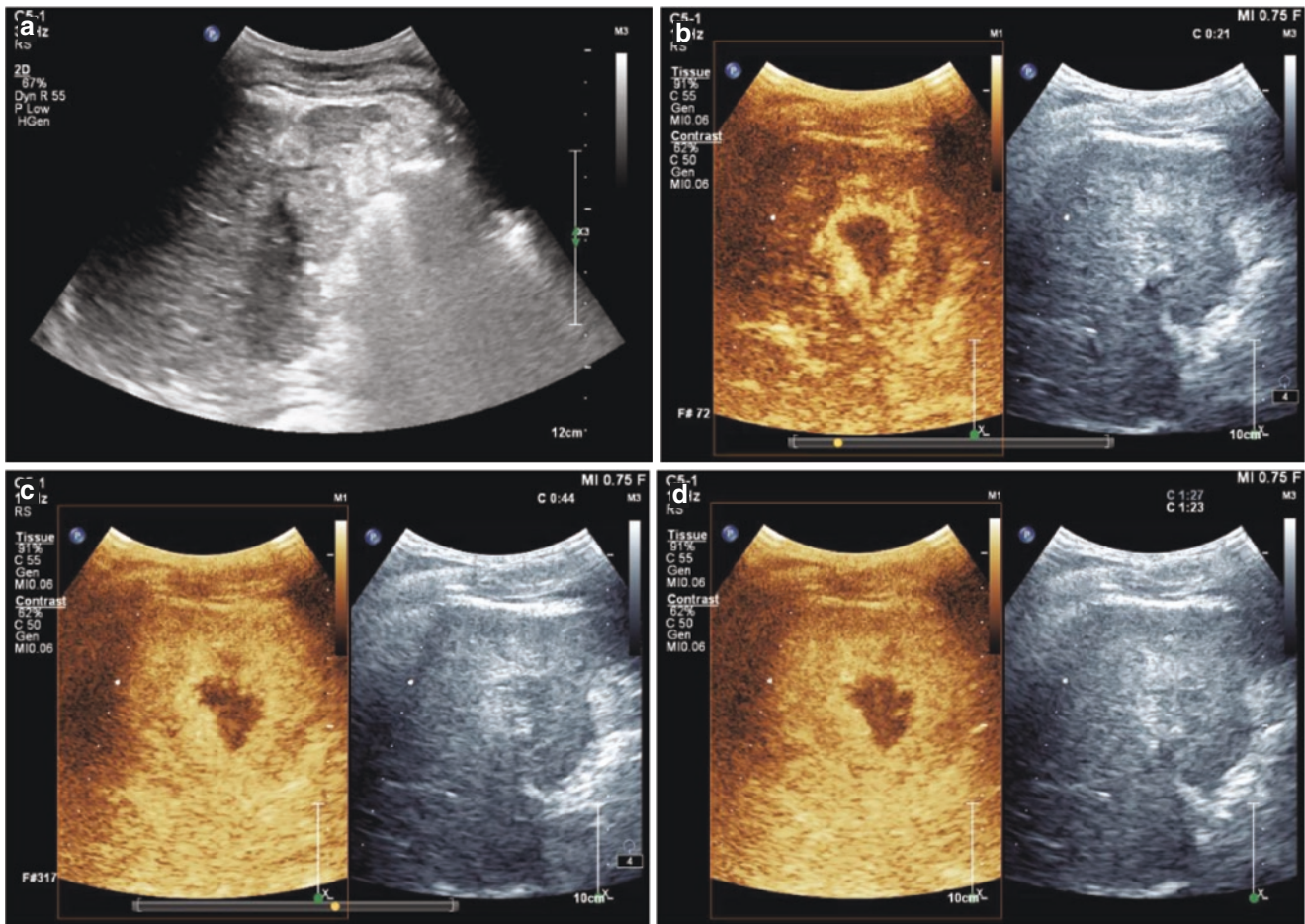
Fig. 4.22 The reactive inflammatory changes occurred after radiofrequency ablation therapy (RFA) in a 47-year-old man with hepatitis B-related hepatocellular carcinoma (HCC). B mode ultrasound examination 1 day after RFA showed a hypoechoic lesion in the right lobe of liver (**a**). After injection of contrast agents, a hyperenhanced peripheral hyperemia of the treated lesion could be detected during arterial phase (**b**), portal venous phase (**c**) to the late phase (**d**) of contrast enhanced ultrasound. This reactive hyperemia may last for 2–3 weeks after local ablation therapy

- Almost all ICCs show wash-out in the portal venous/late phase on CEUS, while ICCs often show the late enhancement on contrast enhanced computed tomography (CT) or contrast enhanced magnetic resonance imaging (MRI).
- Intraoperative ultrasound is valuable to guide surgical resection of ICC, to detect intrahepatic biliary stones, and to guide radiofrequency ablation.
- Tumor markers do not have high sensitivity and specificity to make a diagnosis or rule out ICC.
- Biopsy is not necessary if curative resection is planned.

4.2.3 Differential Diagnosis

4.2.3.1 Hepatocellular Carcinoma

The typical enhancement pattern of HCC on CEUS is arterial phase hyperenhancement followed by wash-out in the portal venous and/or late phases under the background of liver cirrhosis. Some studies suggested that there is an overlap between the wash-in pattern of ICC and HCC on CEUS in liver cirrhosis patients or small tumor. The guidelines of the American Association for the study of Liver Diseases (AASLD) have removed CEUS from the diagnostic modalities for HCC, because of the misdiagnosis probability [26].

The arterial enhancement patterns and temporal presentation between ICCs and HCCs are different. Most HCC lesions manifest global hyperenhancement in arterial phase, whereas most ICC lesions manifest peripheral hyperenhancement. Furthermore, recent studies revealed that the timing of wash-out in ICC was much earlier than that in HCC, as well as the degree of wash-out was more marked in ICC than that in HCC. These two differences may differentiate ICC from HCC. Arterial phase hyperenhancement followed by late (>60 s) wash-out of mild degree is now defined to be a refined diagnosis of HCC on CEUS [21, 23, 24, 27].
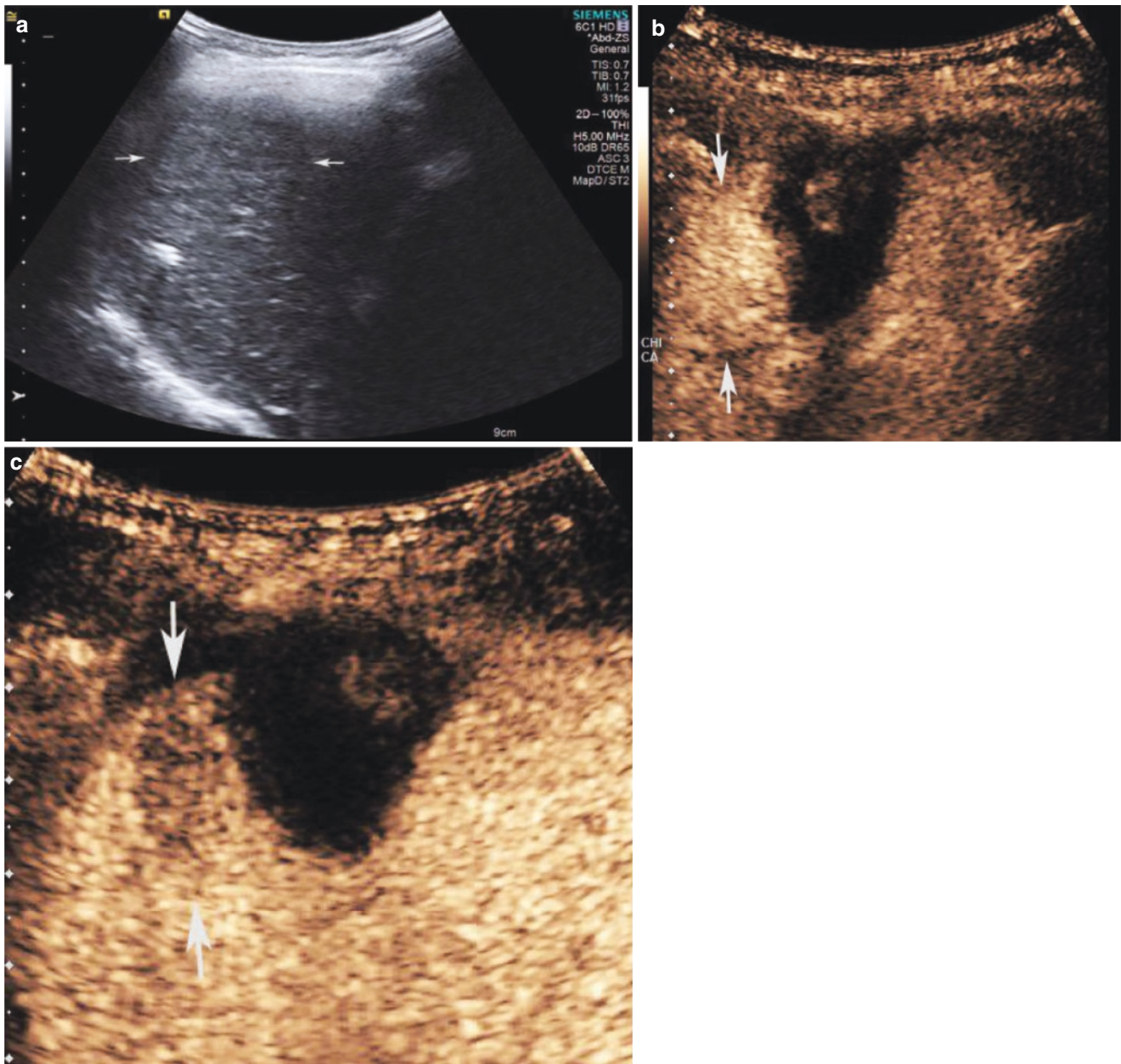
Fig. 4.23 Tumor recurrence after RFA in a 63-year-old woman with hepatitis B-related cirrhosis. B mode ultrasound image obtained 1 month after RFA showed a typical heterogeneous hypoechoic treatment site (arrow) (**a**). CEUS image obtained 18 s after contrast agent injection showed a nodular region of APHE (arrows) near the treatment site (**b**). CEUS image obtained at 89 s showed marked wash-out (arrows) of this nodular (**c**). This patient underwent repeat ablative therapy

4.2.4 Pathology

4.2.4.1 General Features

ICC often occurs in a normal liver. Most ICCs are adenocarcinoma with variable differentiation and fibroplasia. A variable and occasionally abundant fibrous stroma is an important characteristic of ICC. Fibrous encapsulation is not seen. ICC directly invades the surrounding hepatic parenchyma and may spread along the portal tracts. The mass-forming type of ICC can be quite large. The periphery of the tumors contains more abundant, proliferating cells, and the center of the tumors is usually more sclerotic and hypocellular (Fig. 4.28). Central necrosis is common, and there may be focal calcification in these areas. Mucin hypersecretion can be visible dilated ducts. Regional lymph nodes are often involved. Lungs are the most common site when blood-borne metastases occur later [15].
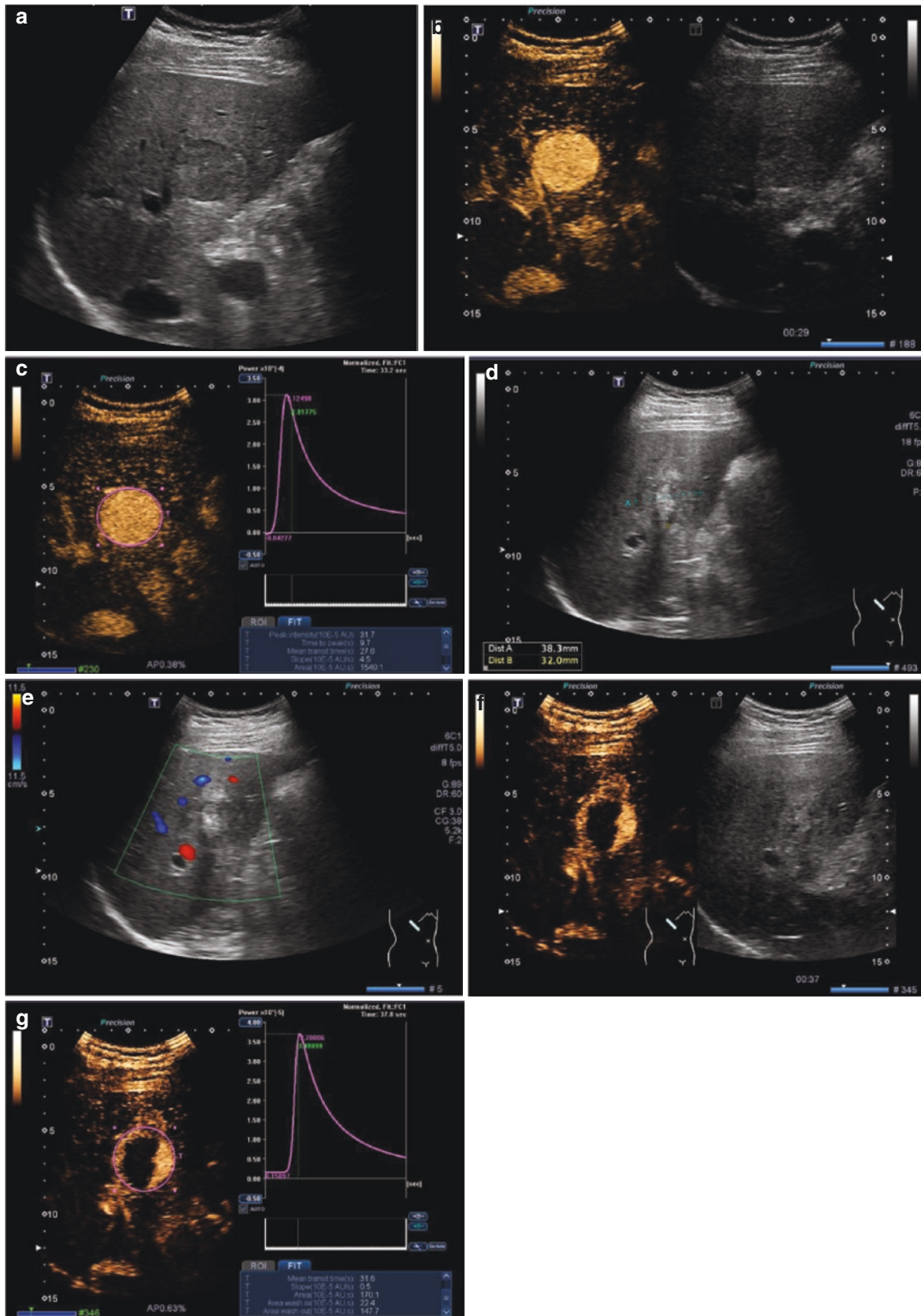
Fig. 4.24 Tumor residual after microwave ablation (MWA) in a 41-year-old woman with hepatitis B-related cirrhosis. B mode ultrasound image (BMUS) obtained 1 day after MWA showed a heterogeneous hypoechoic focal liver lesion located in right lobe of liver (**a**). CEUS image obtained 29 s after contrast agent injection showed complete hyperenhancement of the lesion (**b**). Time intensity curves made quantitative analysis of the tumor perfusion (**c**). One day after MWA, the lesion showed heterogenous on BMUS (**d**), no color flow signals could be detected inside the lesion (**e**). However, CEUS image obtained at 37 s showed APHE (**f**). The residual tumor perfusion was further proved by TIC analysis (**g**). This patient underwent repeat MWA therapy
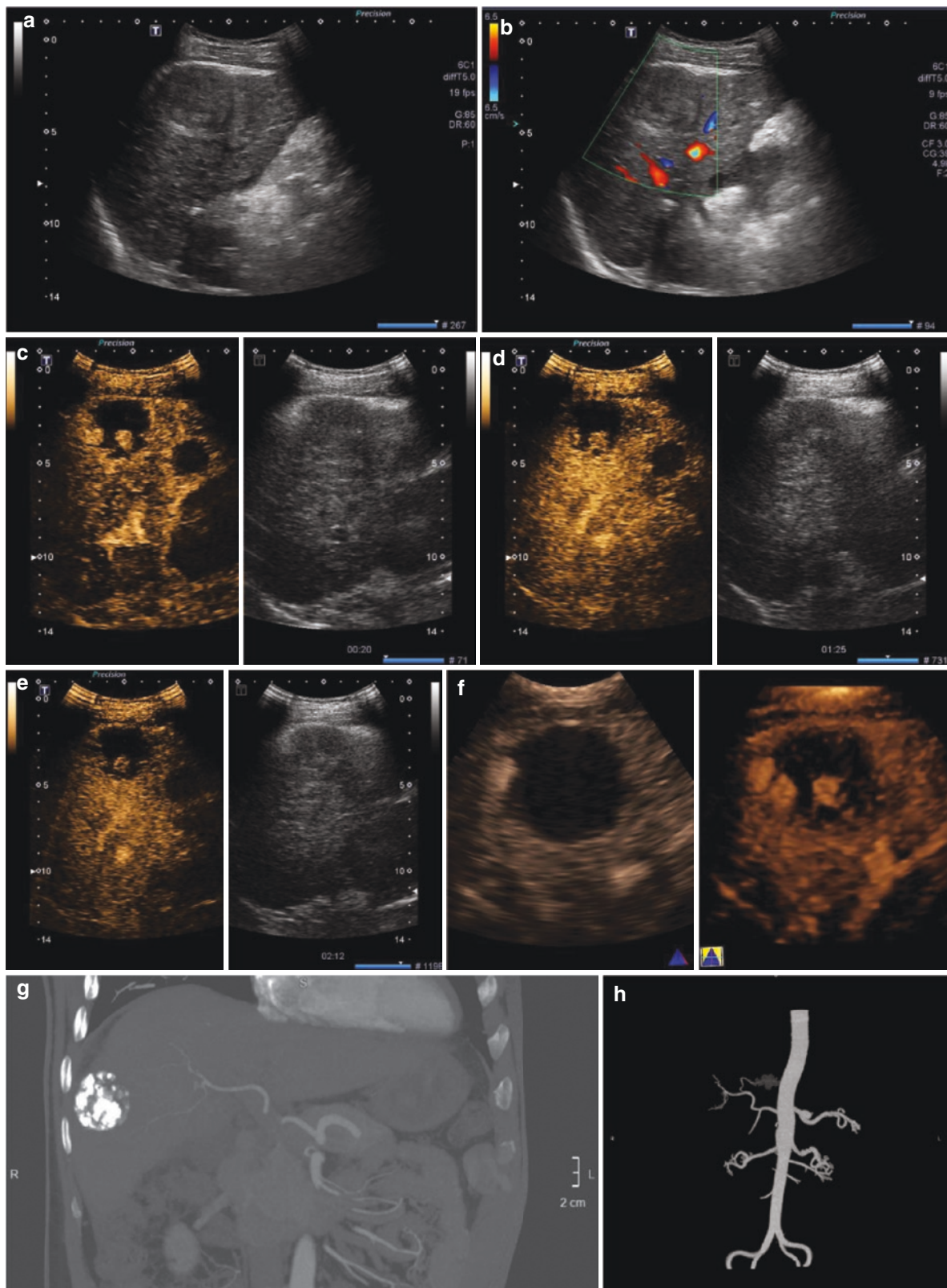
Fig. 4.25 Tumor residual after transarterial chemoembolization (TACE) in a 63-year-old woman with hepatitis B-related cirrhosis. Grayscale US image obtained 1 month after TACE shows a typical heterogeneous treatment lesion (**a**). No color flow signal could be detected inside the lesion (**b**). CEUS image obtained 20 s after contrast agent injection shows a nodular region of APHE (arrows) within the treatment site (**c**). CEUS image obtained at portal venous (**d**) and late phase (**e**) showed isoenhancement without wash-out. Also, the hyperenhanced nodular could be detected on 3D-CEUS (**f**), MRI (**g**), and DSA (**h**). This patient underwent surgery therapy (**i**) and was proved by histopathological results (**j**)
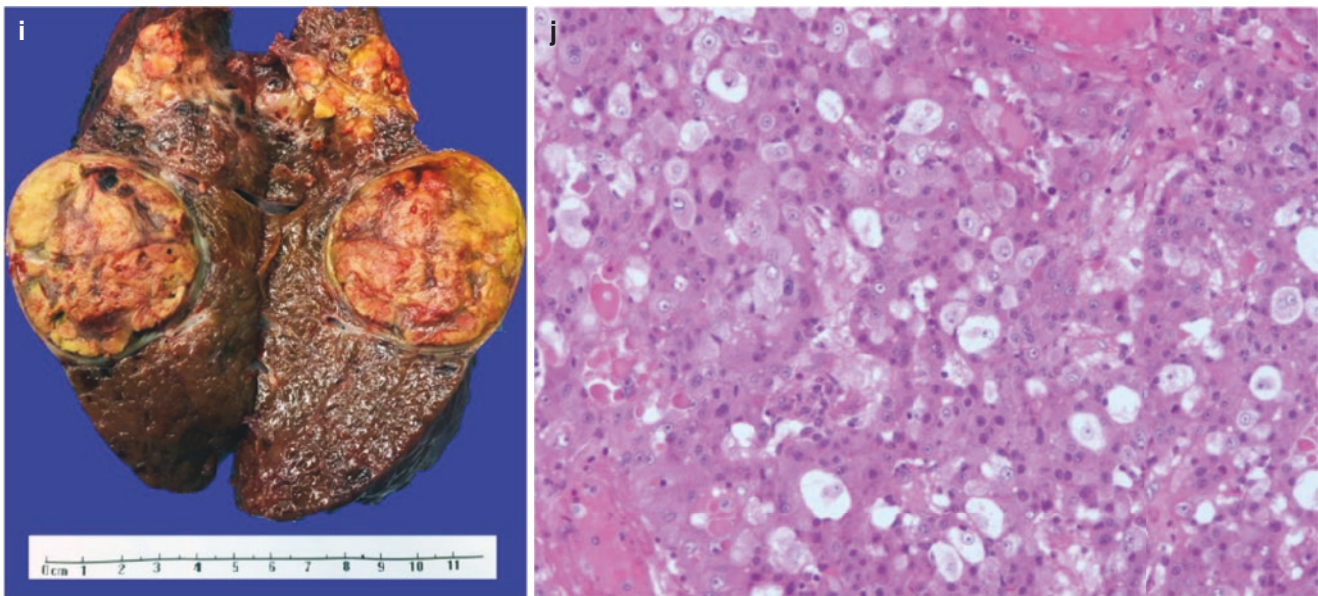
Fig. 4.25 (continued)

4.2.4.2 Staging, Grading, and Classification
Precursor and early lesions
Two types of precursor lesions are considered as precursors or early lesions of ICC arising from the intrahepatic large bile ducts: flat biliary intraepithelial neoplasia (BillN) and papillary intraductal papillary neoplasms (IPN) of the bile duct.

Grading

- Well differentiated
- Moderately differentiated
- Poorly differentiated

TNM classification
Tumor classification depends on the number of lesions, vascular invasion, intrahepatic metastasis, and invasion of adjacent structures.

- T0: No evidence of primary tumor
- T1: Tumor is solitary without vascular invasion
- T2: Multiple tumors (e.g., multifocal disease, satellitosis, and intrahepatic metastasis) with vascular invasion
- T3: Tumor directly invades adjacent structures
- T4: Tumor with any periductal infiltrating component
- N0: No regional lymph nodes metastasis
- N1: Hilar, periduodenal, and peripancreatic lymph nodes metastases
- M0: No distant metastasis
- M1: Distant metastases

4.2.5   Clinical Issues

4.2.5.1 Presentation
ICC is a relatively rare malignancy (accounting for 5–15% of primary liver cancers). Patients with ICC are usually elderly, with a slight male dominance. Etiology of most cases of ICC is not clear, and some cases of ICC are associated with chronic biliary inflammatory, primary sclerosing cholangitis, hepatolithiasis, parasitic biliary infestation, biliary malformations, familial polyposis, congenital hepatic fibrosis, or other risk factors. Clinical symptoms and signs of ICC are often not specific and related to the site of the tumor in the liver, its growth pattern, and the presence of obstruction of biliary tracts. Patients are usually asymptomatic in early stages. ICC without central bile ducts obstruction often attains a large size without being noticed. In advanced stages, patients may present abdominal distension or pain, weight loss, hepatomegaly, or palpable abdominal mass. Biliary tract obstruction is relatively rare, while perihilar cholangiocarcinoma usually presents with cholestasis and cholangitis of the intrahepatic bile ducts [14, 28].

4.2.5.2 Prognosis
ICC is an aggressive cancer with high mortality and poor survival rate as a result of early invasion, widespread metastases, and without effective treatments. The 5-year survival rate after operation is 69% in patients with the intraductal-growth type, and 39% in patients with the mass-forming type. The periductal infiltrating type shows a poor prognosis. The following factors are associated with a poor prognosis: concomitant hepatolithiasis; lymph node spread, macro-
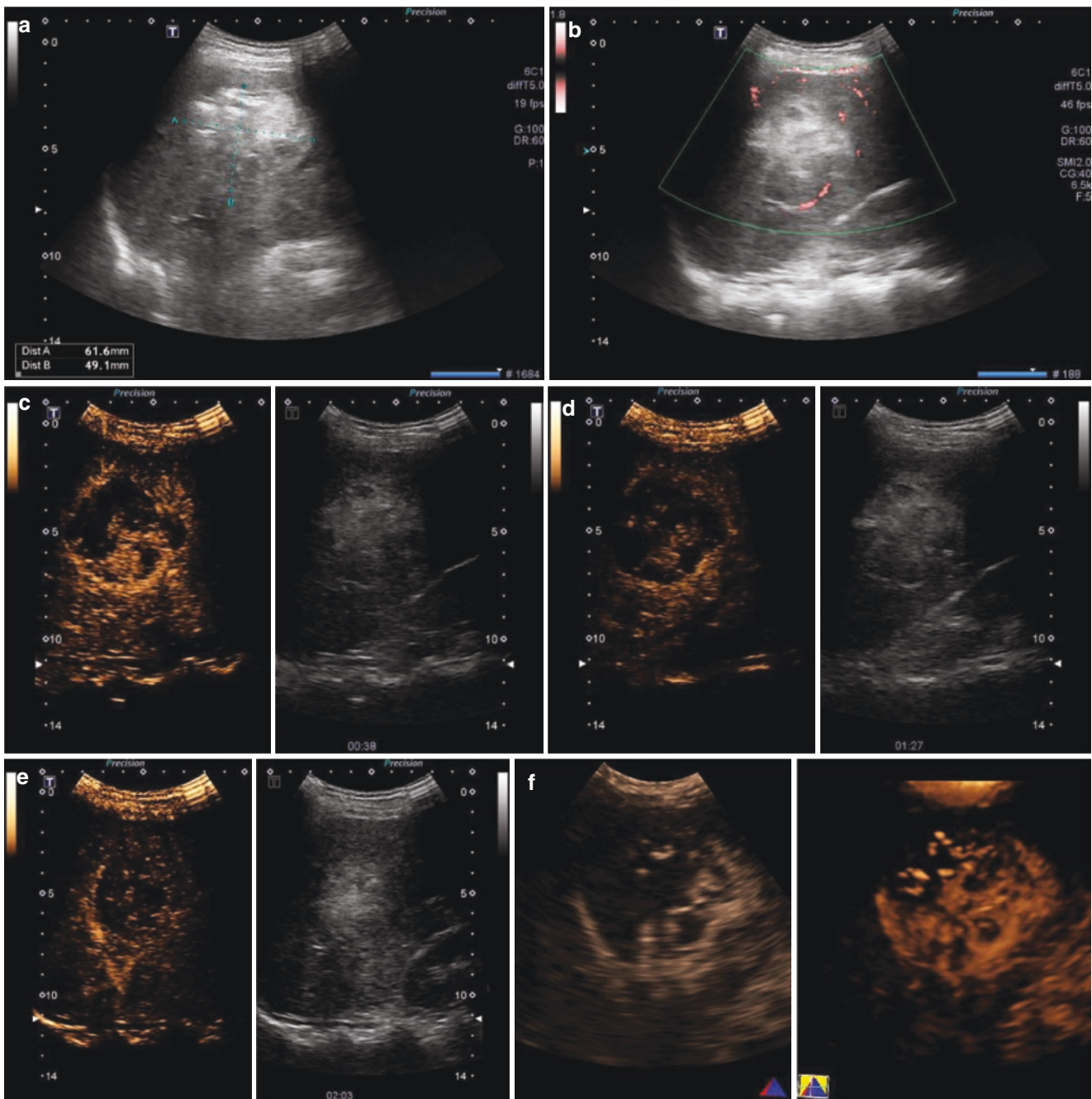
Fig. 4.26 Tumor residual after transarterial chemoembolization (TACE) in a 56-year-old man with hepatitis B-related cirrhosis. Grayscale US image obtained 1 month after TACE shows a typical heterogeneous treatment lesion (**a**). No color flow signal could be detected inside the lesion (**b**). CEUS image obtained 38 s after contrast agent injection shows a nodular region of APHE (arrows) within the treatment site (**c**). CEUS image obtained at portal venous (**d**) and late phase (**e**) showed the hypoenhancement as wash-out. Also, the hyperenhanced nodular could be detected on 3D-CEUS (**f**)
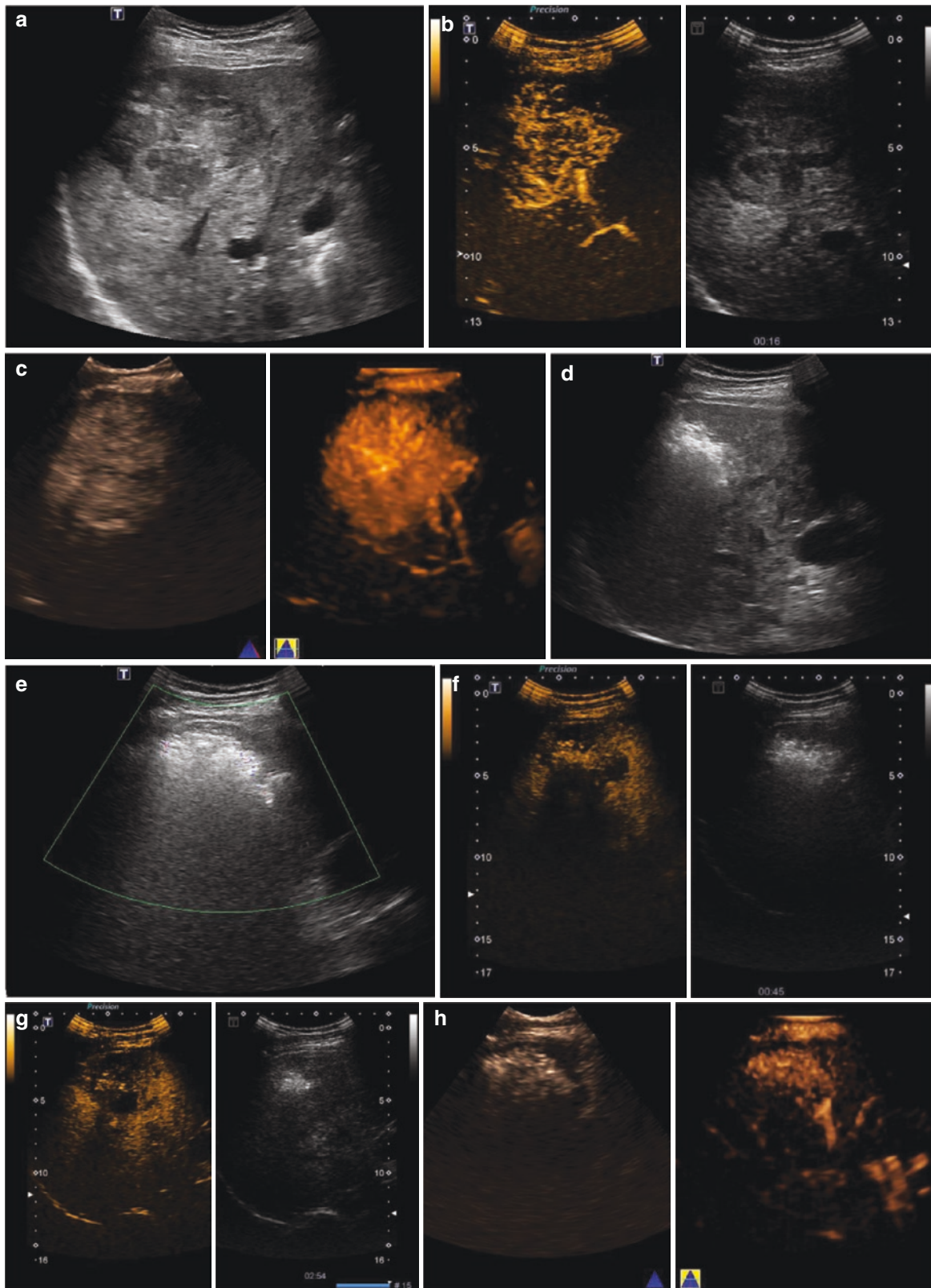
Fig. 4.27 Tumor residual after transarterial chemoembolization (TACE) in a 56-year-old man with hepatitis B-related cirrhosis. Grayscale US image obtained 1 month after TACE shows a typical heterogeneous treatment lesion (**a**). No color flow signal could be detected inside the lesion (**b**). CEUS image obtained 38 s after contrast agent injection shows a nodular region of APHE (arrows) within the treatment site (**c**). CEUS image obtained at portal venous (**d**) and late phase (**e**) showed the hypoenhancement as wash-out. Also, the hyperenhanced nodular could be detected on 3D-CEUS (**f**)
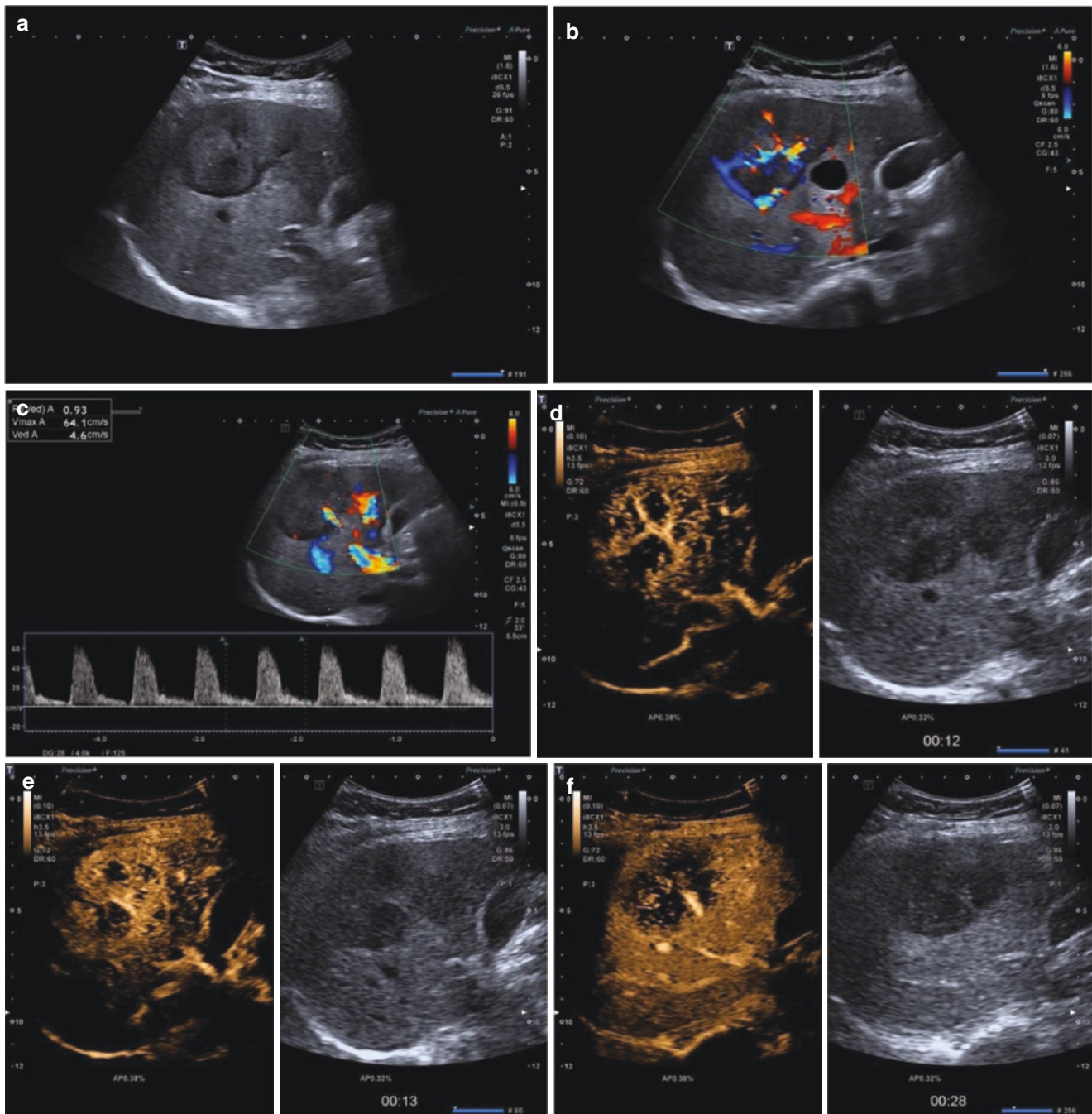
Fig. 4.28 A case of intrahepatic cholangiocarcinoma (ICC) with mass-forming type. A grayscale image revealed an expansile mass with ill-defined border under the capsule of the right lobe of liver (**a**). Color flow imaging showed abundant and branched blood signal inside the lesion (**b**). Arterial Doppler spectrum with high resistance index (RI) as 0.93 was measured (**c**). The lesion showed branched and peripheral rim-like hyperenhancement in the arterial phase (**d**, **e**), and rapidly marked wash-out at 28 s (**f**) with distinct hypoenhancement in the late phase (**g**). The diagnosis of ICC was confirmed with pathology after surgical resection. Macroscopic features of ICC showed that the periphery of the lesion contained abundant, proliferating cells, and the center of the lesion was more sclerotic and hypocellular) (**h**)
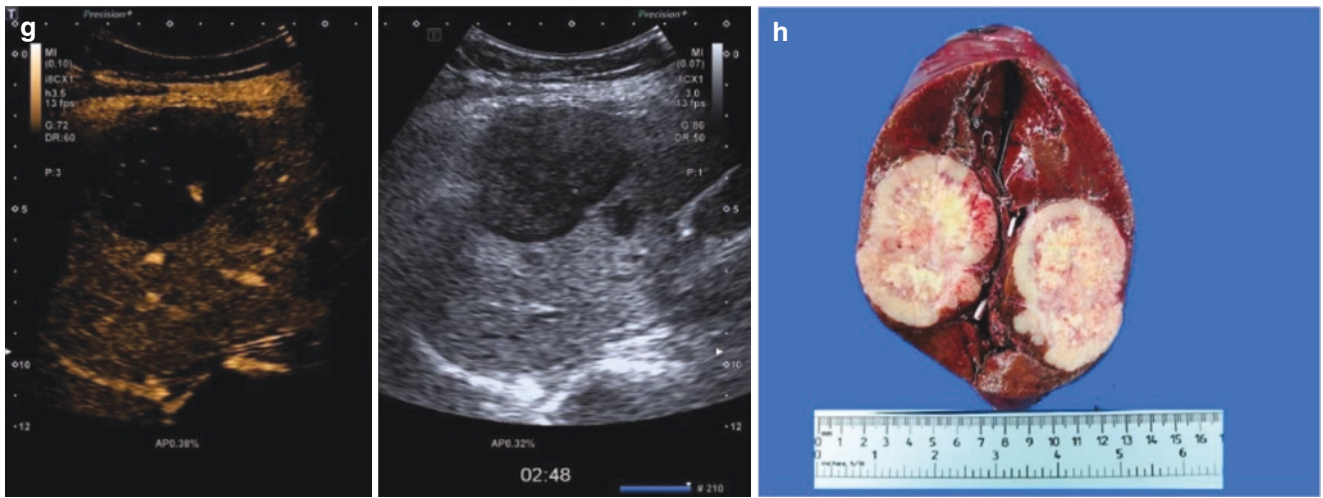
Fig. 4.28 (continued)

Fig. 4.29 A case of intrahepatic cholangiocarcinoma (ICC) with intraductal growth type. A grayscale ultrasound image revealed a polypoid nodule (arrow) within the dilated left hepatic duct (**a**). The lesion within the dilated left hepatic duct showed slightly hyperenhancement (arrow) in arterial phase and gradual enhancement. Localized dilated affected ducts were clearly presented with non-enhancement (arrowhead) (**b**–**e**). The lesion showed mild wash-out at 63 s (**f**) and explicitly in the late phase (**g**) (arrow)
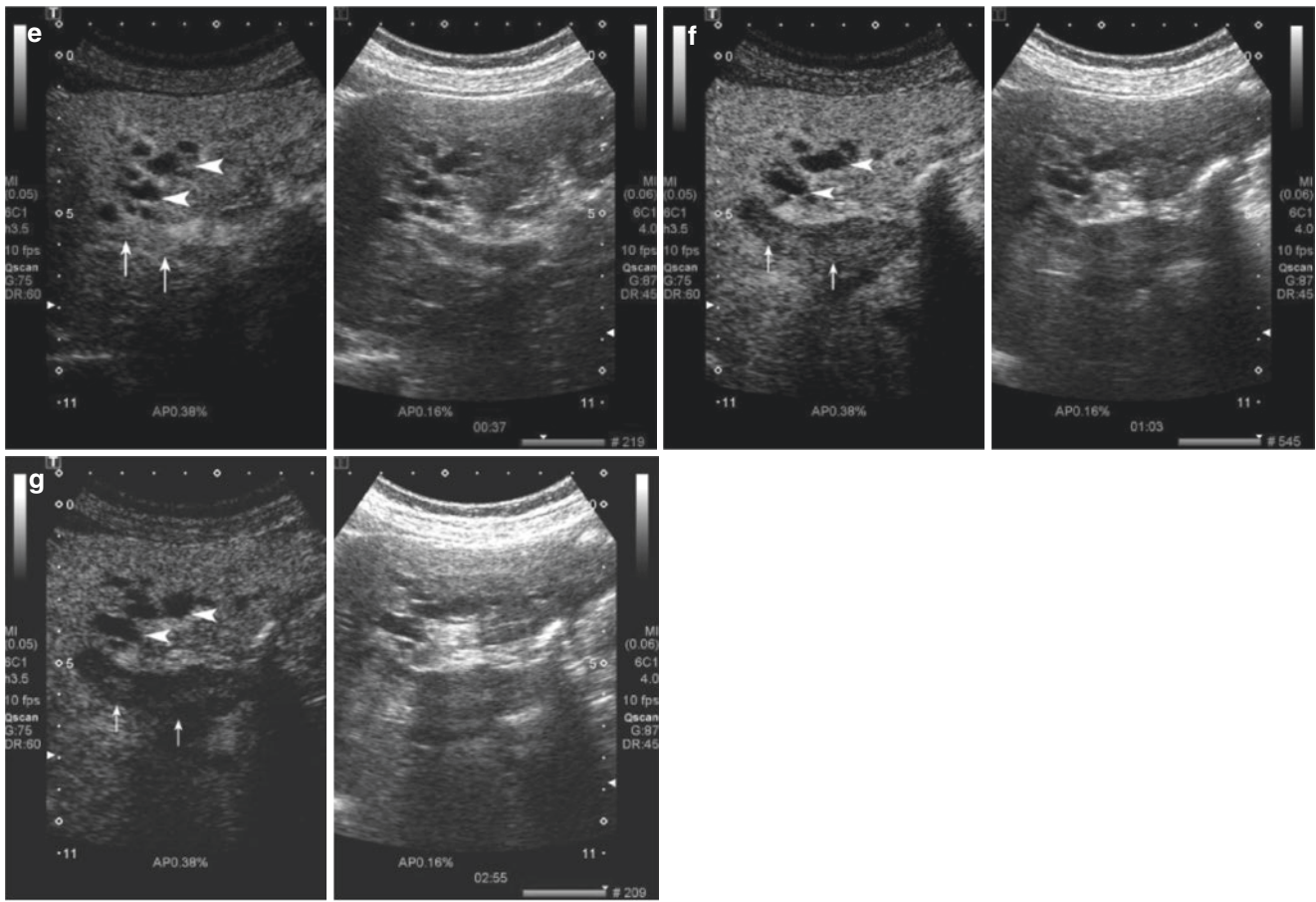
Fig. 4.29 (continued)

scopic vascular invasion, positive surgical margins, intrahepatic metastasis, macroscopic vascular invasion, non-curative resection, advanced TNM stage, poor histological differentiation, squamous cell or sarcomatous elements, and mucin phenotype [14, 28].

4.2.5.3 Treatment

Surgical operation is the unique potentially radical treatment. Few patients have chances for surgical resection as many patients present with advanced disease stage. Transarterial chemoembolization (TACE), ablation, and liver transplantation are not recommended for patients with ICC because of uncertain curative effects. Current researches suggest that chemotherapy may be of benefit to patients with margin invasion and/or nodes metastases after surgical resection or with distant metastases [14, 26–28].

4.3 Liver Metastases

Wen-Ping WangHan-Sheng Xia, and Jia-Ying Cao

4.3.1 Terminology

Focal or diffuse malignant involvement of the liver from extrahepatic origins is termed as liver metastases, which are 18–40 times more common than primary liver tumors. The liver is one of the most common organs for metastasis. The complex dual blood supply mode facilitates the inflow of cancer cells from tumors of other organs and distinct microenvironment of sinusoids permits increased trapping of tumor cells, thus supporting the development and invasion of metastases. The early and exact detection of liver

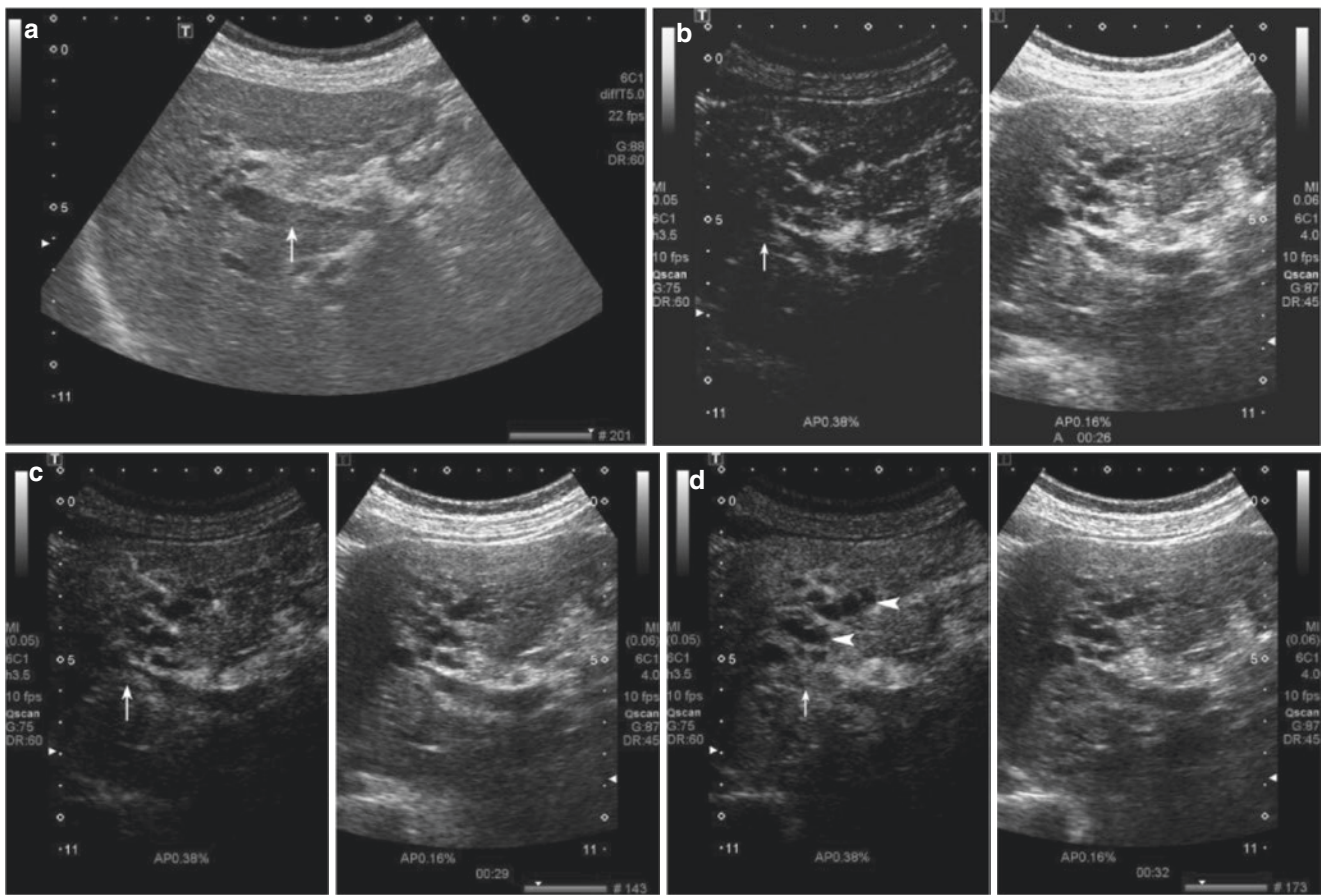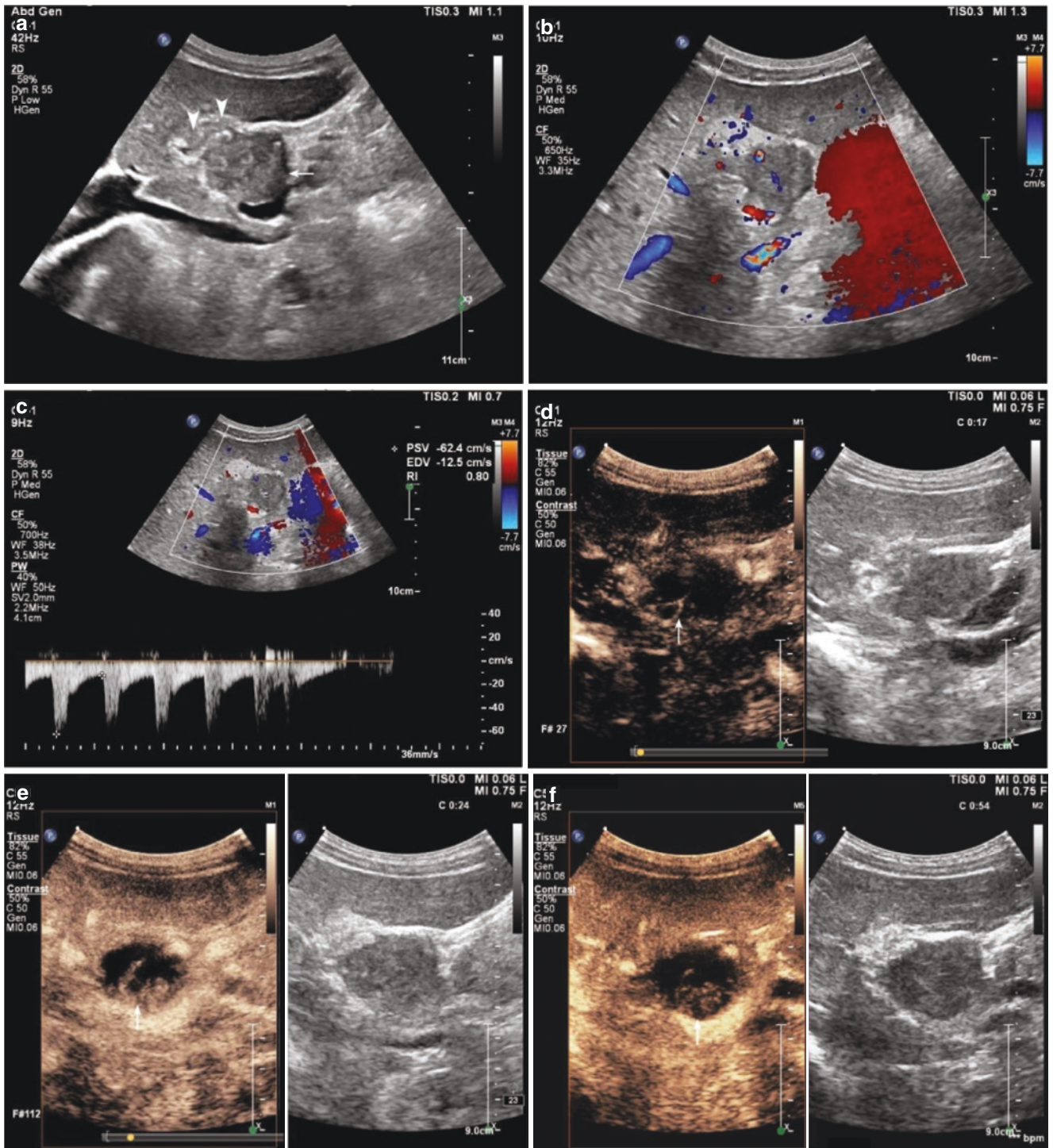**Fig. 4.30** A case of intrahepatic cholangiocarcinoma (ICC) with intraductal growth type. A grayscale ultrasound image revealed a papillary mural nodule within the left hepatic duct (arrow), and adjacent bile duct was invaded (arrowheads) (**a**). Color flow imaging showed blood signal inside the lesion (**b**). Arterial Doppler spectrum with high resistance index (RI) as 0.80 was measured (**c**). The lesion showed peripheral branched hyperenhancement in the arterial phase (arrow) (**d**, **e**). The lesion showed mild wash-out at 54 s (**f**) and explicitly in the portal venous phase (arrow) (**g**). A distant metastasis in the muscular layer of the left lower abdomen was detected and confirmed by biopsy pathology (arrow) (**h**, **i**)
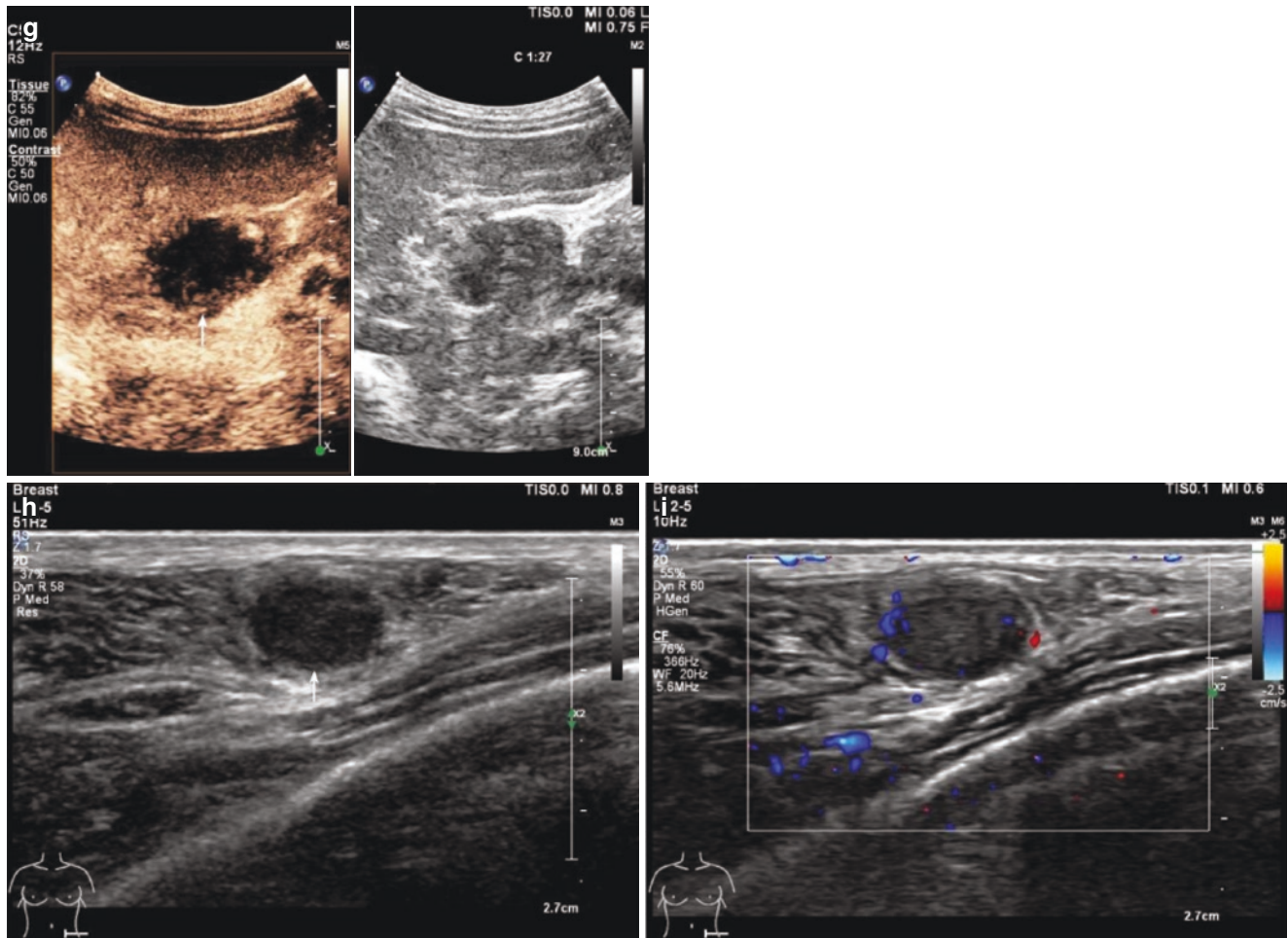
Fig. 4.30 (continued)

metastases is crucial for clinical decision-making and patient management.

4.3.2 Imaging Features

4.3.2.1 Conventional Ultrasound Findings

Conventional ultrasound is the first-line modality for hepatic imaging. It is widely used in routine surveillance, follow-up scanning, and treatment assessment of patients with liver metastases. Most liver metastases occur in normal liver. On US, metastases commonly present as multifocal solid lesions with hypo-, iso-, hyperechoic, or mixed echogenicity depending on the tissue components of the primary tumor and on the presence of necrosis or calcification. Grossly, small lesions may be well-defined hypoechoic nodules; whereas, large lesions are more likely to have heterogeneous echotexture with barely visible margins (Fig. 4.35). A peripheral hypoechoic halo is the most frequent B mode ultrasound feature of liver metastasis, which can also appear as a target sign or "bull's eye" sign owing to alternating layers of hyperechoic and hypoechoic tissue (Fig. 4.36). However, such morphologic changes are non-specific, especially in lesions smaller than 1 cm [29].

4.3.2.2 Contrast Enhanced Ultrasound Findings

With the aid of microbubbles, contrast ratio between liver parenchyma and focal lesions is greatly increased at contrast enhanced ultrasound (CEUS), which can not only stand out the occult lesions on conventional US, but also be more sensitive for small metastases. Moreover, CEUS is a real-time procedure with better temporal and spatial resolution than contrast-enhanced CT or MRI. It is better able to detect hemodynamic changes and detailed vascular information of hepatic tumors regardless of their rate of perfusion, rendering it an excellent tool for detection and characterization of liver metastases [30].
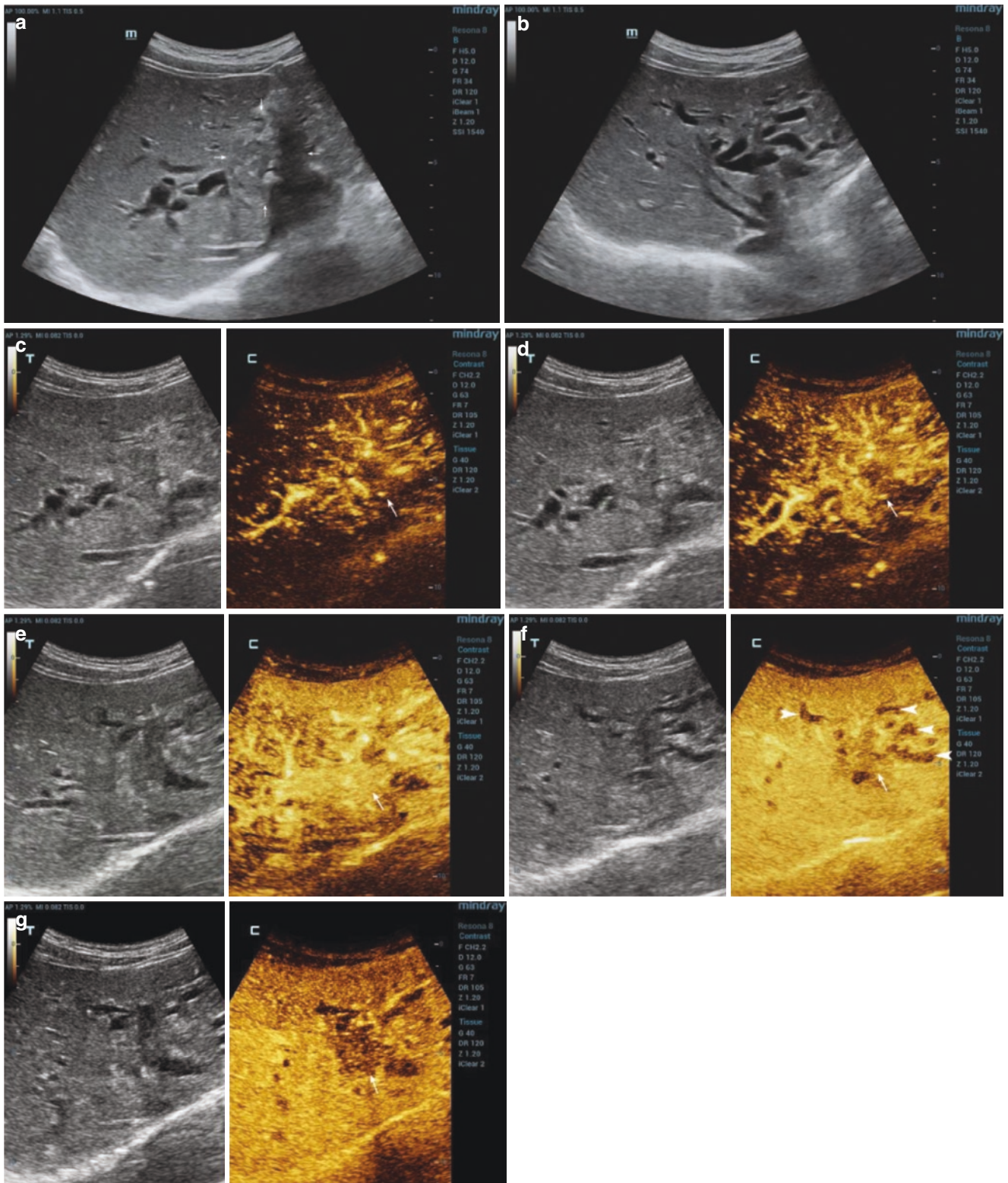
Fig. 4.31 A case of intrahepatic cholangiocarcinoma (ICC) with periductal infiltrating type. A grayscale image revealed a solid mass, adjacent to hepatic hilum, with ill-defined border extending along the intrahepatic bile ducts (arrows) (**a**). The upstream ducts were secondarily dilated and adjacent bile ducts were invaded (**b**). The lesion showed heterogeneously enhancement in the arterial phase and gradually enhancement (arrows) (**c–e**). The lesion showed partly mild washout at 102 s (**f**) and completely in the late phase (**g**) (arrow). The upstream secondarily dilated ducts were clearly observed with nonenhancement (arrowheads)
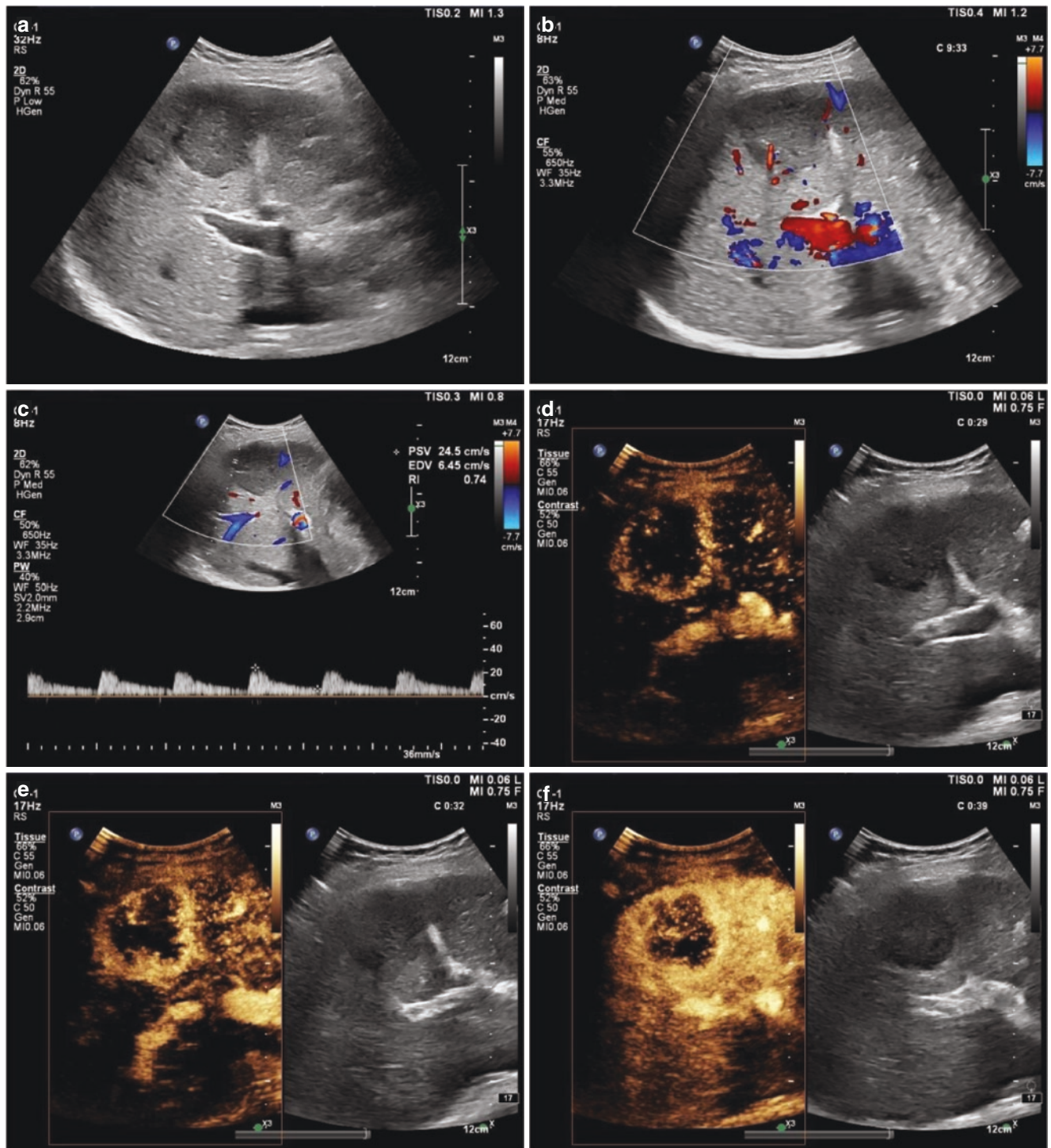
Fig. 4.32 A case of intrahepatic cholangiocarcinoma (ICC) with mass-forming type. B mode ultrasound revealed a hypoechoic mass under the capsule of the right lobe of liver (**a**). Color flow imaging showed a short-linear blood signal inside the lesion (**b**). Arterial Doppler spectrum with high resistance index (RI) as 0.74 was measured (**c**). The lesion showed peripheral rim-like and gradually centripetal hyperenhancement in arterial phase (**d**–**f**). The lesion showed mild wash-out in the portal venous phase (**g**, **h**) and completely in the late phase (**i**). On MRI, the lesion showed hypointense on T1-weighted imaging (**j**) and hyperintense on T2-weighted imaging (**k**). On dynamic enhanced MRI, the lesion showed arterial phase peripheral enhancement followed by progressive and concentric filling in (**l**–**n**). The lesion was confirmed by surgical pathology (**o**)
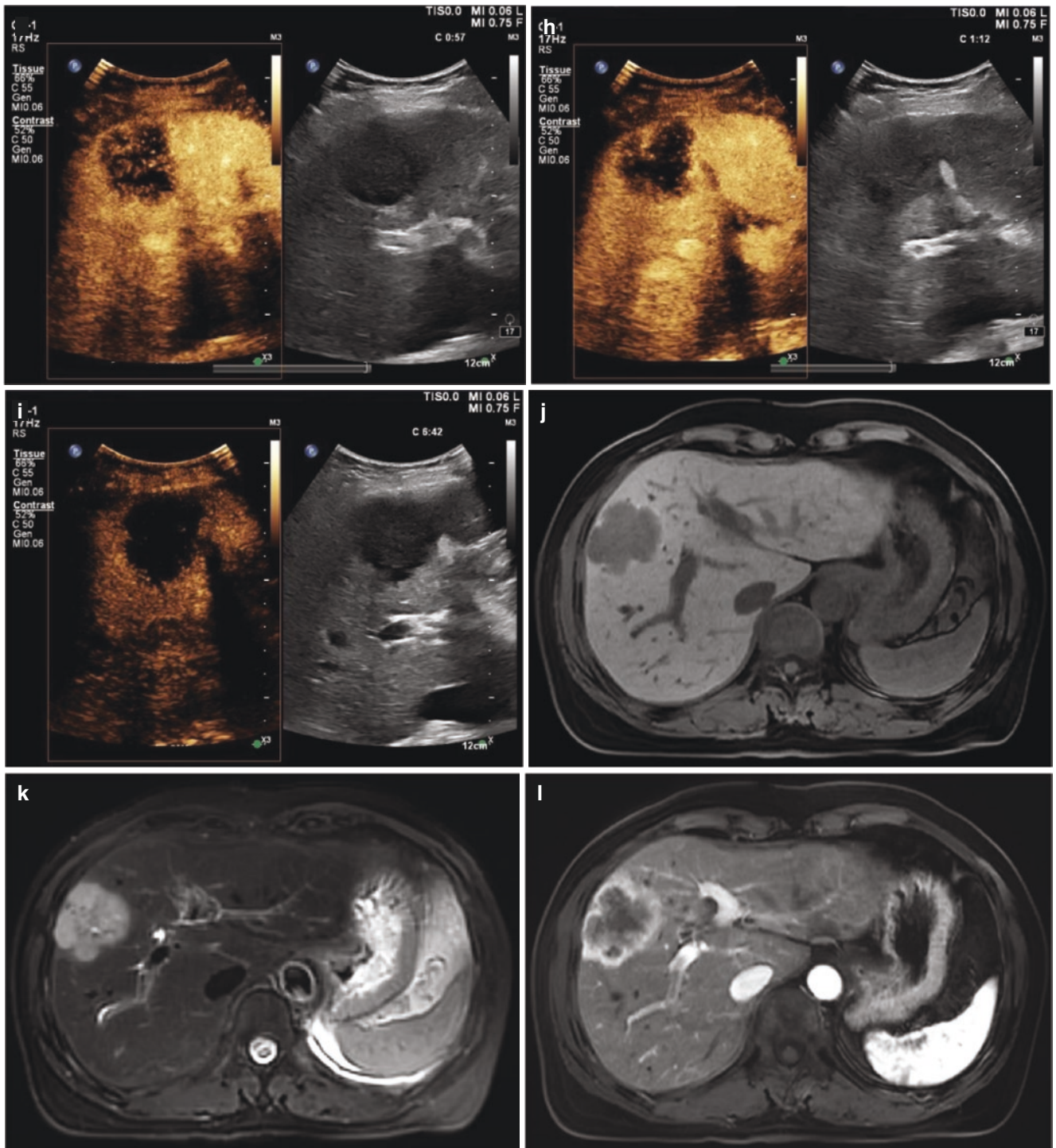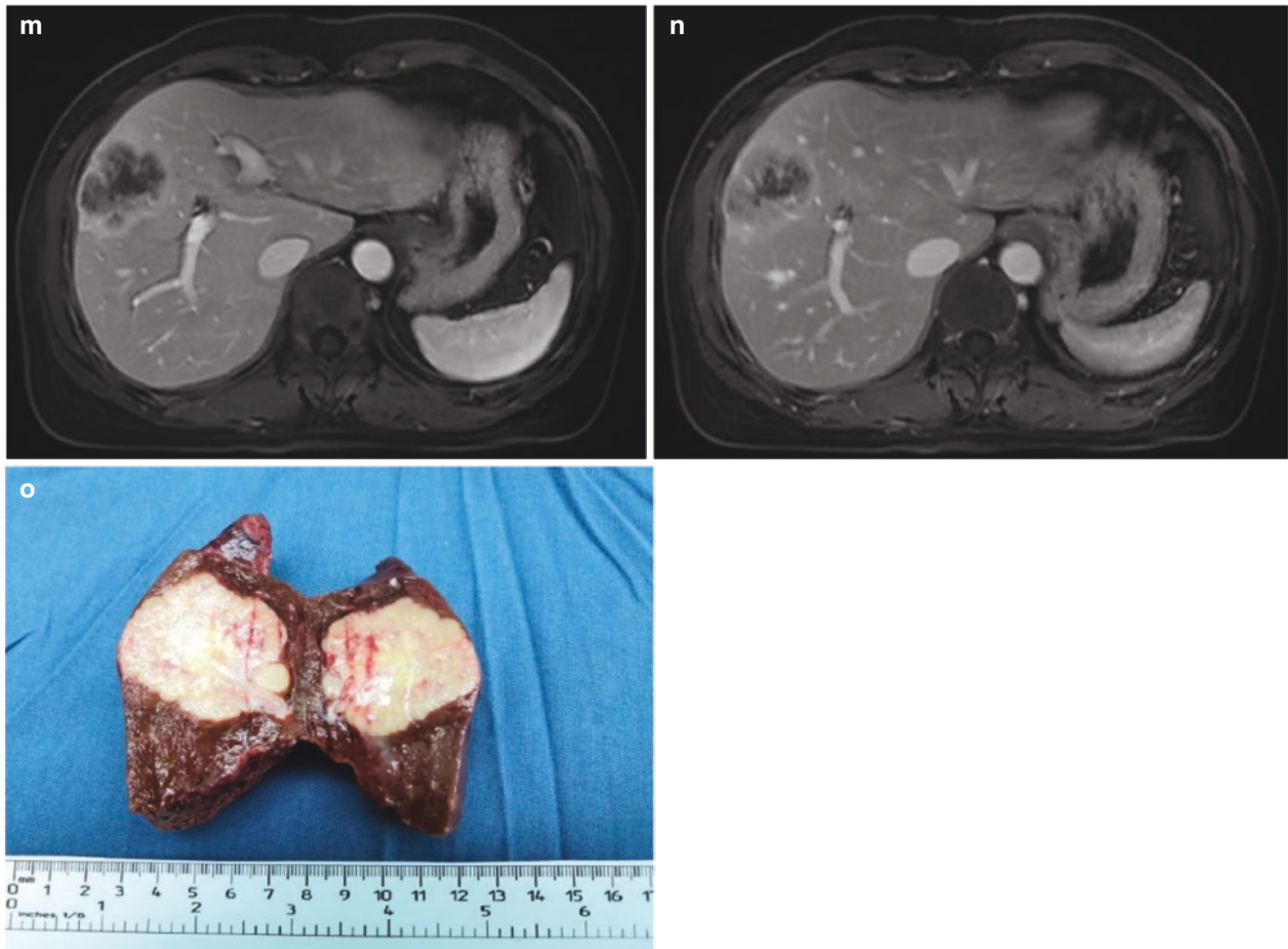
Fig. 4.32 (continued)

Fig. 4.32 (continued)

Typical appearances of liver metastases on CEUS are as follows:

Arterial phase features

Almost all liver metastases show obvious arterial phase enhancement. Generally, there are two enhancement patterns: diffuse homogeneous or heterogeneous hyperenhancement and peripheral rim-like hyperenhancement (Figs. 4.37, 4.38, 4.39, 4.40, 4.41, and 4.42). These patterns are not associated with the degree of tumor vascularity but may be related to nodule size: diffuse hypervascularity is seen more commonly in the lesions smaller than 2 cm, while hepatic metastases larger than 5 cm are more likely to show pronounced rim-like peripheral hyperenhancement [31]. The period for arterial phase enhancement of hepatic metastases is transient and lasts only about 20 s in most cases, which can only be depicted on CEUS and would not be appreciated on CT or MRI imaging. Although such arterial hypervascularity is not specific and provides limited clues for characterization purpose, it may be useful in the treatment response assess-

ment of metastases after local ablation or chemotherapy (Fig. 4.43).

Portal venous and late phase CEUS features

Liver metastases typically present hypoenhancement during the portal venous and late phases after microbubble injection. Rapid and complete wash-out is an invariable evident feature of hepatic metastasis on CEUS. The mass starts to wash-out within 60 s after contrast injection in most cases, and the wash-out onset of some small lesions (≤2 cm) even begins in the late arterial phase (about 20 s after injection). The optimal temporal window to detect metastatic lesions is the early portal venous phase, namely from 40 to 60 s after contrast injection, which provides the best lesion conspicuity. Although hypervascular metastases including neuroendocrine tumors, melanomas, sarcomas, and renal, breast and thyroid neoplasms frequently show a significantly longer wash-out time than hypovascular metastases, virtually almost all metastases unequivocally show complete wash-out after 60 s and remain constant hypoenhancement in the
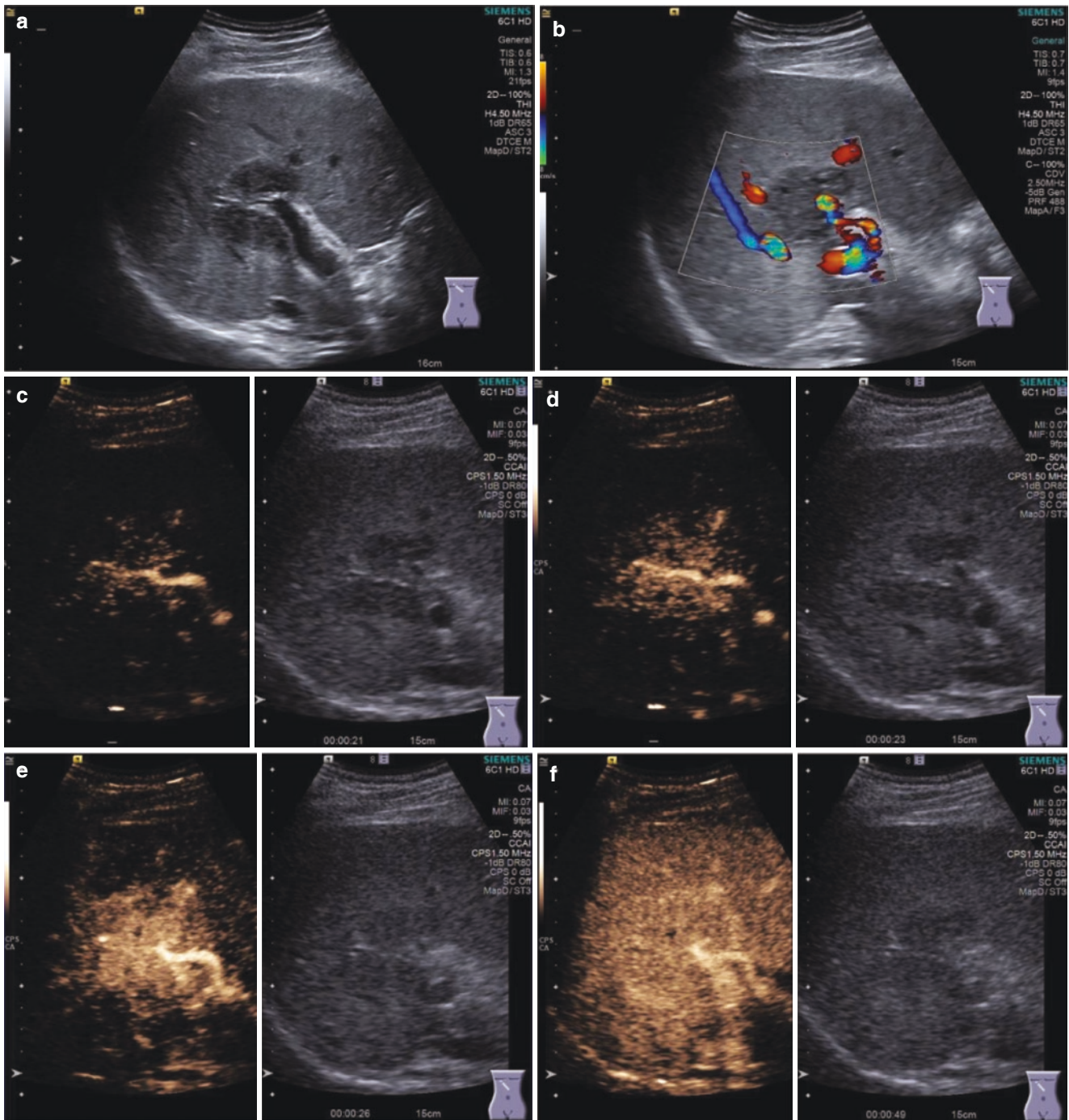
Fig. 4.33 A case of intrahepatic cholangiocarcinoma (ICC) with mass-forming type. B mode ultrasound revealed a hypoechoic mass around the right portal vein (**a**). Color flow imaging showed no blood signal inside the lesion (**b**). The lesion showed centrifugal hyperenhancement in the arterial phase (**c**–**f**). The lesion showed mild wash-out at 82 s (**g**) and distinct hypoenhancement in the late phase (**h**). Gross specimen showed the lesion around the right portal vein (**i**)

Fig. 4.33 (continued)

late phase. Marked wash-out is defined as punched out perfusion defects or black hole within 2 min after contrast injection. It should be noted that if a hyp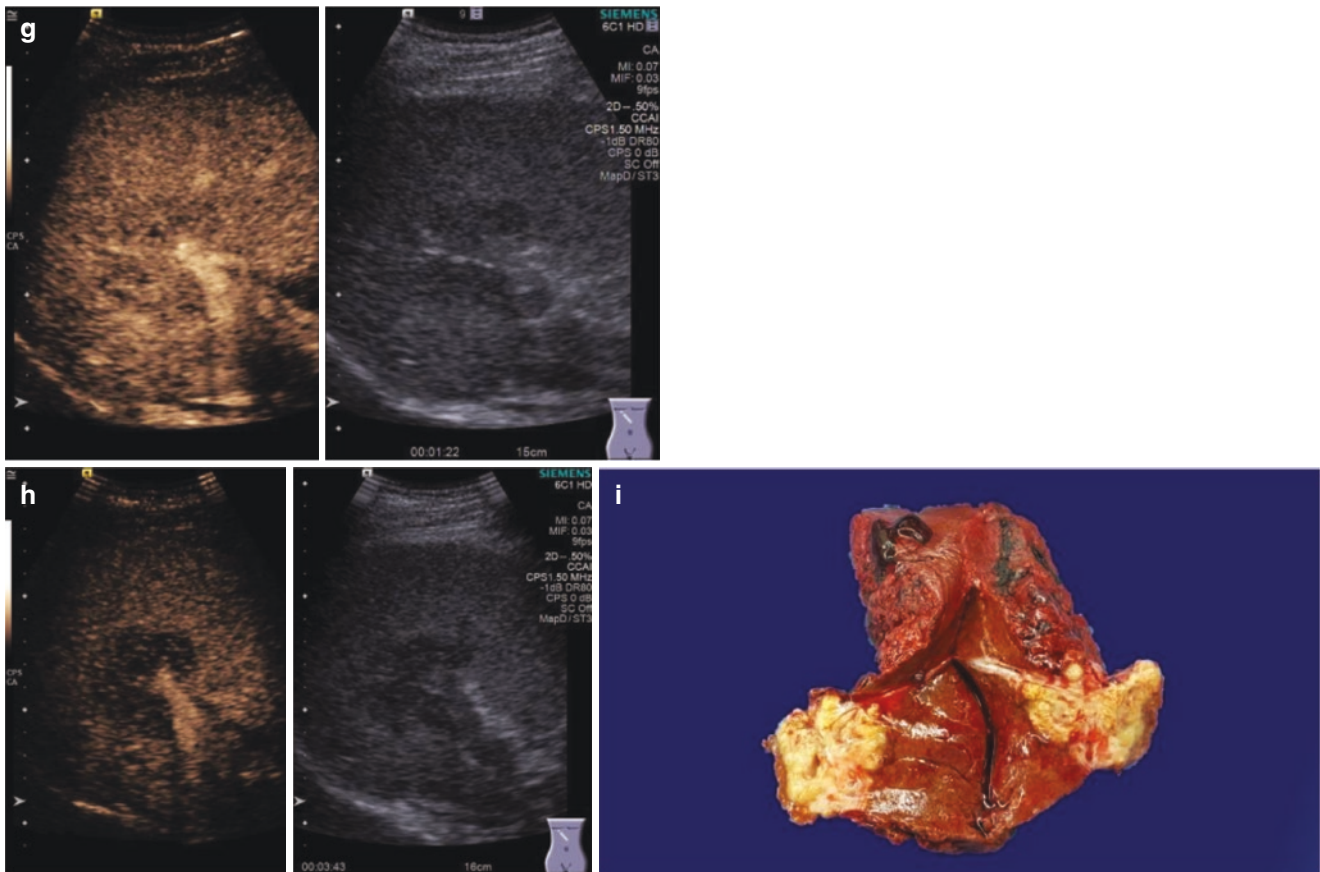oenhanced nodule is relative to the liver but still shows persistent enhancement and eventually becomes marked wash-out after 2 min, the degree of wash-out is still characterized as mild [32, 33].

In HCCs and liver metastases with hypervascularity and a normal liver background on CEUS imaging, various CEUS perfusion parameters on time intensity curve (TIC) may objectively reflect the difference of enhancement patterns between HCCs and liver metastases.

4.3.2.3 CT Findings

Liver metastases present variable enhancement characteristics on contrast enhanced CT. They are best imaged in the portal venous phase and typically appear as a hypoattenuating lesion. Some hypervascular metastases may show marked arterial phase hyperenhancement. However, the benefit of arterial phase observation is controversial for evaluation of such lesions [34].

4.3.2.4 MRI Findings

On non-enhanced MRI, metastases are typically hypointense on T1-weighted images and show various degrees of hyperin-

tensity on T2-weighted images. They show restricted diffusion on DWI and a significant overlap exists for ADC values between metastases and other malignant and benign lesions. Postcontrast MRI imaging features are similar to those of CT. With the use of hepatobiliary-specific contrast agent, metastases show hypointense in hepatobiliary phase, which provides excellent contrast between the liver parenchyma and metastatic lesions and offers superior characterization and greater specificity for diagnosis of liver metastases [34].

4.3.3 Differential Diagnosis

4.3.3.1 Hepatocellular Carcinoma

Most HCCs may occur in cirrhotic liver. Certain atypical HCC, especially poor differentiated HCC tends to show earlier wash-out. However, HCCs frequently show diffuse arterial phase hyperenhancement without a peripheral rim-like, and their degree of wash-out tends to be mild showing substantial enhancement within 2 min after microbubble injection.

4.3.3.2 Intrahepatic Cholangiocarcinoma

ICC usually presents arterial rim-like hyperenhancement and rapid and complete wash-out, posing a challenge for

differential diagnosis. On conventional ultrasound, it frequently shows undefined margin with dilated bile ducts in the peripheral region. On CEUS, it may show patchy hypoechoic areas in the peak enhancement and its size may be significantly increased compared with that of baseline appearance.

4.3.3.3 Focal Fatty Liver Change

Focal fatty sparing can mimic a mass and pose a diagnostic dilemma on conventional US and should be differentiated with metastatic lesions in a steatosis liver background. On CEUS, the lesion typically shows synchronization enhancement and wash-out, which can be considered diagnostic.

4.4 Dysplasia Nodules

Pei-Li Fan, Wen-Ping Wang, and Bei-Jian Huang

4.4.1 Terminology

4.4.1.1 Definitions

Most hepatocellular carcinomas (HCCs) occur in patients with cirrhosis caused by various long-term liver damages including chronic hepatitis B or C virus infections, alcoholic liver disease, nonalcoholic steatohepatitis, or autoimmune hepatitis. Long-term chronic inflammations lead to genetic
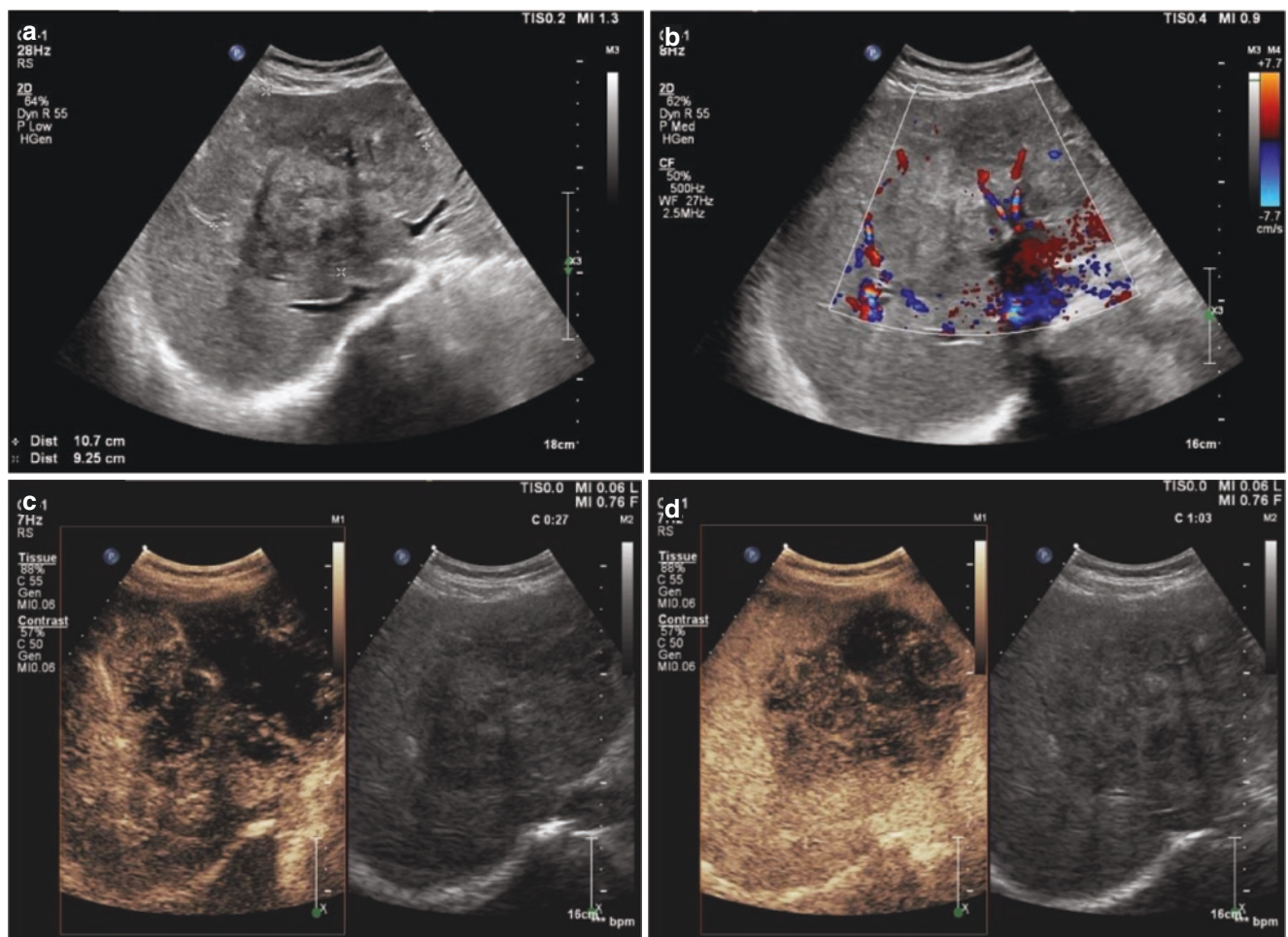

Fig. 4.34 A case of large intrahepatic cholangiocarcinoma (ICC) with satellitosis. B mode ultrasound revealed a heterogeneously hypoechoic mass with an ill-defined border (**a**). Color flow imaging showed a little blood signal inside the lesion (**b**). The lesion showed heterogeneous hypoenhancement in the arterial phase (**c**) and hypoenhancement in the portal venous phase (**d**). The lesion manifested marked wash-out in the late phase (**e**). In the portal venous phase, other small lesions under the capsule showing hypoenhancement were detected around the major lesion (arrow) (**f**). After another injection of contrast agent, the small lesions showed peripheral rim-like hyperenhancement with non-enhancement in the center (arrow) (**g**), and hypoenhancement in the portal venous phase (arrow) (**h**, **i**). The adjacent dilated bile ducts with non-enhancement were detected (arrowheads)
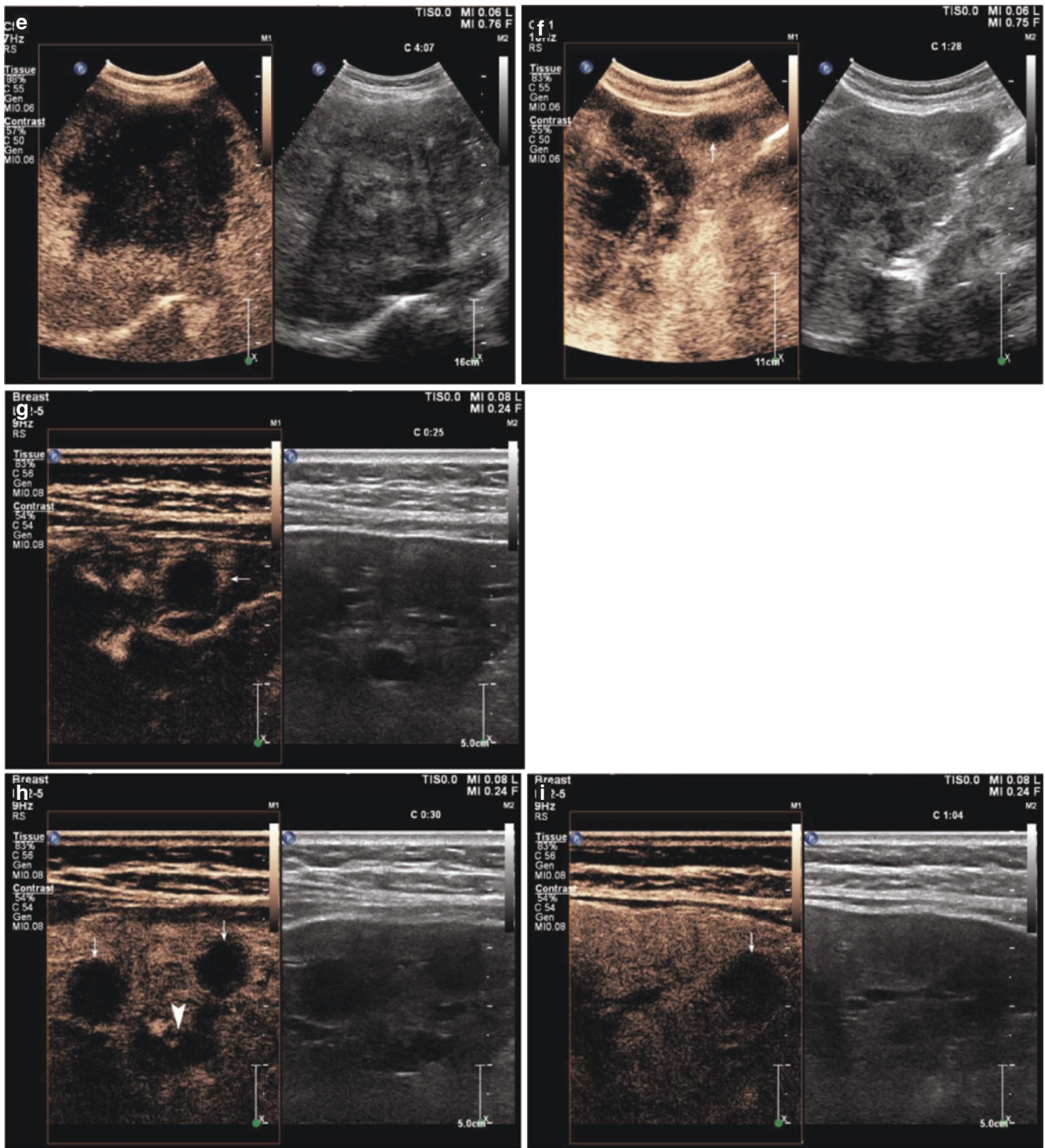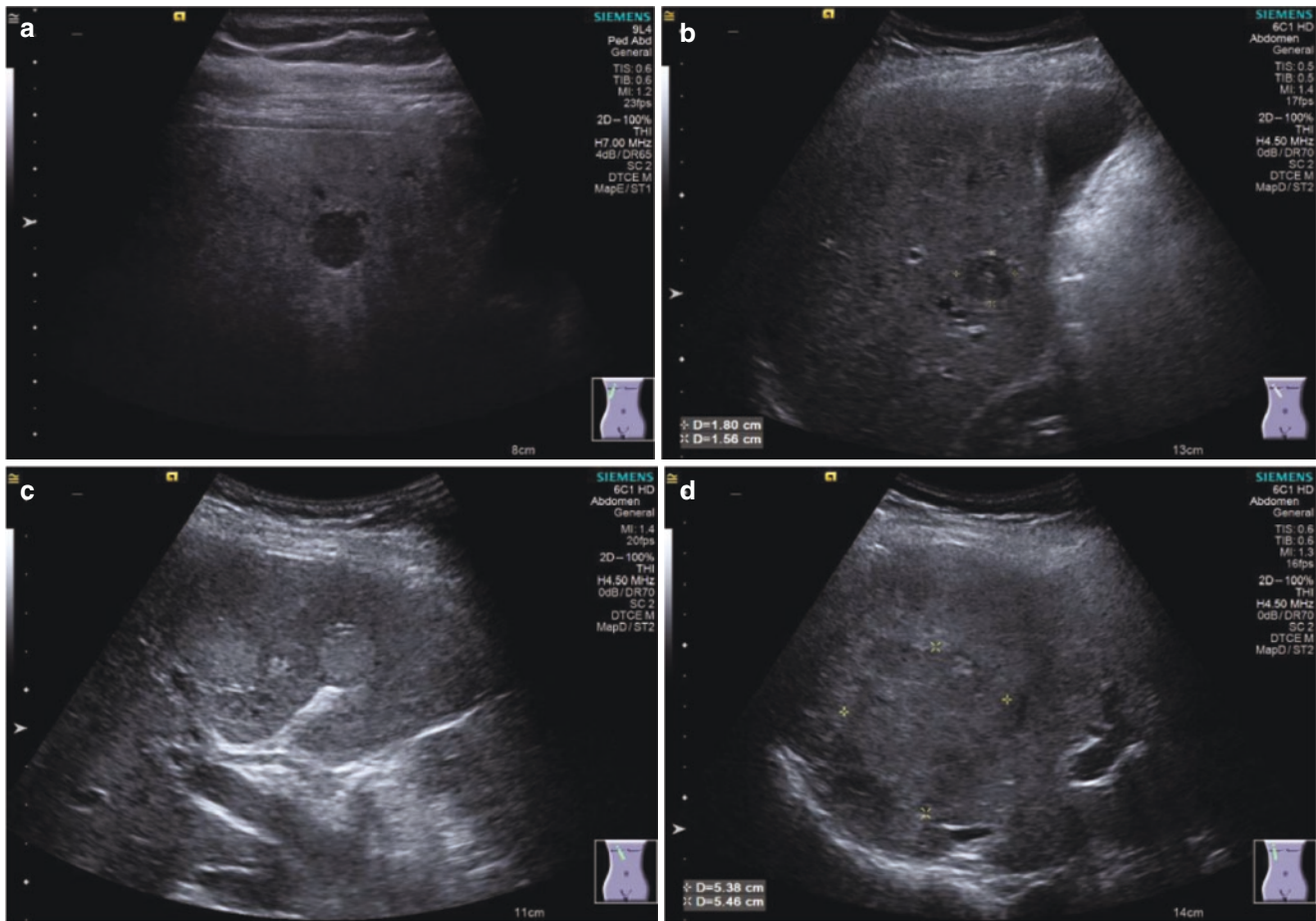
Fig. 4.34 (continued)

Fig. 4.35 Liver metastases with different kinds of echogenicity on B mode ultrasound. Hypoechoic liver metastasis from rectum adenocarcinoma (**a**). Hypoechoic liver metastasis from lung cancer (**b**). Hyperechoic liver metastasis from cecum adenocarcinoma (**c**). Heterogeneously isoechoic liver metastasis from colorectal carcinoma (**d**)

variations leading to hepatocarcinogenesis. Recent data revealed a sequence of changes in hepatic nodules before the occurrence of HCC. Some lesions are considered as precursors of HCCs. In 1995, the International Working Party (IWP) of the World Congresses of Gastroenterology proposed a consensus nomenclature and diagnostic criteria for hepatocellular nodular lesions in cirrhosis, which have been widely adopted. The IWP classified hepatocellular nodular lesions into large regenerative nodule (RN), low-grade dysplastic nodule (LGDN), high-grade dysplastic nodule (HGDN), and HCC. In the latest World Health Organization (WHO) classification of tumors of liver, premalignant lesions of HCCs are classified into large cell change (formerly "dysplasia"), small cell change (formerly "dysplasia"), LGDN, and HGDN. In 2007, the International Consensus Group for Hepatocellular Neoplasia (ICGHN) updated the international consensus on the histopathologic diagnosis of hepatocellular nodular lesions. Stromal invasion, tumor cell invasion into the portal tracts or fibrous septa within vaguely nodular lesions, was defined as a criterion for differential diagnosis of well-differentiated HCC from HGDN [35].

4.4.2 Imaging

The critical alterations during hepatocarcinogenesis detected by imaging methods are simultaneous and gradual decrease of portal tracts, hepatocyte function, Kupffer cell density, and organic anionic transporting polypeptide (OATP) expression, meanwhile development of sinusoidal capillarization and unpaired arterioles. Furthermore, venous drainage changes from hepatic veins to portal veins. In early hepatocarcinogenesis, fat content in the lesions sometimes increases, then in progressed HCC, fat content usually regresses [36].

Nourishing vessel changes in hepatocarcinogenesis in liver cirrhosis are summarized in Fig. 4.44. Three stages according to the pathological and imaging features could be
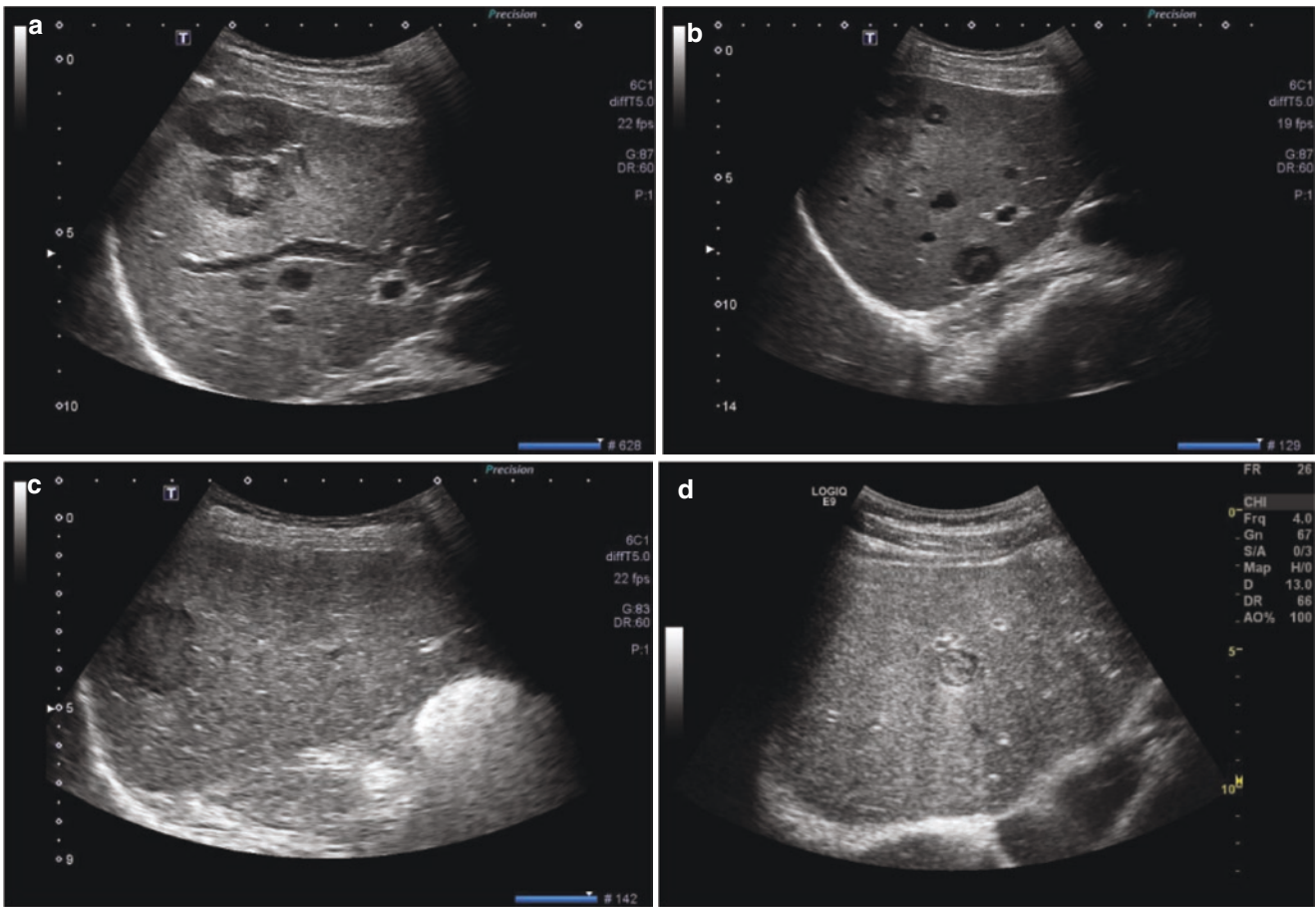
Fig. 4.36 Target sign or "bull's eye" sign on B mode ultrasound. Liver metastases from malignant melanoma (**a**), liver metastases from malignant melanoma (**b**), liver metastases from colon carcinoma (**c**), and liver metastases from gastric stromal tumor (**d**)

divided during hepatocarcinogenesis in liver cirrhosis: premalignant stage (including DNs, especially HGDNs), early HCC stage (including well-differentiated HCCs of the vague margin and HCCs with diameter ≤2 cm), and progressed HCC stage (including moderately- or poorly-differentiated HCCs) [37].

4.4.2.1 Conventional Ultrasound Findings

Ultrasound (US) is a screening method for HCC surveillance because of its convenience, availability, safety, and cost-effectiveness. However, it is challenging to identify DNs in the background of cirrhotic liver because of their vague margin and small size. On B-mode US, DNs could be hypo-, iso-, or hyperechoic, which is overlapped with RNs or small HCCs. When fat content occurs in the lesions, DNs usually manifest hyperechoic.

4.4.2.2 Contrast Enhanced Ultrasound Findings

Based on angiogenesis and hemodynamic changes during hepatocarcinogenesis, several imaging methods could be used to diagnose cirrhosis-associated nodules. After CT and MRI, contrast enhanced ultrasound (CEUS) has been used as a second-line imaging method to detect and recognize various liver lesions.

Blood supply of DNs maybe both from portal vessels and from newly formed unpaired arteries. Portal tracts usually still remain in DNs, but maybe few and scarred. Unpaired arteries increase in both number and size through HGDN and well-differentiated HCC developmental stages. Therefore, DNs typically show isoenhancement (Fig. 4.45) or hypoenhancement in arterial phase and isoenhancement on subsequent phases on CEUS, as compared to the surrounding liver. In transient phases before the development of unpaired arter-
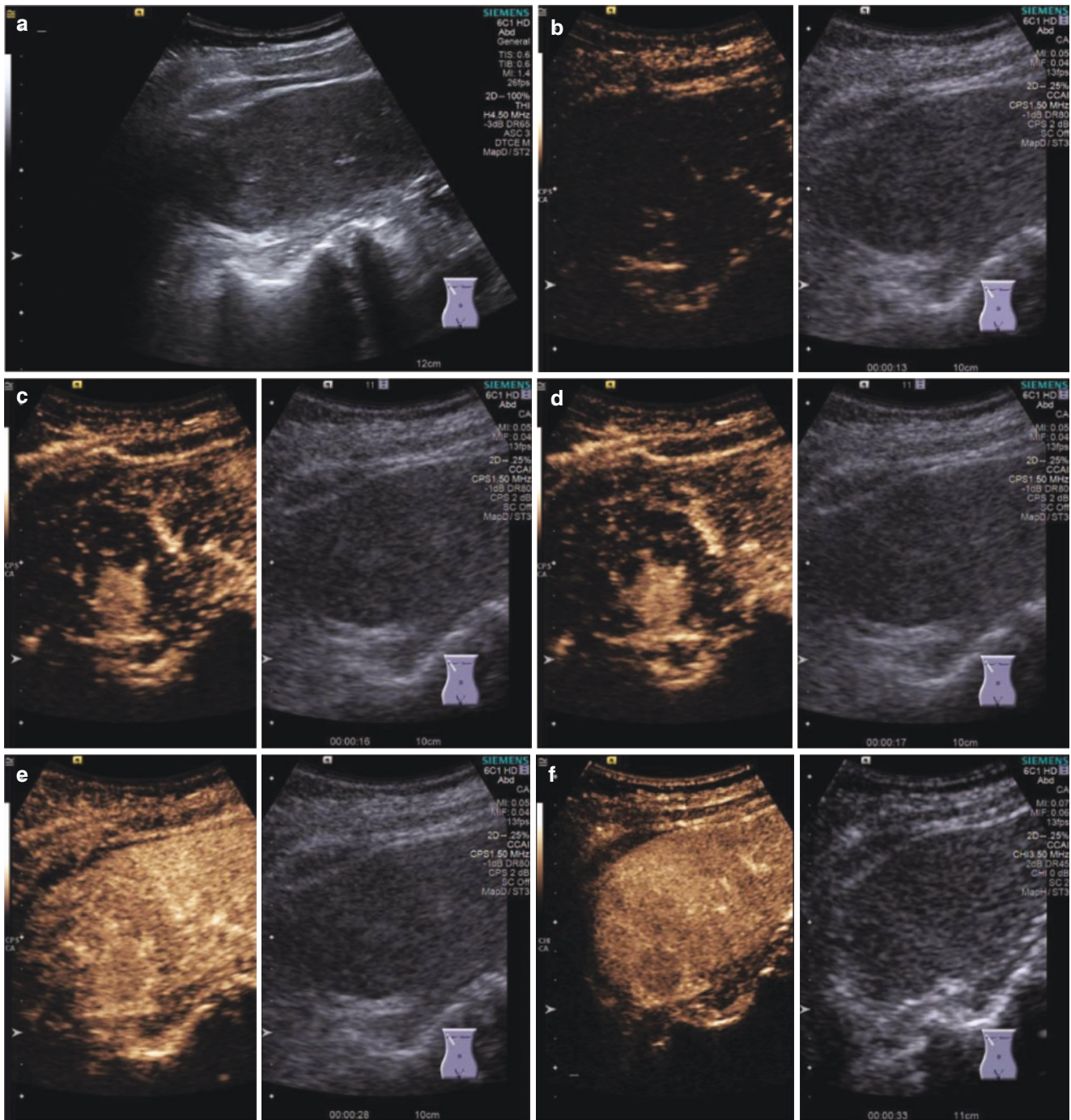
Fig. 4.37 A case of liver metastasis from breast cancer. A slightly hyperechoic lesion was found near the diaphragm in right hepatic lobe on B mode ultrasound (**a**). It was enhanced rapidly and homogeneously in arterial phase of CEUS (**b**–**e**). At 33 s after injection of SonoVue, the lesion showed rapid wash-out (**f**). It was observed hypoenhancement in both portal venous and late phases (**g**). Time intensity curve (TIC) reflected the lesion rapid "wash-in and wash-out" process (**h**)
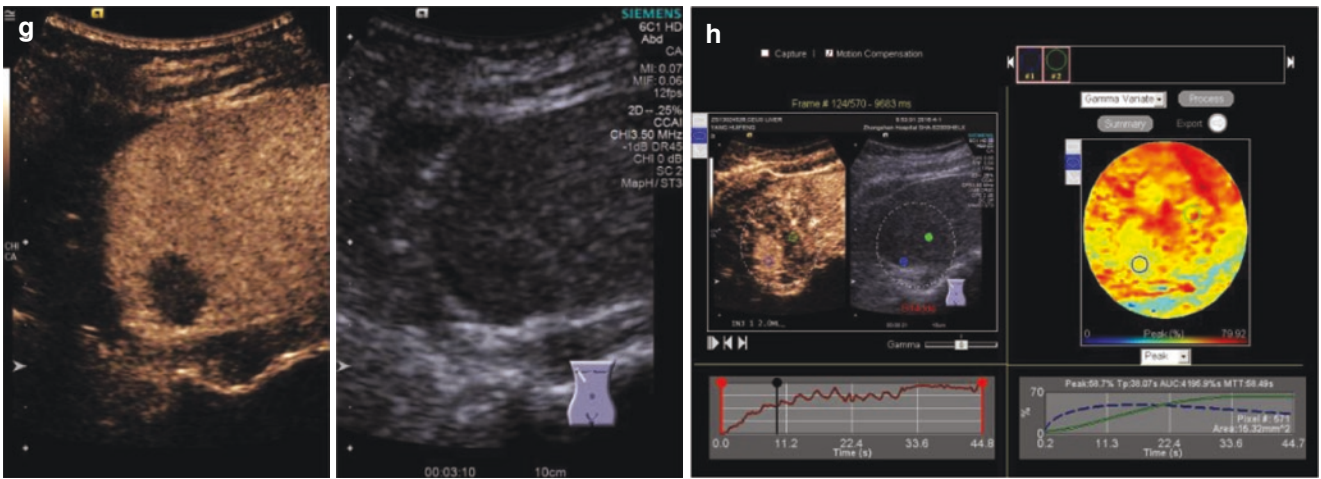
Fig. 4.37 (continued)
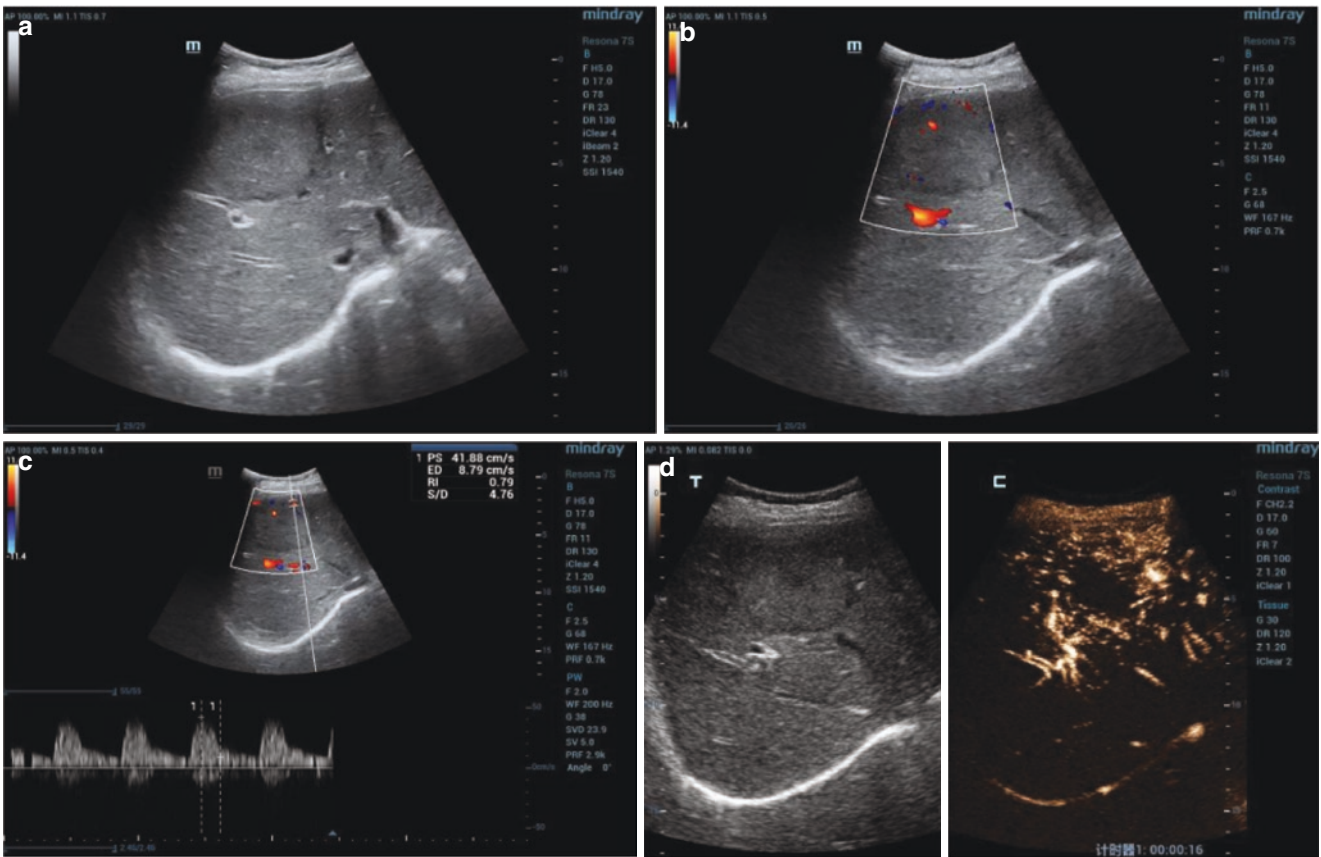
Fig. 4.38 A case of liver metastases from colon carcinoma. The lesion showed isoechoic clearly on B mode ultrasound (**a**). Few color flow signals can be detected (**b**). Arterial Doppler spectrum with low resistance index (RI) as 0.79 was measured (**c**). The lesion showed branch-like hyperenhancement in the peripheral region of the lesion and fill-in rapidly in arterial phase (**d–f**). At 33 s after injection of SonoVue, the lesions showed wash-out obviously (**g**), and became hypoenhancement in portal venous (**h**) and late phases (**i**)

Fig. 4.38 (continued)

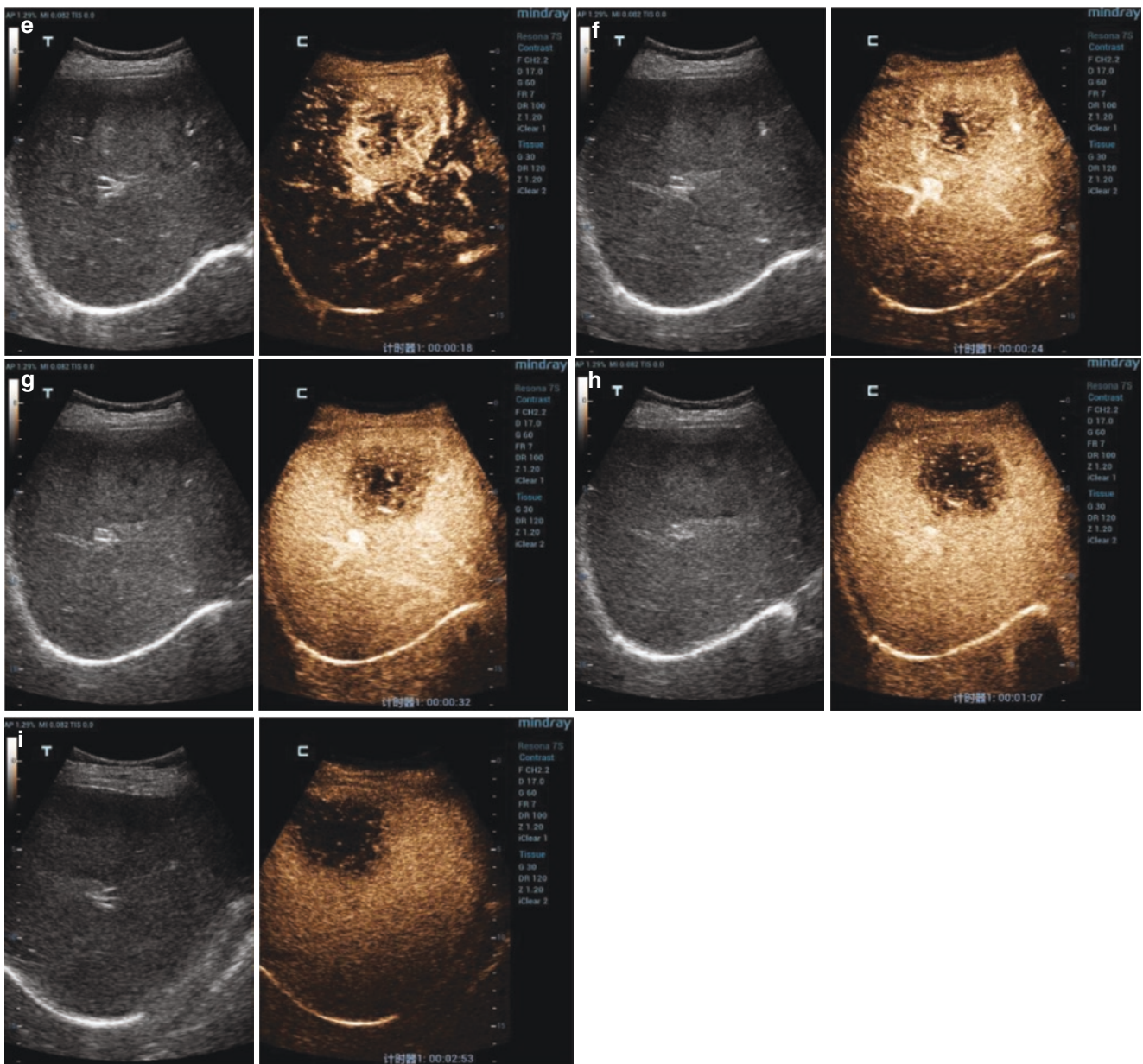ies, some DNs could manifest hypoenhancement in arterial phase (Figs. 4.46 and 4.47), because normal arterial and portal supplies reduce simultaneously [38–40].

Three types of ultrasound contrast agents (UCAs) are commonly used in liver today, including SonoVue (sulfur hexafluoride with a phospholipid shell), Definity/Luminity (octafluoropropane with a lipid shell), and Sonazoid (perflubutane with a phospholipid shell: hydrogenated egg phos-

phatidyl serine). The first two UCAs are similar in CEUS imaging manifestation. Both of them belong to vascular pool agents with slow removal over about 5 min after intravenous injection. Sonazoid is a liver-specific contrast agent that is phagocytosed by Kupffer cells on the late phase (termed "postvascular phase" or "Kupffer phase"), and can persist for several hours in the liver and spleen. By contrast, malignant liver lesions usually have few or no Kupffer cells and mani-

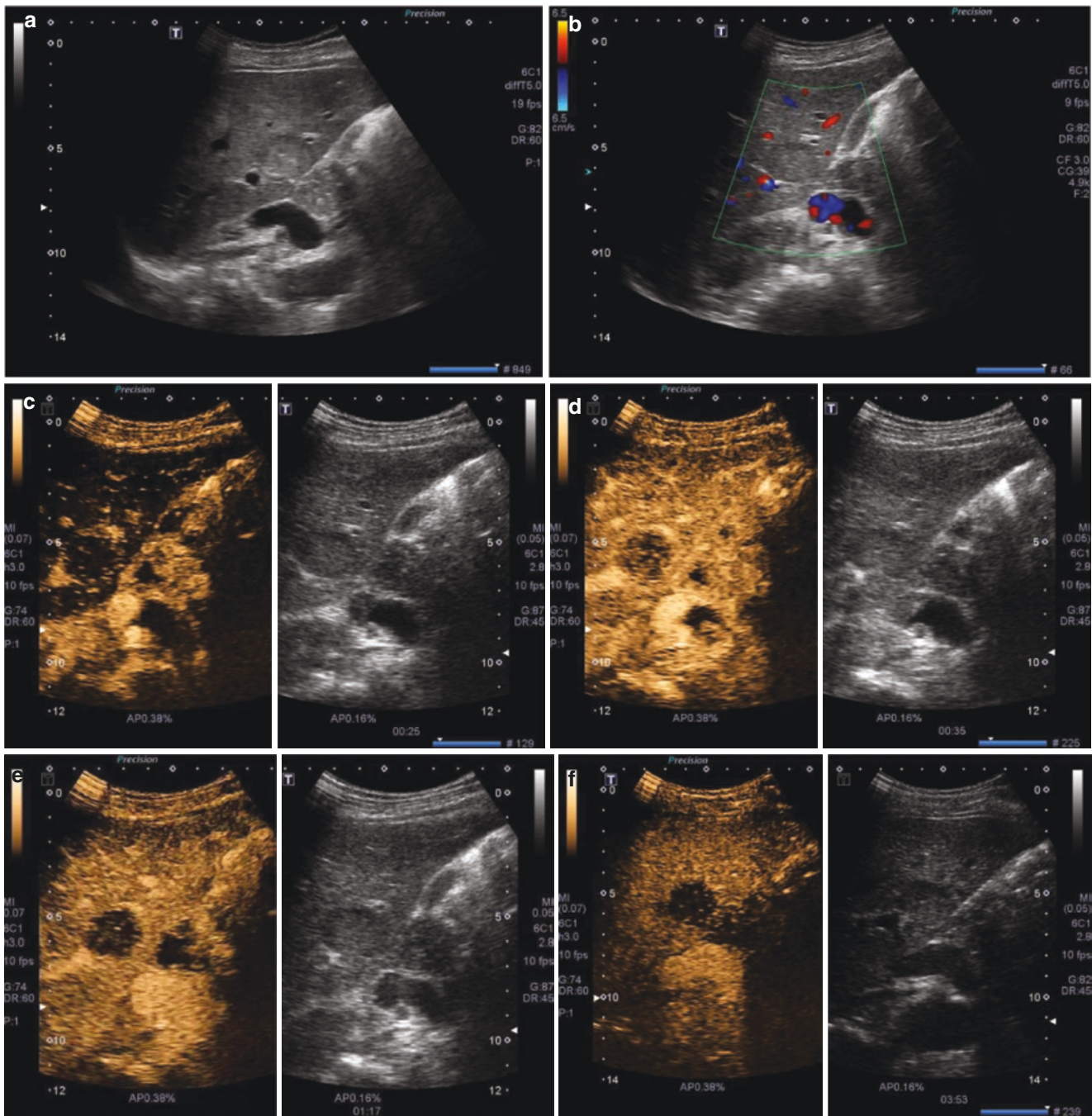**Fig. 4.39** A case of liver metastases from colon carcinoma. B mode ultrasound revealed an isoechoic focal liver lesion in right hepatic lobe (**a**). No color flow signal can be detected inside the lesion (**b**). It showed rim-like hyperenhancement in arterial phase on contrast enhanced ultrasound (CEUS) (**c**, **d**) and rapid wash-out in portal venous and late phases (**e**, **f**)
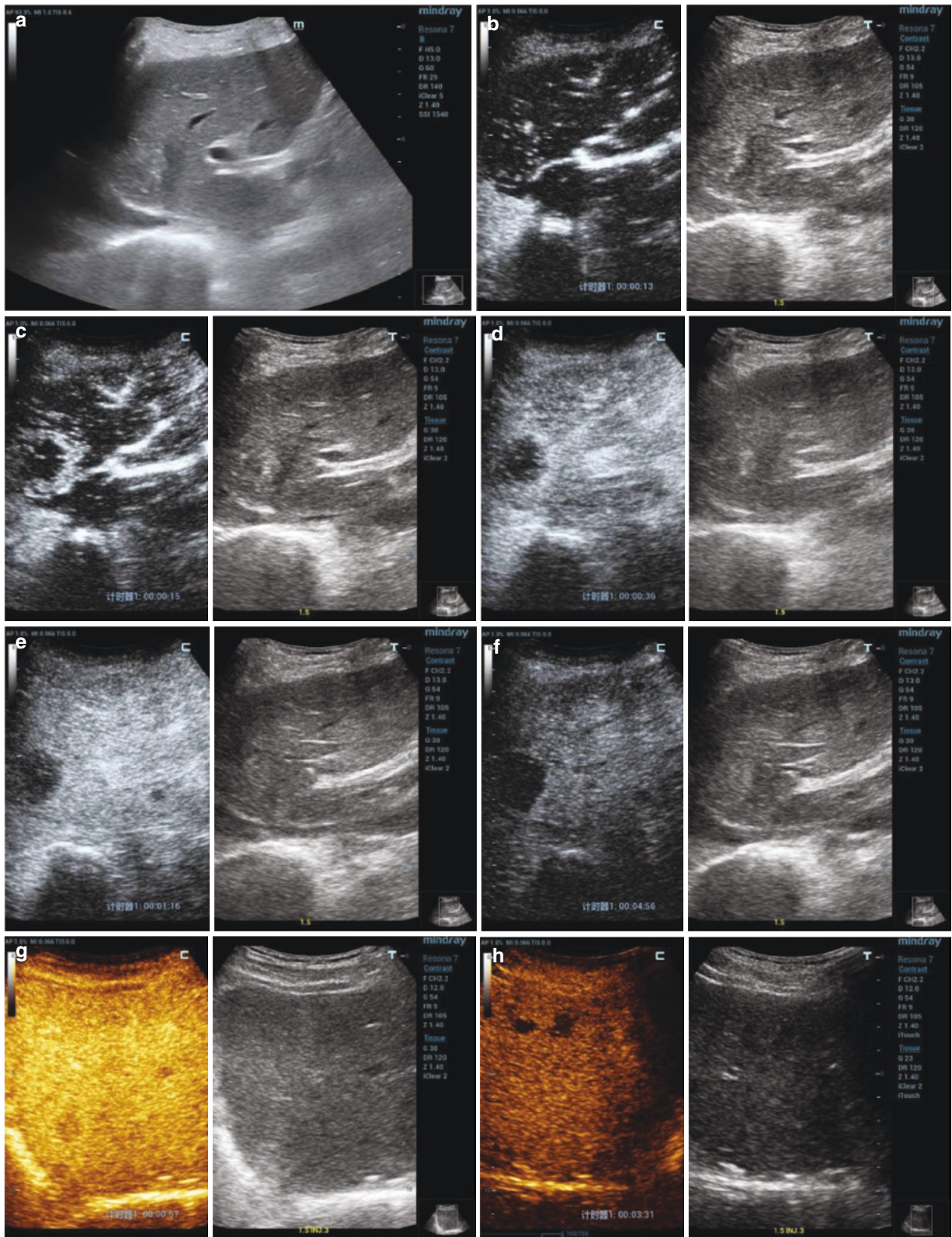
Fig. 4.40 A case of multiple liver metastases from colon carcinoma. B mode ultrasound showed a slightly hyperechoic lesion in left hepatic lobe (**a**). The lesion showed peripheral rim-like hyperenhancement during arterial phase (**b**–**d**). The lesion showed obvious hypoenhancement in portal venous and late phases (**e**, **f**). More lesions smaller than 1 cm in diameter were detected during late phase (**g**, **h**), while these small lesions were invisible on B mode ultrasound
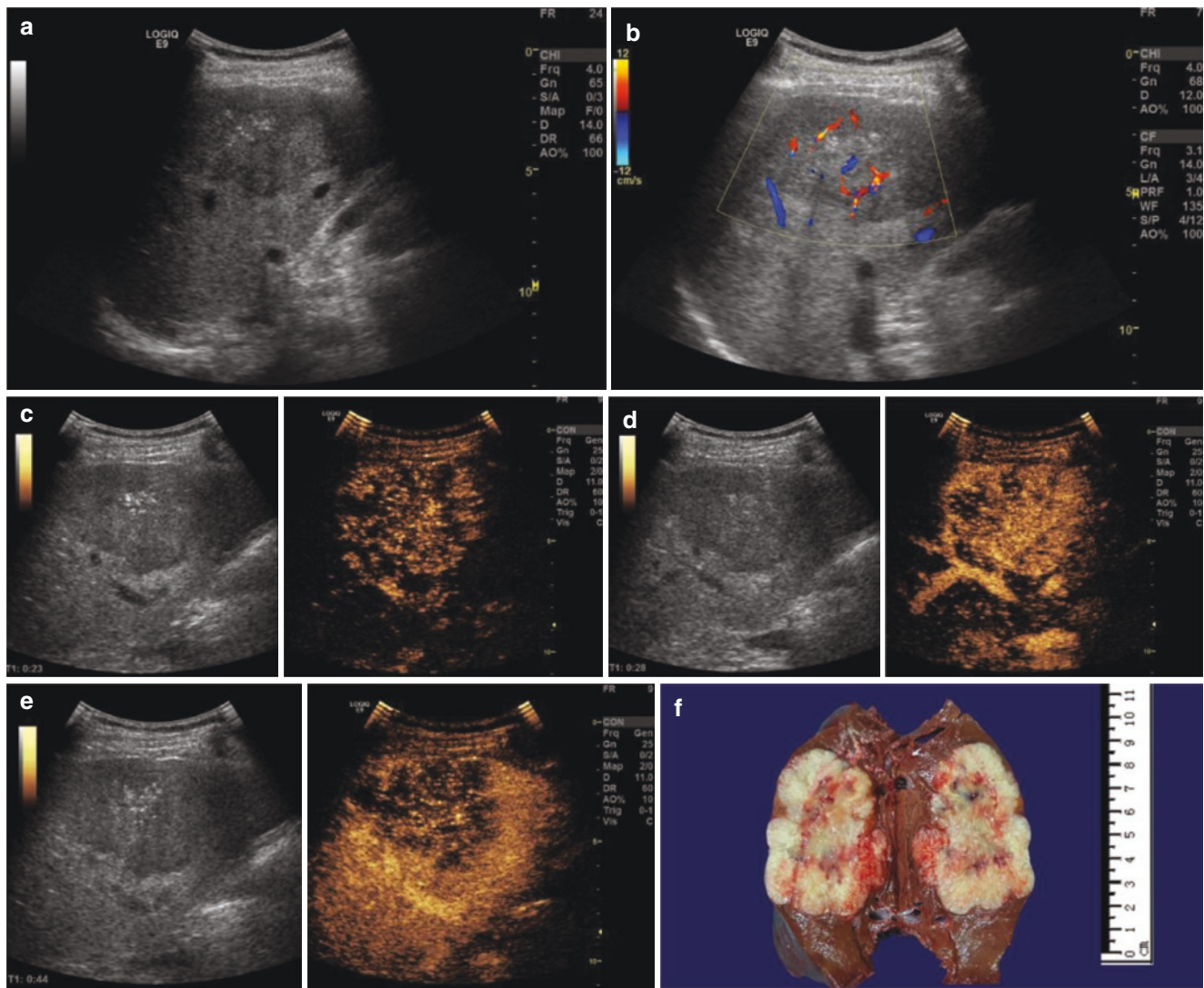
Fig. 4.41 Liver metastases from colon carcinoma. B mode ultrasound showed a heterogeneously isoechoic lesion near the surface of right hepatic lobe, and there were several scattered calcifications in the lesion (**a**). Color flow signals could be detected inside the lesion (**b**). The lesion showed rapid and heterogeneous hyperenhancement in arterial phase on contrast enhanced ultrasound (CEUS) (**c**, **d**). At 44 s after injection of SonoVue, the lesion showed obviously heterogeneous hypoenhancement (**e**). The diagnosis was confirmed by surgery and pathology (**f**)

fest contrast defect. The Kupffer defect is commonly assessed in the Kupffer phase beginning 6–10 min after intravenous injection and lasting for an hour or more. No DNs showed hypoenhancement in the Kupffer phase [41].

4.4.2.3 CT Findings
Most DNs show non-hypervascularity on arterial phase and isoattenuation on portal venous phase because of the relatively decreased normal arterial and portal venous flow. However, some HGDNs may show hyperenhancement owing to increased neoangiogenesis suggesting the potential probability of HCC transformation [36].

4.4.2.4 MRI Findings
Since MRI can provide better soft-tissue contrast and information of tissue components, current studies suggest MRI is more useful than other imaging methods to identify DNs and HCCs in the background of liver cirrhosis. Pathological changes during hepatocarcinogenesis, including increased cellular density, increased neoangiogenesis followed by decreased portal tracts and decreased OATP expression, could be reflected by various MRI techniques. Compared to CT or MRI with extracellular contrast agents, Gd-EOB-DTPA-enhanced MRI (using a kind of liver-specific contrast agent) can improve the diagnostic accuracy of DNs and
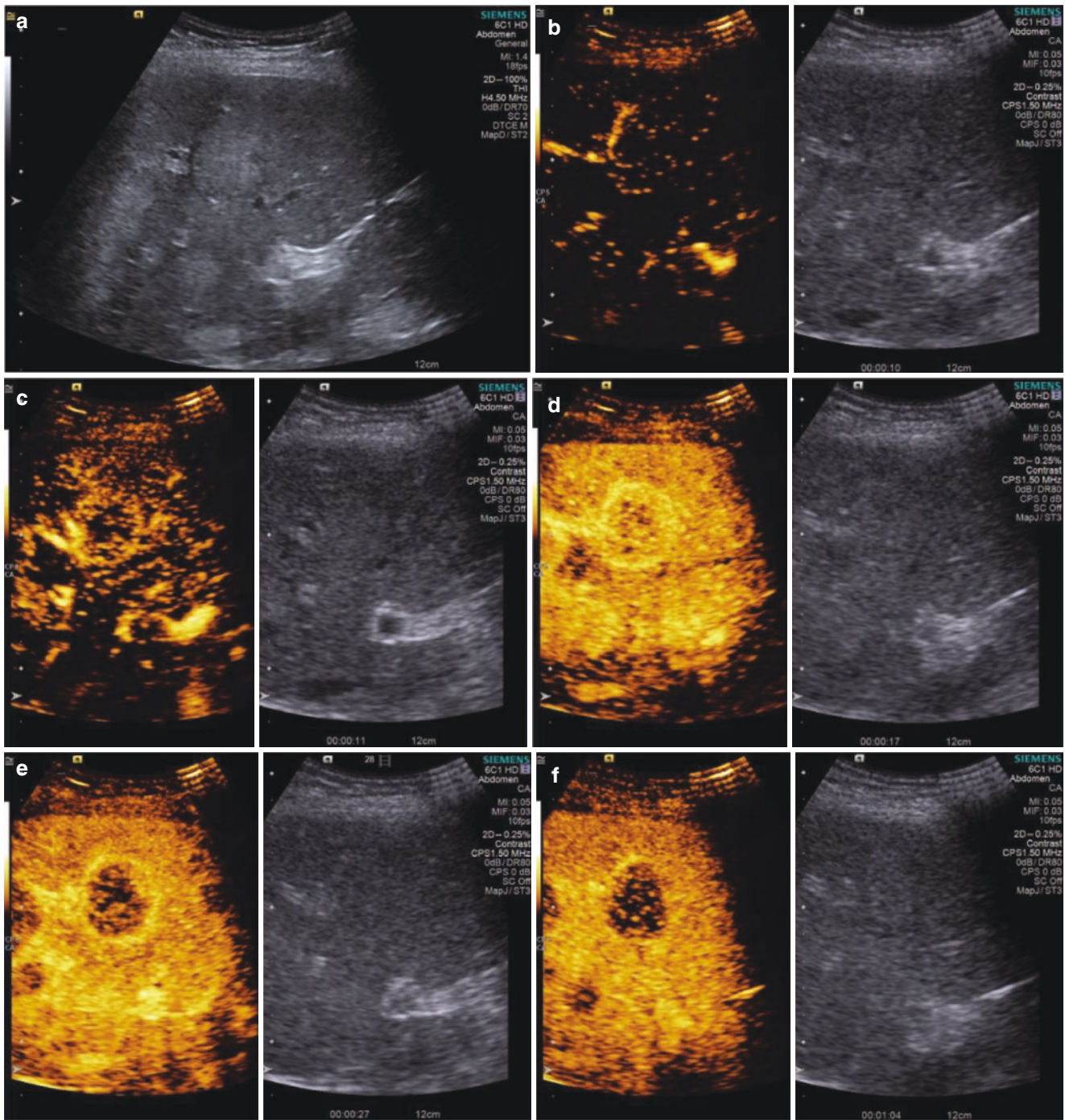
Fig. 4.42 A case of multiple liver metastases of colon carcinoma. B mode ultrasound image revealed several slightly hyperchoic lesions with unclear boundaries in right lobe of liver (**a**). The lesion showed rim-like enhancement and rapid fill-in immediately during early arterial phase (**b–d**). The lesion showed rapid wash-out in late arterial phase (**e**) and portal venous phase (**f**). In this phase, more lesions with clear boundaries can be observed (**g**, **h**)
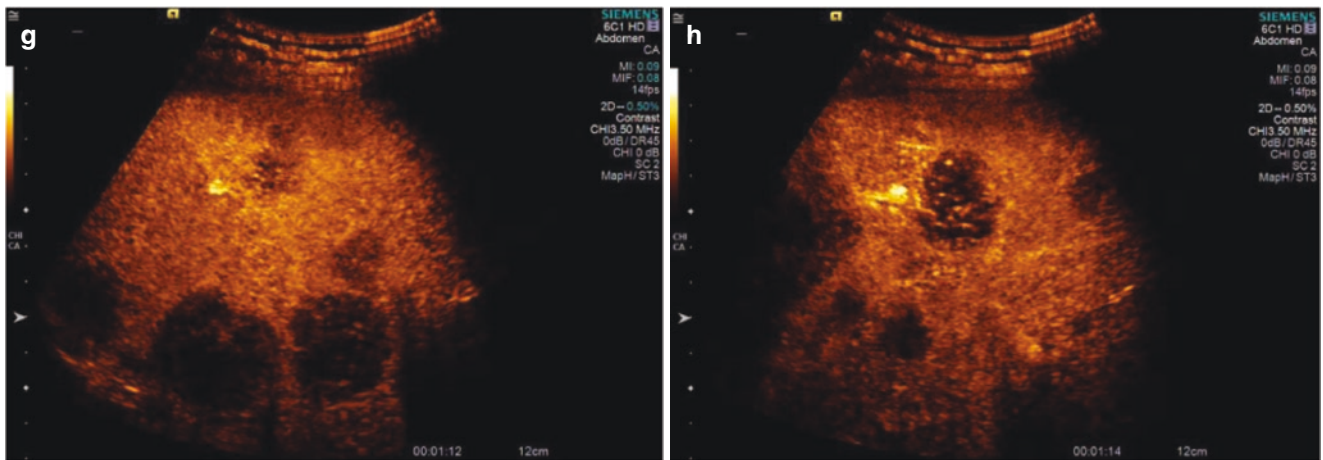
Fig. 4.42 (continued)
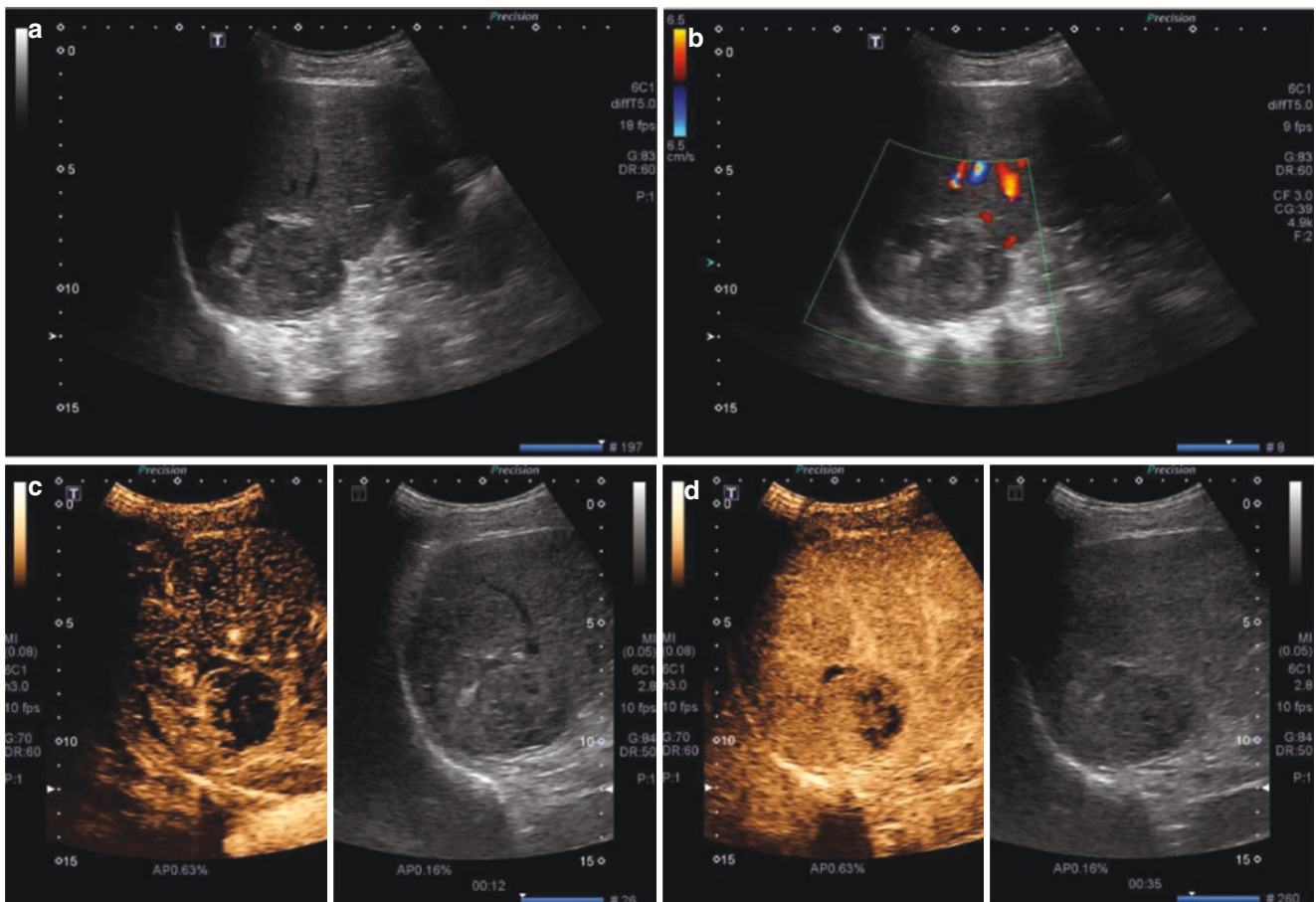
Fig. 4.43 A case of liver metastasis from nasopharyngeal carcinoma. B mode ultrasound revealed a heterogeneous isoechoic lesion in right lobe of liver (**a**). Color flow signals could be detected around the lesion (**b**). The lesion showed heterogeneous enhancement during arterial phase (**c**, **d**). The lesion showed rapid wash-out in portal venous and in late phases (**e**, **f**). On 1 day after TACE treatment, the lesion was hyperechoic on B mode ultrasound (**g**). No color flow signal could be detected (**h**). The lesion showed nonenhancement during CEUS (**i**)

Fig. 4.43 (continued)

Fig. 4.44 Nourishing vessels changes in hepatocarcinogenesis in cirrhotic liver. Hepatocellular carcinoma (HCC)

HCCs and the sensitivity for the detection of HCCs, especially small HCCs. Before neoangiogenesis in an overt HCC, imaging feature of non-enhancement followed by hypointense on hepatobiliary phase is a strong predictor of precancerous lesion or malignancy (Fig. 4.45) [41].
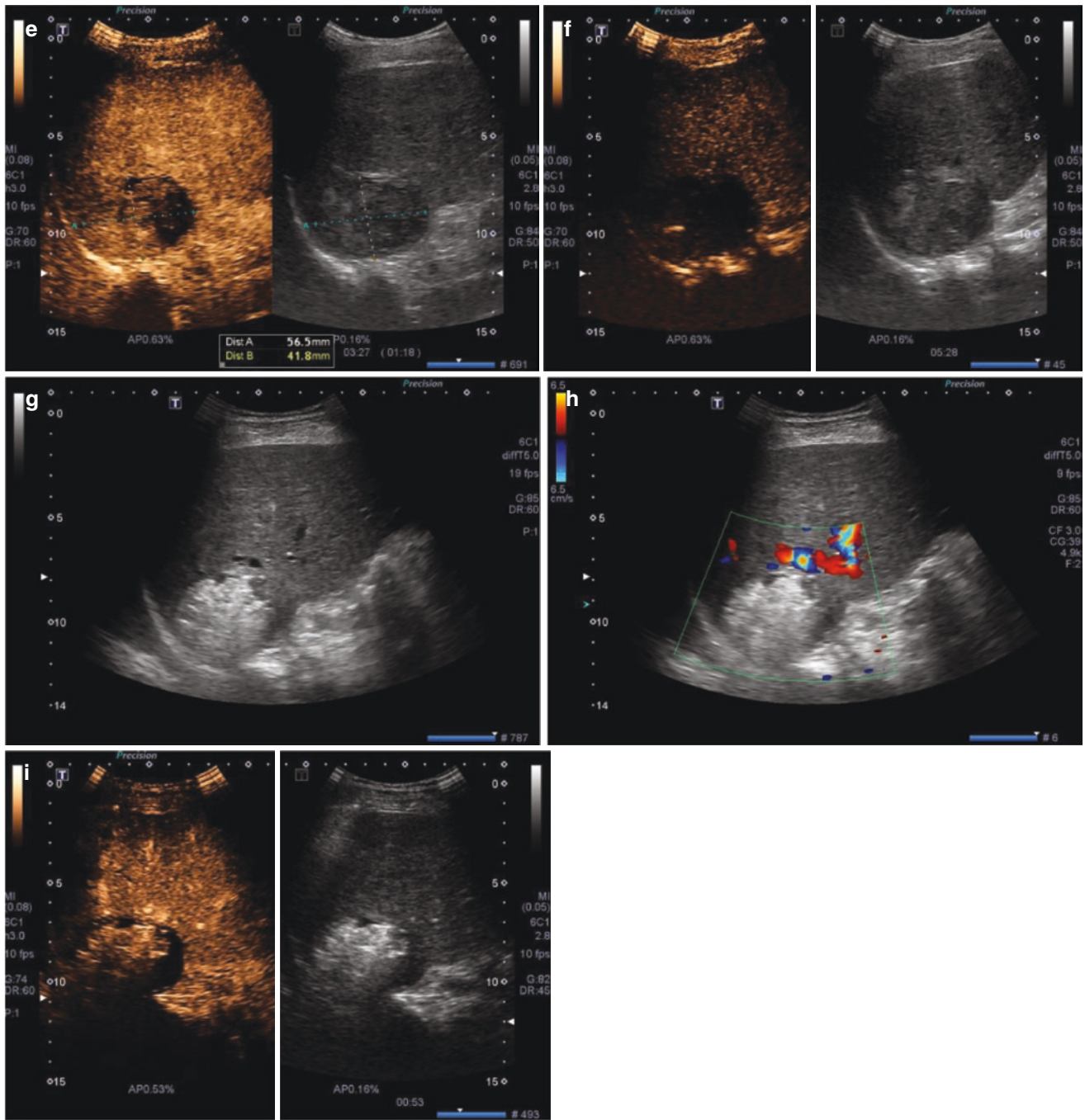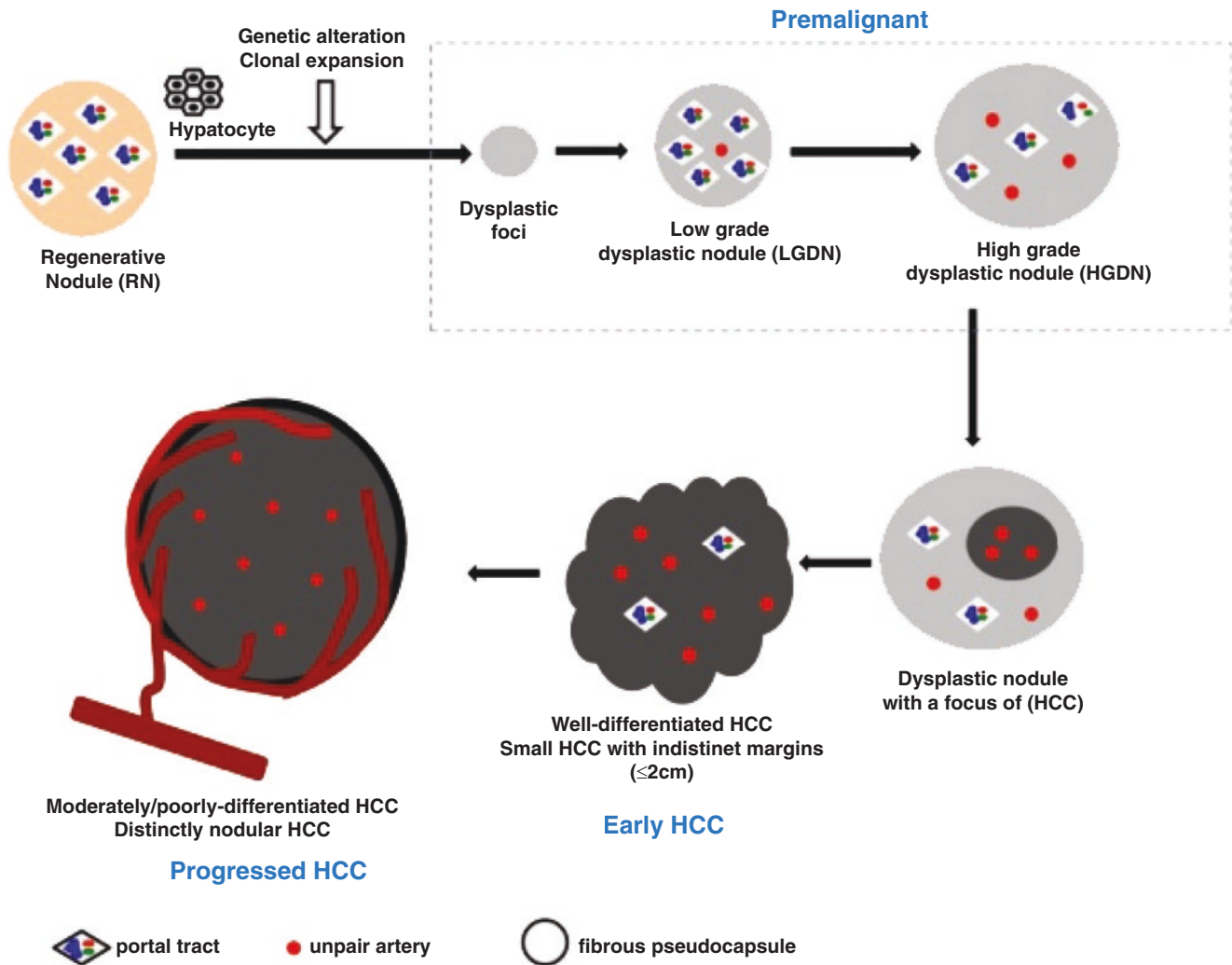
4.4.2.5 Best Imaging Protocol Advices

- US every 6 months is universally recommended for patients with high risk of HCC. When DNs are present, they are usually small and difficult to be distinguished from RNs by US.
- On CEUS, DNs typically show iso-or hypoenhancement on the arterial phase and isoenhancement on subsequent phases.
- On Gd-EOB-DTPA-enhanced MRI, non-enhancement followed by hypointense on hepatobiliary phase is a strong predictor of precancerous lesion or malignancy (HGDN or early HCC).

4.4.3 Differential Diagnosis

Regerative nodulars

Regerative nodulars (RNs) are usually smaller than 10 mm and innumerable in liver cirrhosis. On CEUS, RNs usually show isoenhancement in the arterial phase. Nearly all RNs show isoenhancement in the portal venous and late phases.

Well-differentiated hepatocellular carcinoma

About 40% of well-differentiated hepatocellular carcinoma (HCCs) demonstrated non-hyperenhancement in the arterial phase on CEUS. Some well-differentiated HCCs manifesting arterial hypoenhancement are confirmed pathologically to have fewer unpaired arteries. Furthermore, 60–90% of well-differentiated HCCs showed almost complete isoenhancement in the portal vein phase and late phase, even though Sonazoid is used. Therefore, DNs and well-differentiated HCCs maybe both hypoenhancement in the

Fig. 4.45 Features of dysplasia nodular (DN) on conventional ultrasound and contrast enhanced ultrasound (CEUS). A hyperechoic lesion in the right lobe of liver, with ill-defined margin (arrow) (**a**). Color flow imaging showed portal veins signals around the lesion (**b**). Arterial phase isoenhancement on CEUS (arrow) (**c**). Persisting isoenhancement during portal venous and late phase on CEUS (arrow) (**d**). The lesion showed slight hyperintensity on T1-weighted in-phase image (arrow) (**e**) and loss of signal on out-of-phase on pre-enhanced T1-weighted imaging, suggesting fat content in the lesion (arrow) (**f**). Isointensity on pre-enhanced T2-weighted imaging (arrow) (**g**). Non-enhancement on arterial phase on Gd-EOB-DTPA-enhanced MRI (arrow) (**h**). Hypointensity on hepatobiliary phase on Gd-EOB-DTPA-enhanced MRI (**i**)
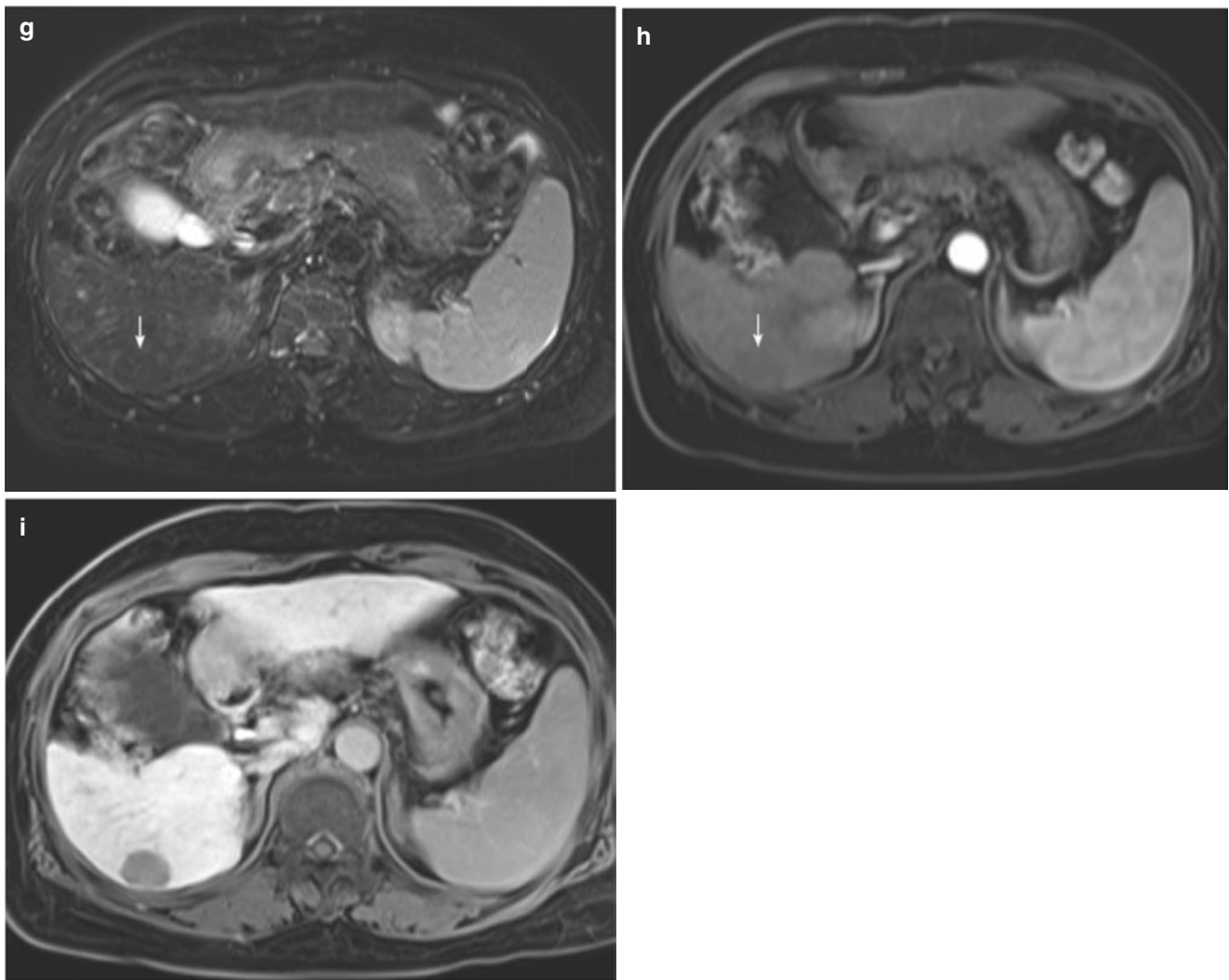
Fig. 4.45 (continued)

arterial phase and isoenhancement in the late phase or in the Kupffer phase on CEUS [36, 39]. To a certain extent, imaging features between HGDNs and well-differentiated HCCs are overlapping, accurate recognition of HGDNs and well-differentiated HCCs is still challenging, not only on CEUS but also on CT and MRI.

The American Association for the Study of Liver Diseases (AASLD) recommends that biopsy is necessary for hepatic lesions less than 2 cm in liver cirrhosis without typical HCC imaging findings, whereas biopsy is not needed for hepatic lesions with characteristic HCC imaging finding [42]. It should be noted that biopsy diagnosis of hepatic border nodules may be also a challenge, because minute biopsy specimens may be inadequate to detect stromal invasion. Core liver biopsy is more recommended than fine needle aspiration, because the specimen obtained is more sufficient and suitable for assessment. Furthermore, the tissue block obtained can be assessed by immunohistochemical technique.

4.4.4 Pathology

4.4.4.1 General Features
DNs may be single or multiple, and may have distinct or indistinct margins on gross examination. The size of DNs ranges from few millimeters to few centimeters. The diameter of most DNs is <15 mm. Based on varying degrees of atypia, DNs are divided into LGDN and HGDN [35].

Low-grade dysplasia nodular
Low-grade dysplasia nodular (LGDNs) usually have no true capsule, but are still distinct from the surrounding cirrhotic liver parenchyma with fibrous tissue around. LGDNs show moderate cell density increase with a homogeneous pattern, and have no cytologic atypia. Large cell changes could be usually found, but there have no architectural changes. Pseudoglands or markedly thickened trabeculaes are nonexistent. Some HGDNs have a few unpaired arteries. Nodule-
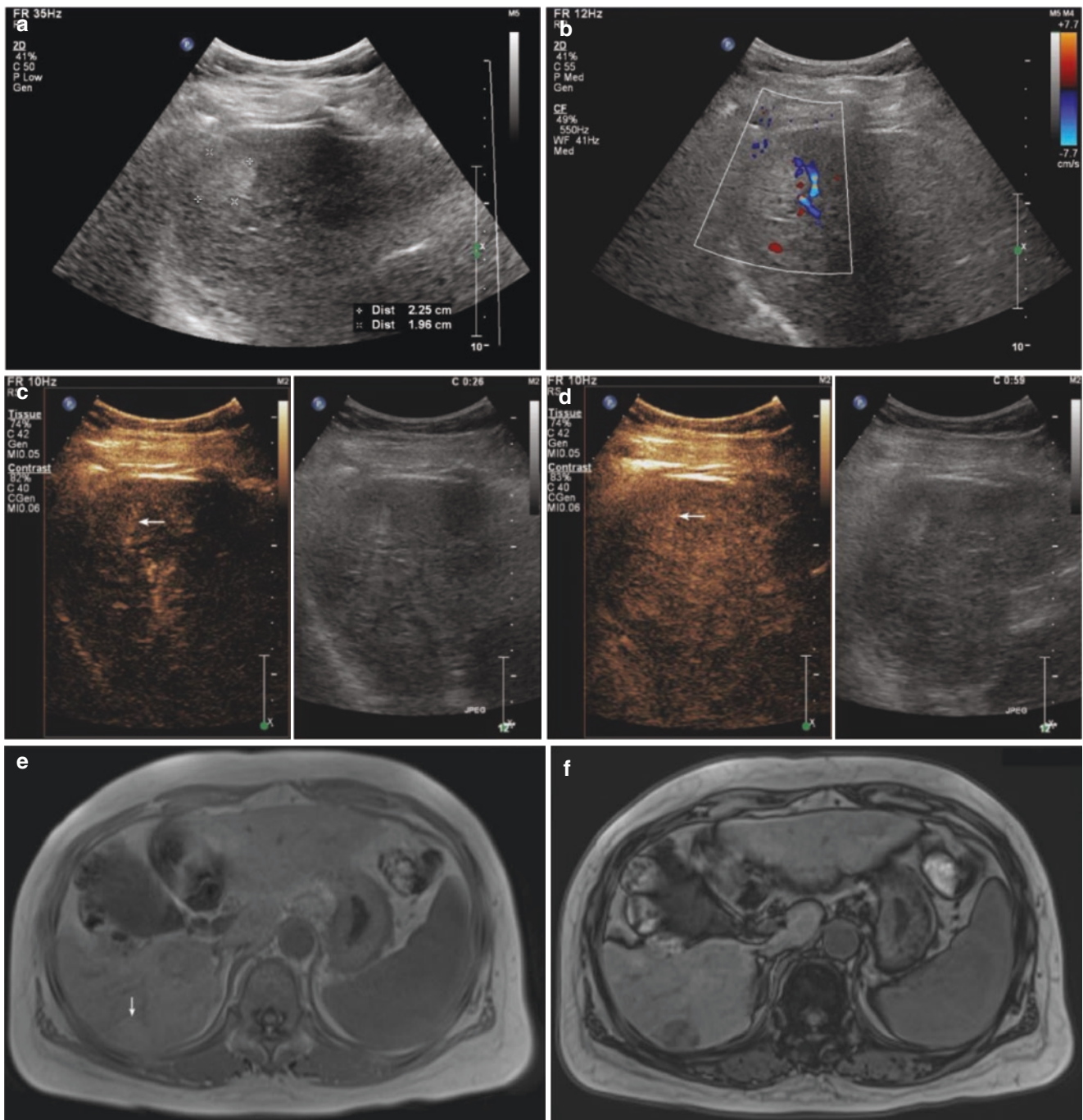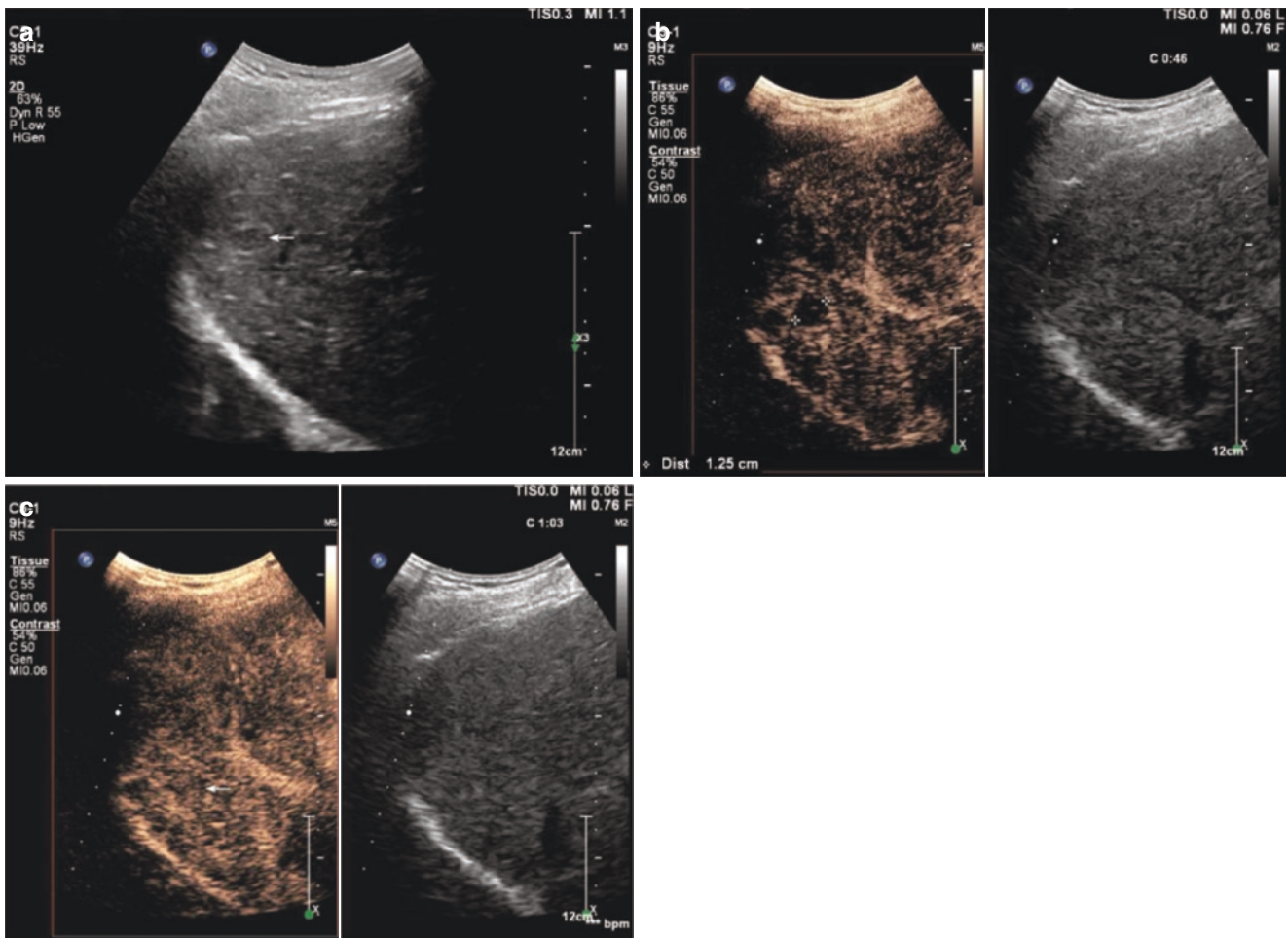
Fig. 4.46 Features of dysplasia nodular (DN) on conventional ultrasound and contrast enhanced ultrasound (CEUS). A hypoechoic lesion in the right lobe of liver (arrow) (**a**). Arterial phase hypoenhancement on CEUS (**b**). Isoenhancement on portal venous and late phases (arrow) (**c**)

in-nodule type do not appear in LGDNs. Recognition from LGDNs to large regenerative nodules (RNs) is difficult or impossible. Fortunately, there has no significant clinical application value to make a distinction between LGDNs and large RNs at present.

High-grade dysplasia nodular

High-grade dysplasia nodulars (HGDNs) have a distinct or vague margin in the background of cirrhosis. They also lack true capsules, similar to LGDNs. HGDNs commonly have architectural and/or cytologic atypia, but the atypia is not enough to diagnose as HCCs. Increased cell density with an irregular trabecular pattern is often present, and it is usually more than 2–3 times higher than the liver parenchyma. Small cell change is the most commonly seen in HGDNs. Large cell change sometimes can be seen in HGDNs. Other cytological changes, including clear cell change, focal fatty change, and resistance to iron accumulation distinguish

HGDN from LGDN. Most HGDNs have some but not in great number of unpaired arteries. Nodule-in-nodule type is occasionally found in HGDNs. The subnodule is usually well-differentiated HCC with a well-defined margin. The most appropriate term for such lesions is "HCC arising in DN." Definite distinction between HGDN and well-differentiated HCC may be difficult, especially on needle biopsy material. Stromal invasion is a diagnostic criterion for the distinction of HGDN and well-differentiated HCC, and immunostaining for keratins 7 or 19 may be useful for an accurate diagnosis of stromal invasion.

4.4.5   Clinical Issues

4.4.5.1 Presentation

DNs may be single or multiple in cirrhotic liver, and are occasionally found in non-cirrhotic liver.
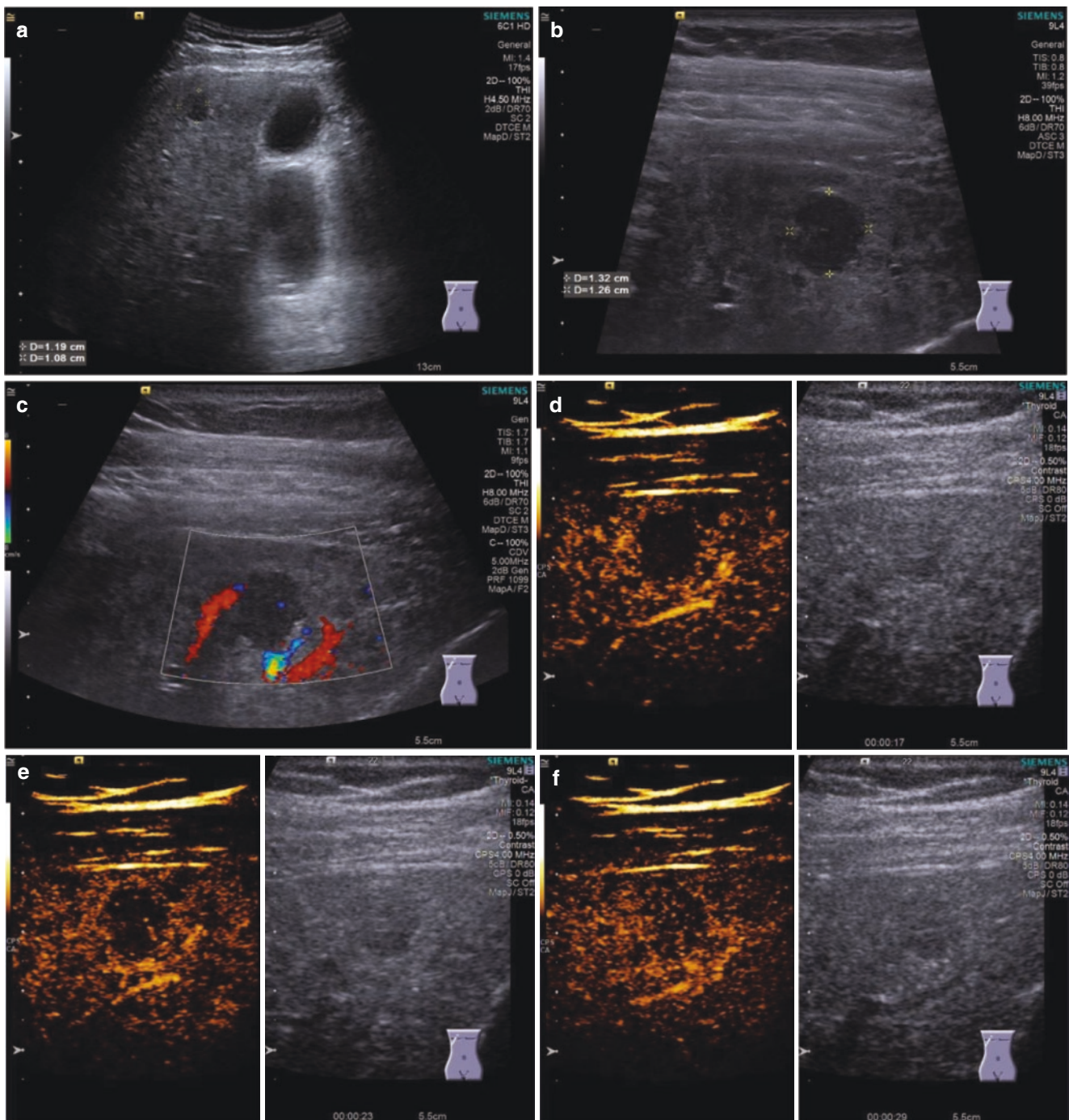
Fig. 4.47 Features of dysplasia nodular (DN) on conventional ultrasound and contrast enhanced ultrasound (CEUS). A hypoechoic lesion in the right lobe of liver was detected by B mode ultrasound with low-frequency transducer (4.5 MHz) (**a**) and high-frequency linear trans-ducer (8.0 MHz) (**b**). Dotted blood signal inside the lesion on color flow imaging (**c**). Arterial phase hypoenhancement followed by gradual isoenhancement on portal venous and late phases on CEUS (**d**–**g**)

Fig. 4.47 (continued)

4.4.5.2 Prognosis

A previous study reported that 27–70% of DNs would enlarge; and the rate of evolution to malignancy was 40–80% [43, 44].

4.4.5.3 Treatment

It is very important to observe the changes in nodule size and blood supply in DNs during the follow-up period in order to predict the development of HCCs as soon as possible.

References

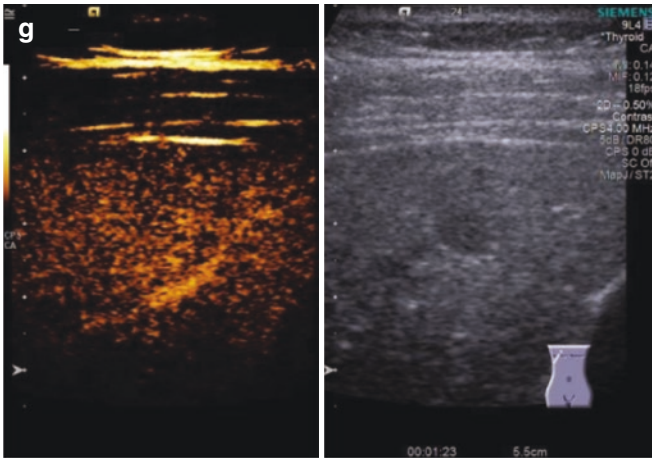1. Bansal S, Gui J, Merrill C, Wong JK, Burak KW, Wilson SR. Contrast-enhanced US in local ablative therapy and secondary surveillance for hepatocellular carcinoma. Radiographics. 2019;39:1302–22.
2. Villanueva A. Hepatocellular carcinoma. N Engl J Med. 2019;380:1450–62.
3. Leoni S, Piscaglia F, Granito A, Borghi A, Galassi M, Marinelli S, Terzi E, et al. Characterization of primary and recurrent nodules in liver cirrhosis using contrast-enhanced ultrasound: which vascular criteria should be adopted? Ultraschall Med. 2013;34:280–7.
4. Dietrich CF, Teufel A, Sirlin CB, Dong Y. Surveillance of hepatocellular carcinoma by medical imaging. Quant Imaging Med Surg. 2019;9:1904–10.
5. Yanagisawa K, Moriyasu F, Miyahara T, Yuki M, Iijima H. Phagocytosis of ultrasound contrast agent microbubbles by Kupffer cells. Ultrasound Med Biol. 2007;33:318–25.
6. Kudo M, Hatanaka K, Kumada T, Toyoda H, Tada T. Double-contrast ultrasound: a novel surveillance tool for hepatocellular carcinoma. Am J Gastroenterol. 2011;106:368–70.
7. Numata K, Fukuda H, Nihonmatsu H, Kondo M, Nozaki A, Chuma M, Morimoto M, et al. Use of vessel patterns on contrast-enhanced ultrasonography using a perflubutane-based contrast agent for the differential diagnosis of regenerative nodules from early hepatocellular carcinoma or high-grade dysplastic nodules in patients with chronic liver disease. Abdom Imaging. 2015;40:2372–83.
8. Lencioni R, Piscaglia F, Bolondi L. Contrast-enhanced ultrasound in the diagnosis of hepatocellular carcinoma. J Hepatol. 2008;48:848–57.
9. Choi BI, Lee JM, Kim TK, Dioguardi Burgio M, Vilgrain V. Diagnosing borderline hepatic nodules in hepatocarcinogenesis: imaging performance. AJR Am J Roentgenol. 2015;205:10–21.
10. Quaia E. State of the art: LI-RADS for contrast-enhanced US. Radiology. 2019;293:4–14.
11. Dietrich CF, Dong Y, Kono Y, Caraiani C, Sirlin CB, Cui XW, Tang A. LI-RADS ancillary features on contrast-enhanced ultrasonography. Ultrasonography. 2020;39:221–8.
12. Jang HJ, Kim TK, Wilson SR. Small nodules (1-2 cm) in liver cirrhosis: characterization with contrast-enhanced ultrasound. Eur J Radiol. 2009;72:418–24.
13. Knieling F, Waldner MJ, Goertz RS, Zopf S, Wildner D, Neurath MF, Bernatik T, et al. Early response to anti-tumoral treatment in hepatocellular carcinoma–can quantitative contrast-enhanced ultrasound predict outcome? Ultraschall Med. 2013;34:38–46.
14. Weber SM, Ribero D, O'Reilly EM, Kokudo N, Miyazaki M, Pawlik TM. Intrahepatic cholangiocarcinoma: expert consensus statement. HPB (Oxford). 2015;17(8):669–80.
15. Nakanuma Y, Curado MP, Franceschi S, et al. Intrahepatic cholangiocarcinoma. In: Bosman FT, Carneiro F, Hruban RH, et al., editors. WHO classification of tumours of the digestive system. 4th ed. Lyon: International Agency for Research on Cancer; 2010. p. 217–24.
16. Liu GJ, Wang W, Lu MD, et al. Contrast-enhanced ultrasound for the characterization of hepatocellular carcinoma and intrahepatic cholangiocarcinoma. Liver Cancer. 2015;4(4):241–52.
17. Wildner D, Pfeifer L, Goertz RS, et al. Dynamic contrast-enhanced ultrasound (DCE-US) for the characterization of hepatocellular carcinoma and cholangiocellular carcinoma. Ultraschall Med. 2014;35(6):522–7.
18. Galassi M, Iavarone M, Rossi S, et al. Patterns of appearance and risk of misdiagnosis of intrahepatic cholangiocarcinoma in cirrhosis at contrast enhanced ultrasound. Liver Int. 2013;33(5):771–9.
19. Claudon M, Dietrich CF, Choi BI, et al. Guidelines and good clinical practice recommendations for contrast enhanced ultrasound (CEUS) in the liver–update 2012: a WFUMB-EFSUMB initiative in cooperation with representatives of AFSUMB, AIUM, ASUM, FLAUS and ICUS. Ultraschall Med. 2013;34(1):11–29.
20. Vilana R, Forner A, Bianchi L, et al. Intrahepatic peripheral cholangiocarcinoma in cirrhosis patients may display a vascular pattern similar to hepatocellular carcinoma on contrast-enhanced ultrasound. Hepatology. 2010;51(6):2020–9.
21. Li F, Li Q, Liu Y, et al. Distinguishing intrahepatic cholangiocarcinoma from hepatocellular carcinoma in patients with and without risks: the evaluation of the LR-M criteria of contrast-enhanced ultrasound liver imaging reporting and data system version 2017. Eur Radiol. 2020;30(1):461–70.
22. Guo LH, Xu HX. Contrast-enhanced ultrasound in the diagnosis of hepatocellular carcinoma and intrahepatic cholangiocarcinoma: controversy over the ASSLD guideline. Biomed Res Int. 2015;2015:349172.
23. Wildner D, Bernatik T, Greis C, Seitz K, Neurath MF, Strobel D. CEUS in hepatocellular carcinoma and intrahepatic cholangiocellular carcinoma in 320 patients – early or late washout matters: a subanalysis of the DEGUM multicenter trial. Ultraschall Med. 2015;36(2):132–9.
24. Kono Y, Lyshchik A, Cosgrove D, et al. Contrast Enhanced Ultrasound (CEUS) Liver Imaging Reporting and Data System

(LI-RADS®): the official version by the American College of Radiology (ACR). Ultraschall Med. 2017;38(1):85–6.

25. Fábrega-Foster K, Ghasabeh MA, Pawlik TM, Kamel IR. Multimodality imaging of intrahepatic cholangiocarcinoma. Hepatobiliary Surg Nutr. 2017;6(2):67–78.

26. Heimbach JK, Kulik LM, Finn RS, et al. AASLD guidelines for the treatment of hepatocellular carcinoma. Hepatology. 2018;67(1):358–80.

27. Galle PR, Forner A, Llovet JM, et al. EASL Clinical Practice Guidelines: management of hepatocellular carcinoma. J Hepatol. 2018;69(1):182–236.

28. Seo N, Kim DY, Choi JY. Cross-sectional imaging of intrahepatic cholangiocarcinoma: development, growth, spread, and prognosis. AJR Am J Roentgenol. 2017;209(2):64–75.

29. Dietrich CF, Tana C, Caraiani C, Dong Y. Contrast enhanced ultrasound (CEUS) imaging of solid benign focal liver lesions. Expert Rev Gastroenterol Hepatol. 2018;12:479–89.

30. Dong Y, Zhang XL, Mao F, Huang BJ, Si Q, Wang WP. Contrast-enhanced ultrasound features of histologically proven small (</=20 mm) liver metastases. Scand J Gastroenterol. 2017;52:23–8.

31. D'Onofrio M, Crosara S, De Robertis R, Canestrini S, Mucelli RP. Contrast-enhanced ultrasound of focal liver lesions. AJR Am J Roentgenol. 2015;205:W56–66.

32. Lu Q, Zhang XL, Han H, Huang BJ, Ding H, Wang WP. Value of perfusion parameters for differentiating hepatocellular carcinoma and liver metastasis with hypervascularity and a normal hepatic background on contrast-enhanced ultrasound imaging. J Ultrasound Med. 2019;38:2601–8.

33. Schulz A, Dormagen JB, Drolsum A, Bjornbeth BA, Labori KJ, Klow NE. Impact of contrast-enhanced intraoperative ultrasound on operation strategy in case of colorectal liver metastasis. Acta Radiol. 2012;53:1081–7.

34. Choi SH, Kim SY, Park SH, Kim KW, Lee JY, Lee SS, Lee MG. Diagnostic performance of CT, gadoxetate disodium-enhanced MRI, and PET/CT for the diagnosis of colorectal liver metastasis: systematic review and meta-analysis. J Magn Reson Imaging. 2018;47:1237–50.

35. Pathologic diagnosis of early hepatocellular carcinoma: a report of the international consensus group for hepatocellular neoplasia. Hepatology 2009;49:658–664.

36. Park HJ, Choi BI, Lee ES, Park SB, Lee JB. How to differentiate borderline hepatic nodules in hepatocarcinogenesis: emphasis on imaging diagnosis. Liver Cancer. 2017;6:189–203.

37. Theise ND, Curado MP, Franceschi S, Hytiroglou P, Kudo M, Park YN, Sakamoto M, Torbenson M, Wee A. Hepatocellular carcinoma. In: Bosman FT, Carneiro F, Hruban RH, et al., editors. WHO classification of tumours of the digestive system. 4th ed. Lyon: International Agency for Research on Cancer; 2010. p. 195–254.

38. Shin SK, Kim YS, Choi SJ, Shim YS, Jung DH, Kwon OS, Choi DJ, et al. Contrast-enhanced ultrasound for the differentiation of small atypical hepatocellular carcinomas from dysplastic nodules in cirrhosis. Dig Liver Dis. 2015;47:775–82.

39. Claudon M, Dietrich CF, Choi BI, Cosgrove DO, Kudo M, Nolsøe CP, Piscaglia F, et al. Guidelines and good clinical practice recommendations for Contrast Enhanced Ultrasound (CEUS) in the liver – update 2012: a WFUMB-EFSUMB initiative in cooperation with representatives of AFSUMB, AIUM, ASUM, FLAUS and ICUS. Ultrasound Med Biol. 2013;39:187–210.

40. Pei-li F, Han-sheng X, Hong D, Dong Y, Ling-li C, Wang W-p. Characterization of early hepatocellular carcinoma and high-grade dysplastic nodules on contrast-enhanced ultrasound: correlation with histopathologic findings. J Ultrasound Med. 2020;39:1799–808.

41. Ohama H, Imai Y, Nakashima O, Kogita S, Takamura M, Hori M, Seki Y, et al. Images of Sonazoid-enhanced ultrasonography in multistep hepatocarcinogenesis: comparison with Gd-EOB-DTPA-enhanced MRI. J Gastroenterol. 2014;49:1081–93.

42. Heimbach JK, Kulik LM, Finn RS, Sirlin CB, Abecassis MM, Roberts LR, Zhu AX, et al. AASLD guidelines for the treatment of hepatocellular carcinoma. Hepatology. 2018;67:358–80.

43. Kobayashi M, Ikeda K, Hosaka T, Sezaki H, Someya T, Akuta N, Suzuki F, et al. Dysplastic nodules frequently develop into hepatocellular carcinoma in patients with chronic viral hepatitis and cirrhosis. Cancer. 2006;106:636–47.

44. Sato T, Kondo F, Ebara M, Sugiura N, Okabe S, Sunaga M, Yoshikawa M, et al. Natural history of large regenerative nodules and dysplastic nodules in liver cirrhosis: 28-year follow-up study. Hepatol Int. 2015;9:330–6.